Università degli Studi di Parma

Facoltà di Scienze MM. FF. NN.

Dottorato di Ricerca in Scienze Chimiche

MODIFIED and UNMODIFIED β-CYCLODEXTRINS as MYCOTOXIN RECEPTORS

Tutor: Prof. Rosangela Marchelli

Coordinatore: Prof. Marta Catellani

Dottorando: Roberto Pela

XX Ciclo – Triennio 2005-2007

...a mia Mamma.

"…Non so cosa dirvi davvero…Tre minuti alla nostra più difficile sfida professionale...Tutto si decide oggi…Ora noi, o risorgiamo come squadra, o cederemo un centimetro alla volta, uno schema dopo l'altro, sino alla disfatta. Siamo all'inferno adesso, signori miei. Credetemi!...E…possiamo rimanerci, farci prendere a schiaffi oppure aprirci la strada lottando verso la luce. Possiamo scalare le pareti dell'inferno un centimetro alla volta!

Io però non posso farlo per voi, sono troppo vecchio…Mi guardo intorno, vedo i vostri giovani volti e penso…certo che…ho commesso tutti gli errori che un uomo di mezza età possa fare. Si perché io ho sperperato tutti i miei soldi, che ci crediate o no. Ho cacciato via tutti quelli che mi volevano bene e da qualche anno mi da anche fastidio la faccia che vedo allo spechio.

Sapete col tempo, con l'età tante cose ci vengono tolte ma questo fa … fa parte della vita.

Però tu lo impari solo quando quelle cose le cominci a perdere…e scopri che la vita è un gioco di centimetri. E così è il football! Perché in entrambi questi giochi, la vita e il football, il margine d'errore è ridottissimo. Capitelo…Mezzo passo fatto un po' in anticipo o in ritardo e voi non ce la fate. Mezzo secondo troppo veloci o troppo lenti e mancate la presa. Ma i centimetri che ci servono sono dappertutto, sono intorno a noi, ci sono in ogni break della partita, ad ogni minuto, ad ogni secondo.

In questa squadra si combatte per un centimetro! In questa squadra massacriamo di fatica noi stessi e tutti quelli intorno a noi, per un centimetro! Ci difendiamo con le unghie e con i denti per un centimetro! Perché sappiamo che quando andremo a sommare tutti quei centimetri, il totale allora farà la differenza tra la vittoria e la sconfitta, la differenza tra vivere e morire.

E voglio dirvi una cosa: in ogni scontro è colui il quale è disposto a morire che guadagnerà un centimetro…E io so che se potrò avere un'esistenza appagante sarà perché sono disposto ancora a battermi e a morire per quel centimetro. La nostra vita è tutta lì! In questo consiste, e in quei dieci centimetri davanti alla faccia.

Ma io non posso obbligarvi a lottare! Dovrete guardare il compagno che avete accanto, guardarlo negli occhi. Io scommetto che ci vedrete un uomo determinato a guadagnare terreno con voi. Che ci vedrete un uomo che si sacrificherà volentieri per questa squadra, consapevole del fatto che quando sarà il momento voi farete lo stesso per lui.

Questo è essere una squadra, signori miei!

Perciò…o noi risorgiamo adesso, come collettivo, o saremo annientati individualmente…E' il football ragazzi! E' tutto qui.

Allora, che cosa volete fare?..."

Dal film: "Ogni maledetta domenica". Regia di Oliver Stone. Protagonista…un magistrale Al Pacino!!

Chi non avesse mai visto e sentito Al Pacino recitare in questo film, non può certo dire di aver goduto di tutto ciò che la vita ha da offrirgli!!

Preface

"Supramolecular chemistry in water is a constantly growing research area because noncovalent interactions in aqueous media are important for obtaining a better understanding and control of the major processes in nature."

Water is unique.[1] It provides an environment for life and mediates, regulates and controls many processes in nature. As a consequence of its many anomalous properties, water provides both a challenge and opportunities.[2] Water is used more and more as a reaction medium, because it is an inexpensive "green" solvent and its usage has minimal ecological impact. Furthermore, its unique properties give rise to accelerated reaction rates and enhanced reaction selectivities.

Water molecules form an infinite dynamic network of hydrogen bonds with localized and structured clustering. This very favourable process is the main reason not only for the deviation of a variety of its physical properties, but also for the hydrophobic effect; on the other hand, polar molecules experience strong hydration by water and participate in the hydrogen-bonding network, which dramatically influences the properties of the solvatated species. These properties of water provide two main challenges for supramolecular chemistry in aqueous media: how to gain (high) water solubility and how to avoid, or exploit the strong involvement of water in noncovalent processes.

One of the goals of supramolecular chemistry is the creation of synthetic receptors that have both a high affinity and a high selectivity for binding of guests in water.

Enzymes and antibodies show strong and selective host-guest recognition through multiple weak, noncovalent interactions between the functional groups on the binding partners.[3] These natural systems provide the inspiration for the rational design of synthetic receptors that can be used to understand the binding forces that contribute to the formation of complexes.[4] Most synthetic receptors have been studied so far in organic solvents, although most recognition events in nature take place in aqueous medium. The design of synthetic receptors which can be used in water represents a special challenge. First, the host needs to be soluble in water. This severely limits the type of building blocks which can be used for its construction. Second. Special interactions and approaches have to be chosen to overcome the competitive influence of water. Another important feature of large water-soluble receptor is the encapsulation of several (different) guests, thus allowing molecular interactions to be studied within a confined space and carry out chemical reactions in aqueous media.

[1] P. Ball, H_2O: A Biography of Water, Phoenix Press, London, **2000**.

[2] a) D. Laage, J. T. Hynes, *Science* **2006**, 311, 811-835; b) R. Ludwig, *Angew. Chem. Int. Ed.* **2006**, 45, 3402-3405;

c) J. E. Kliyn, J. B. F. N. Engberts, *Nature* **2005**, 435, 746-747; d) D. Chandler, *Nature* **2002**, 417, 491; e) R. Ludwing, *Angew. Chem Int. Ed.*, **2001**, 40, 1808-1827.

[3] *Highlights in Bioorganic Chemistry: Methods and Application* (Eds. C. Shmuck, H. Wennemers), Wiley-VCH, Weinheim, **2004**.

[4] a) S. Kubik, C. Reyheller, S. Stuwe, *J. Inclusion Phenom. Macrocyclic Chem.* **2005**, 52, 137-187; b) R. J. Fitzmaurice, G. M. Kyne, D. Douheret, J. D. Kilburn, *J. Chem. Soc. Perkin Trans. 1*, **2002**, 841-864.

Index

1 Introduction 9
1.1 Cyclodextrins: an overview 9
1.2 Mycotoxins: an overview 22
2 Aim of the Work 35
3 Investigating CD-Mycotoxin Interactions using a "Natural" Force Field 37
3.1 General 37
3.2 Structure and objectives of the chapter 38
3.3 Computational approach 38
3.4 Studying of AFB_1-CD interactions 40
3.5 Computational studying of OTA-CD interactions 51
3.6 Experimental 58
4 Synthesis of Positively Charged β-CD as OTA Receptors 65
4.1 General 65
4.2 Methods for modifying CDs: an overview 66
4.3 Structure and objectives of the chapter 70
4.4 Tosylation of β-CD at the 2-position 72
4.5 Characterization of 2A, 2X-ditosyl-β-CDs. 78
4.6 Synthesis of 2-guanidinium-2-(S)-β-CD. 96
4.7 Tosylation of β-CD at the 6-position 98
4.8 Synthesis of 6-guanidinium-β-CD 99
4.9 Synthesis of multi-charged CD derivatives 99
4.10 Experimental 102
5 Positively Charged CDs for the Recognition of Ochtatoxin A 117
5.1 Introduction 117
5.2 Aim of the work 119
5.3 Results and discussion 120
5.4 Conclusions 127
5.5 Materials and methods 128
6 Host:Guest Interactions of β-CD with Zearalenone: Spectroscopic Evidences 131
6.1 Introduction 131
6.2 Aim of the work 133
6.3 Results and discussion 134
6.4 Conclusions 148
6.5 Materials and methods 149

Chapter 1

Introduction

1.1 Cyclodextrins: an overview

1.1.1 General.

Molecular recognition is a very fundamental process. It may be said that without molecular recognition, there would be no life on this world since enzymes, antibodies, membranes and their receptors, carriers and channels all work through this principle.[1]

In the late nineteenth century (1984), Fisher proposed the *"lock and key"* idea,[2] according to which molecular recognition may be represented by the lock as the molecular receptor and the key as the substrate that is recognized to give a defined receptor-substrate complex. With such a model, chemists have not only been able to design synthetic systems with fascinating properties observed in natural systems but also to create novel organic chemistry of great interest to both science and technology.

In the mid-1980s, molecular recognition became a new area in chemistry. Whereas (organic) chemists in the past, up to the late 1970, were predominantly concerned with covalent bonds in molecules, culminating with the golden age of the complex natural product syntheses, more recently they developed a new direction for science and thinking called *"supramolecular chemistry"*, the chemistry beyond the molecule,[3] where noncovalent bonds and spatial fit between molecular individuals that form a specific "host-guest" complex are in the foreground.[4] According to a general approach, molecular recognition is therefore defined as the study of multi-molecular entities and assemblies said supramolecular complexes, formed between two or more chemical species held together by noncovalent forces.[5]

Among all the potential hosts, from relatively simple receptors containing one or more binding sites to dipodal, tripodal receptors, clips, appropriate functionalized ciclophanes, crown ethers, azamacrocycles, etc., cyclodextrins are an important class of compounds within these water-soluble supramolecular platforms, for the following reasons:

- they are natural products, produced from starch by a relatively simple enzymatic conversion;

- they are produced in thousands of tons per year by means of environmentally friendly technologies;
- since their ability to give inclusion complexes, imported properties of the complexed compounds can be modified significantly. This “unprecedented “molecular encapsulation” is already widely utilized in many industrial products, technologies and analytical methods;
- any toxic effect is secondary and can be eliminated by selecting the appropriate cyclodextrin type or derivative or mode of application;
- as a result of the previous point, cyclodextrins are largely consumed by humans as ingredients for drugs, foods and/or cosmetics.

1.1.2 Structure and properties of CDs.

Cyclodextrins are a family of cyclic oligomers composed of α-(1→4)-linked D-glucopyranose units in the $^4C_1$ chair conformation. As a consequence of this peculiar structure, the molecule features a conical cavity that is essentially hydrophobic in nature.

The most common cyclodextrins have six-, seven and eight glucopyranose units and are referred to as α-, β- and γ-cyclodextrin, respectively. Larger cyclodextrins have also been identified and isolated but have little value in terms of applications.[6] The cavity is limited by hydroxyl groups of different chemical character. Those located at the narrower side come from position 6 of the glucopyranose ring (primary side), while those located at the wider entrance are secondary and therefore are less prone to chemical transformation (secondary side). The reactivity of the hydroxyl groups strongly depends on the reaction conditions. The nonreducting character of cyclodextrins makes them behave as polyols.

Figure 1.1 shows a sketch of the characteristic structural features of cyclodextrins. On the side where the secondary hydroxyl groups are situated, the cavity is wider than on the other side where free rotation of the primary hydroxyls reduces the effective diameter of the cavity.

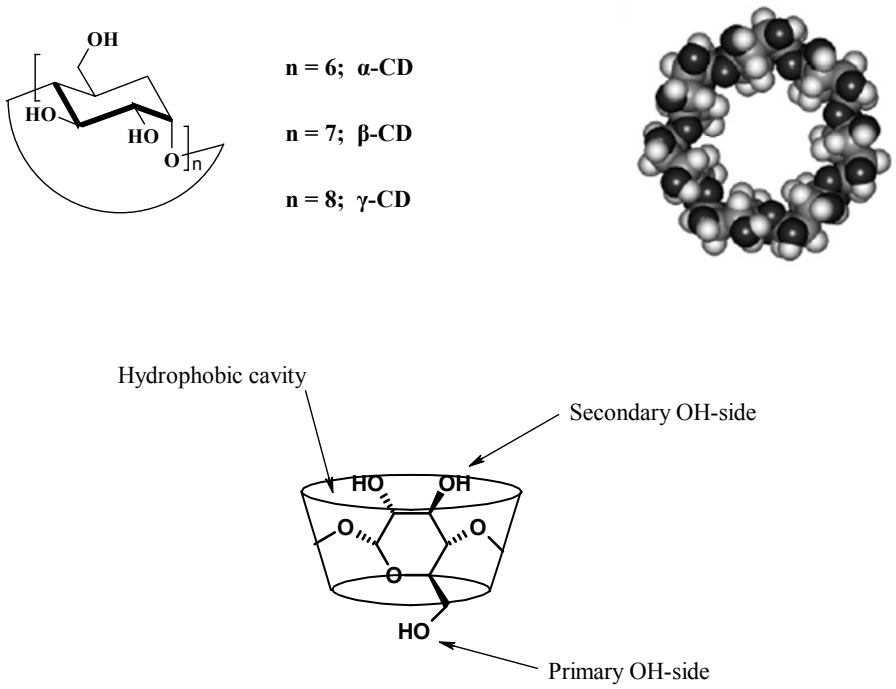

Figure 1.1: Structure of cyclodextrins.

The inner diameter of the cavity in unmodified cyclodextrins varies from 5 to 10 Å, and it is about 8 Å in depth. The nonbonding electron pairs of the glucosidic oxygen bridges are directed toward the inside of the cavity, producing a high electron density there and giving some Lewis-base character.

In the β-cyclodextrin, a complete secondary belt, due to a series of hydrogen bonds formed between the C2-OH group of one glucopyranoside unit and the C3-OH group of the adjacent glucopyranose unit, is formed, thus causing a rather rigid structure. This intramolecular H-bond formation is probably responsible for the lower solubility of β-cyclodextrin in water.

On the other hand, the H-bond belt is incomplete in the α-cyclodextrin molecule, because one glucopyranose unit is in a distorted position. Consequently, instead of six possible H-bonds, only four can be established simultaneously. The γ-cyclodextrin, forming less hydrogen intramolecular bonding, possesses a more flexible structure; therefore, it is the most soluble of the three cyclodextrins.

The most important characteristics of cyclodextrins are summarized in Table 1.1.

Table 1.1: Characteristics of α-, β- and γ-cyclodextrins. From ref. [7]

	α	β	γ
No. of glucose units	6	7	8
MW	972	1135	1297
Solubility in water, g · 100 ml^{-1} at room temp.	14.5	1.85	23.2
$[\alpha]_D$ 25 °C	150±0.5	162.5±0.5	177.4±0.5
Cavity diameter, Å	4.7-5.3	6.0-6.5	7.5-8.3
Height of torus, Å	7.9±0.1	7.9±0.1	7.9±0.1
Diameter of outher periphery, Å	14.6±0.4	15.4±0.4	17.5±0.4
Approx volume of cavity, $Å^3$	164	262	427
Approx cavity volume in 1 mol CD (ml)	104	157	256
in 1 g CD (ml)	0.10	0.14	0.20
Crystal forms (from water)	Hexagonal plates	Monoclinic parallelograms	Quadratic prisms
Crystal water, wt %	10.2	13.2-14.5	8.13-17.7

In the early 1950 and during the past decade, a series of the larger cyclodextrins were isolated and studied.[8] For example, the nine membered δ-cyclodextrin was isolated from the commercially available cyclodextrin conversion mixture by chromatography. δ-cyclodextrin showed a greater aqueous solubility than β-cyclodextrin, but less than α- and γ-cyclodextrin. It was the least stable among the cyclodextrins known at that time: their hydrolysis rate increases in the order of α-CD < β-CD < γ-CD < δ-CD. Moreover, δ-cyclodextrin did not show any significant effect on slightly soluble drugs in water, except in the case of some large guest molecules.

Table 1.2: Incl. complexing capacity of α- to θ-CD studied by capillary electrophoresis. From ref. [7].

Compound	Inclusion complex formation constant (M-1)							
	α	β	γ	δ	ε	ζ	η	θ
Benzoic acid	16	23	3	3	3	5	4	4
2-methylbenzoic acid	13	13	7	6	6	5	6	7
3-methylbenzoic acid	26	49	6	3	5	6	7	8
4-methylbenzoic acid	36	66	8	2	4	6	6	7
2,4-dimethylbenzoic. acid	45	42	8	3	4	5	7	6
3,5-dimethoxybenzoic. acid	47	63	10	8	9	10	9	12
salicylic acid	11	65	13	9	8	8	9	10
3-phenylpropionic acid	35	79	7	2	3	5	4	6
4-tert-butylbenzoic acid	51	457	59	60	4	9	19	31
ibuprofen	55	2006	59	1013	-	10	44	225
1-adamantanecarboxylic acid	114	501	42	8	-	4	4	8

Several studies on the complex-forming ability of the larger cyclodextrins were performed (see Table 1.2).

These results were in agreement with that obtained by computer graphic studies, underlining that the real cavity of the larger cyclodextrins are even smaller than the γ-cyclodextrin cavity, since they are not regularly cylinder shaped structures but they are collapsed, as shown in Figure 1.2.

Figure 1.2: "Collapsed cylinder" structure of the δ-CD. From ref. [7].

Therefore, considering their smaller cavities, the driving force of the complex formation, that is the displacement of the water molecules by a guest in the cyclodextrin cavity, is weaker than in the case of α-, β- and γ-cyclodextrins. Thus, their utilization as inclusion complex agents still remain rather restricted.

1.1.3 Cyclodextrin derivatives.

For several reasons (price, availability, approval status, cavity dimensions, etc.) β-cyclodextrin is the most widely used and represents at least 95% of all produced and consumed cyclodextrins.

However, its anomalous low aqueous solubility is a serious barrier to its wider utilization. Fortunately, by chemical or enzymatic modifications, the solubility of all cyclodextrins can be improved markedly.

Considering that cyclodextrins contain 18 (α-cyclodextrin), 21 (β-cyclodextrin) and 24 (γ-cyclodextrin) hydroxyl groups, the number of possible derivatives are unlimited. By 2000, the syntheses of more than 1500 derivatives have been published. For example, in β-cyclodextrin, 21 hydroxyl groups can be modified by substituting the hydrogen atom or the hydroxyl group with a variety of groups, such as alkyl, hydroxyalkyl, carboxyalkyl, amino, thio, tosyl, glucosyl, maltosyl, and thousands of ethers, esters, anhydro, deoxy, acidic, basic, etc., derivatives can be prepared by chemical or enzymatic reactions. The aim of such derivatizations may be: to improve the solubility of the cyclodextrin derivatives (and its complexes); to improve the fitting and/or the association between the cyclodextrin and its guest, with concomitant stabilization of the guest, reducing its reactivity and mobility; to attach specific (catalytic) groups to the binding site (e.g. in enzyme modelling); or to form insoluble, immobilized cyclodextrin-containing structures and polymers, e.g. for chromatographic purposes.

Industrially, in ton amounts, the following cyclodextrins are actually the most produced: methylated β-cyclodextrin, such as heptakis(2,6-di-O-methyl)-β-cyclodextrin (DIMEB) and the

randomly methylated β-cyclodextrin (RAMEB); hydroxyalkylated cyclodextrins (hydroxypropyl-β-CD and hydroxypropyl-γ-CD); acetylated cyclodextrins (acetyl-γ-CD); reactive cyclodextrins (chlorotriazinyl-β-CD); and branched cyclodextrins (glucosyl-and maltosyl-β-CD).

However, the actual or potential uses of native cyclodextrins or their derivatives in pharmaceuticals, foods, cosmetics, chemical products and technologies are widely summarized in many reviews, as well as in some cyclodextrin monographs,[9] and confirm, unanimously, the correctness of the prognosticated steady increase of the cyclodextrin market during the last two decades. While a series of cyclodextrin-containing products, or cyclodextrin-using technologies is widely known in the food, cosmetic and pharmaceutical industries, for the coming decade, significant new applications are expected from the use of cyclodextrins in environmental protection, in biotechnology and in several industries, like the textile industry.

1.1.4 CD inclusion complexes.

Cyclodextrins can be considered as empty capsules of molecular size. When their cavities include a molecule of another substance, it is called an "inclusion complex".

Considering that no covalent bond is established between the host and the guest, the dissociation/association equilibrium in solution is one of the most characteristic features of the host-guest association. In Figure 1.3 a schematic illustration of a cyclodextrin inclusion complex formation is reported.

Inclusion complexes are entities involving two or more molecule, in which one of the molecules, the "host", includes, totally or in part, a "guest" molecule, only by physical interactions, that is, without covalent binding. Cyclodextrins are typical host molecules and may include a great variety of molecules having the size of one or two condensed benzene rings, or even larger ones which have a side chain of comparable size.

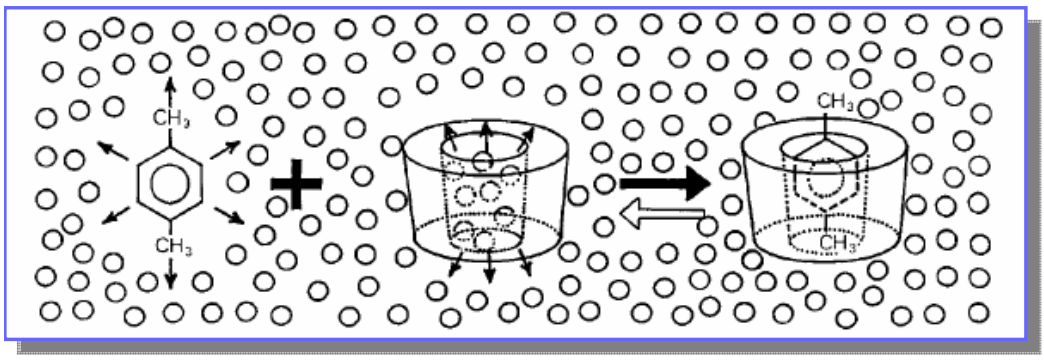

Figure 1.3: Schematic illustration of inclusion complexation of p-xylene by a CD. The small circles represent the water molecules. From ref. [7].

Complex formation is a dimensional fit between host cavity and guest molecule. The lipophilic cavity of cyclodextrin molecules provide a microenvironment into which appropriately sized non-polar moieties can enter to form inclusion complexes.[10] Noncovalent bonds are broken or formed during formation of the inclusion complex.[11] The main driving force of complex formation is the release of enthalpy-rich water molecules from the cavity. Water molecules are displaced by more hydrophobic guest molecules present in the solution to attain an apolar-apolar association and decrease of cyclodextrin ring strain resulting in a more stable lower energy state.

The binding of guest molecules within the host cyclodextrin is not fixed or permanent but rather is a dynamic equilibrium. Binding strength depends on how well the "host–guest" complex fits together and on specific local interactions between surface atoms.

Inclusion in cyclodextrins exerts a profound effect on the physicochemical properties of guest molecules as they are temporarily locked or caged within the host cavity giving rise to beneficial modifications of guest molecules, which are not achievable otherwise.[12] These properties are: solubility enhancement of highly insoluble guests, stabilisation of labile guests against the degradative effects of oxidation, visible or UV light and heat, control of volatility and sublimation, physical isolation of incompatible compounds, chromatographic separations, etc.

The potential guest list for molecular encapsulation in cyclodextrins is quite varied and includes such compounds as straight or branched chain aliphatics, aldehydes, ketones, alcohols, organic acids, fatty acids, aromatics, gases, and polar compounds such as halogens, oxyacids and amines.[12]

The ability of a cyclodextrin to form an inclusion complex with a guest molecule is a function of two key factors. The first is steric and depends on the relative size of the cyclodextrin to the size of the guest molecule or certain key functional groups within the guest. If the guest is the wrong size, it will not fit properly into the cyclodextrin cavity. The second critical factor is the thermodynamic interactions between the different components of the system (cyclodextrin, guest, solvent). For a complex to form, there must be a favourable net energetic driving force that pulls the guest into the cyclodextrin.

In general, therefore, there are four energetically favourable interactions that help shift the equilibrium to form the inclusion complex:

- the displacement of polar water molecules from the apolar cyclodextrin cavity;
- the increased number of hydrogen bonds formed as the displaced water returns to the larger pool;
- a reduction of the repulsive interactions between the hydrophobic guest and the aqueous environment;
- an increase in the hydrophobic interactions as the guest inserts itself into the apolar cyclodextrin cavity.

Once inside the cyclodextrin cavity, the guest molecule makes conformational adjustments to take maximum advantage of the weak noncovalent forces that exist.

Most frequently the host:guest ratio is 1:1, but this is the simplest case. However, 2:1, 1:2, 2:2, or even more complicated associations, and higher order equilibria exist, almost always simultaneously.

Complex formation can be explained through an equilibrium established between dissociate and associate species that is expressed by the complex stability constant K_a. Thus, the association of the cyclodextrin (CD) and the guest (D) molecules, and the dissociation of the formed cyclodextrin/guest complex is governed by a thermodynamic equilibrium (equation 1 and 2 shown in Figure 1.4).

$$\mathbf{CD + D \rightleftharpoons CD{\cdot}D} \qquad (1)$$

$$\mathbf{K_a = \frac{[CD{\cdot}D]}{[CD][D]}} \qquad (2)$$

Figure 1.4: Equilibrium of complexation (1) and the complex stability constant K_a (2).

The most important primary consequence due to the interaction between a poorly soluble guest and a cyclodextrin in aqueous solution are as follow:

- a significantly increase of the concentration of the guest in the dissolved phase, while the concentration of the dissolved cyclodextrin decrease (this is not always true, since in the case of ionized guests or hydrogen bond establishing compounds may enhance the solubility of the cyclodextrin;

- the spectral properties of the guest are modified. For example the chemical shifts of the anisotropically shielded atoms are modified in the NMR spectra. Also when chiral guests are included into the chiral cavity, they become optically active, and show strong induced Cotton effects on the circular dichroism spectra. Further, the maximum of the UV spectra are shifted by several nm, as well as the fluorescence is very strongly improved, since the emission of the guest into the cavity results protected from external quenchers;

- the reactivity of the included molecule is modified. In most cases the reactivity decreases since the guest is stabilized, but in many cases cyclodextrin, behaving as an artificial enzyme, can catalyzes several guest transformations and to modify the reaction pathways;

- the formerly hydrophobic guest, upon complexation, become hydrophilic: its chromatographic mobility, therefore, may be modified.

A wide variety of spectroscopic methods are frequently employed to determine equilibrium constants for cyclodextrin complexation. The choice of the method and the experimental procedure depend on the spectral properties of the guest and/or the host used. In the case of aliphatic guests lacking in intense absorption bands in the accessible UV-vis region, some chromophoric compounds (e.g. azo dyes) are added to the cyclodextrin solutions as a competitive binder, and the binding constants are determined by differential UV spectroscopy.[13] The interaction of cyclodextrin with aromatic guest compounds, which possess strong absorption bands in the UV-vis region, instead, can be studied without adding any chromophoric dyes.

Similarly, in the case of fluorescent guests, the association constant can be determined exploiting emission change of the substrate against the cyclodextrin concentration according to the Benesi-Hildebrand model.[14]

NMR titration is also used to obtain the thermodynamic quantities for cyclodextrin complexation. A mathematical approach similar to that employed in the absorption and fluorescence spectroscopic determination is used. NMR spectroscopy is widely used in chiral discrimination studies using cyclodextrins.[15]

Circular dichroism (CD) spectroscopy is one of the best methods for the observation of the complexation behaviour of chromophoric guests with cyclodextrins, since all natural cyclodextrins are inherently chiral and the spectral changes caused by the inclusion of guest molecules are often more exaggerated in the CD spectra than in the UV spectra.[16]

Recently, use of scanning probe techniques such as atomic force microscopy has allowed measurements of the force involved in the inclusion processes at a single-molecule level,[17] opening new and exciting prospects in supramolecular chemistry.

1.1.5 Spectral changes.

1.1.5.1 Modification of absorption spectra by CDs.

The high electron density prevailing inside the cyclodextrin cavity affects the electrons of the incorporated molecules. This results in characteristic changes in various spectral properties of both the host and the guest.

Since the spectral changes of coloured molecules in the presence of cyclodextrins was first observed in 1951 by Cramer,[18] the effect of cyclodextrins on UV and visible spectra of various guest molecules has been studied.[19] In Figure 1.5 is reported the UV spectra of Amphotericin B in water and in aqueous γ-cyclodextrin solutions.[20]

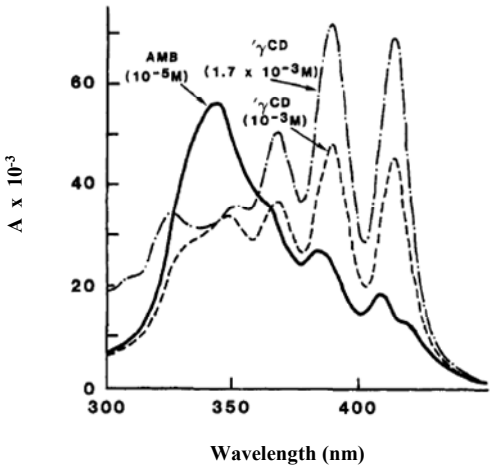

Figure 1.5: UV spectrum of Amphotericin B in water and in aqueous γ-CD solutions. From ref.[20].

Generally, a bathochromatic shift and an absorbance change (increase or decrease) can be observed in the presence of cyclodextrins. The changes in absorbance upon adding cyclodextrins have been used to calculate the association constants.

The complexation of analytes and/or colouring reagents can effectively change their properties. Some of the most useful effects are as follows:

- increased solubility of apolar analytes and/or reagents in aqueous media;
- increased stability of sensitive reagents and the colour complexes in aqueous or non aqueous solutions;
- increased sensitivity of the coloured reaction through intensification of UV absorption;
- improved selectivity of coloured reaction.

These effects make cyclodextrins useful auxiliaries in the spectrophotometric determinations of a wide variety of compounds and elements.

1.1.5.2 Induced circular dichroism.

By adding cyclodextrin to an aqueous solution of a potential achiral guest, an induced Cotton effect will be observed on the circular dichroism spectra, which can be attributed to the optical activity of the guest molecule induced by inclusion into the cyclodextrin chiral cavity, and partly to conformational changes of the same cavity.

The Cotton effect is only observed when the guest molecule, or more exactly its chromophore moiety, is really included in the cyclodextrin cavity. An outer surface association of a potential

guest to the cyclodextrin molecule may lead to some modification of the spectral properties, but not to induce circular dichroism.[21]

It has been notated that the sign and the intensity of the induced Cotton effects are quite sensitive to the orientation of the guest chromophore in the cyclodextrin cavity. In particular, Cotton effects with opposite signs will be observed depending on if the electric dipole moment of the guest coincides with the axis of the cyclodextrins or, instead, if they are perpendicular to each other.

This characteristic property can be explained showing results obtained by Corradini et al.[22] In their work they reported a spectroscopic study on different conformations assumed by two DNS modified cyclodextrins, the 6-deoxy-6-N-(N'-dansylethylenediamino)-β-cyclodextrin (CD-en-DNS) and the 6-deoxy-6-N-(N'-dansyldiethylenetriamino)-β-cyclodextrin, (CD-dien-DNS), in aqueous solutions (Figure 1.6).

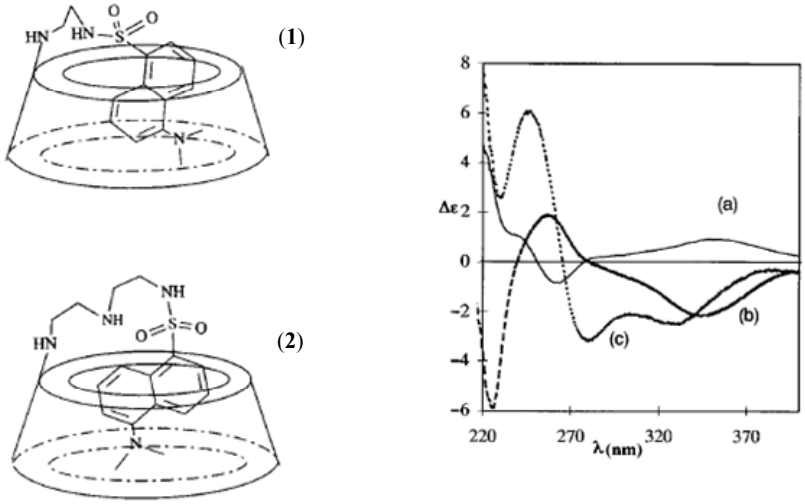

Figure 1.6: Circular dichroism spectra of (a) CD-dien-DNS (2), (b) CD-en-DNS (1) and (c) CD-dien-DNS: copper(II) = 1:1.

As shown in Figure 1.6, opposite sign of each CD band was obtained, thus showing a different type of inclusion for the two dansyl groups of the two derivatives. The orientation of the dansyl groups seemed to be dependent on the length of the spacer: the shorter one induces axial complexation, while the longer one induces equatorial complexation. Line (c) was obtained adding copper(II) to the aqueous solution of compound **2** (CD-dien-DNS: copper(II) = 1:1). This caused a drastically change of the CD signal, since a negative band similar to that obtained for compound **1** was observed. Probably the copper(II) complexation induced an axial inclusion of the dansyl group, similar to that observed for **1**, due to the more rigid conformation of the linking moiety on the rim (Figure 1.7).

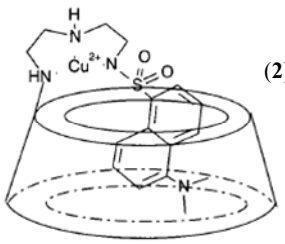

(**2**)

Figure 1.7: Copper(II) complexation model for CD-dien-DNS (2).

1.1.5.3 Cyclodextrins in NMR spectroscopy.

^{1}H-NMR spectra of cyclodextrins and their inclusion complexes were first investigated by Denmarco and Thakkar.[23] These authors found that when the aromatic moiety of a guest molecule is included in the cyclodextrin cavity, protons located within the cavity (H-3 and H-5) are susceptible to anisotropic shielding by the aromatic moiety, and thus an upfield shift is observed. Protons located on the exterior of the cavity (H-2, H-4 and H-6) are relatively unaffected. Following this pioneering work, NMR spectroscopy became the most powerful tool for the study of inclusion complex formation between cyclodextrins and a variety of guest molecules. Initially, the investigation were only carried out in solution by ^{1}H-NMR, but now ^{13}C-NMR, ^{15}N-NMR, ^{19}F-NMR and ^{31}P-NMR spectroscopic methods have been used for the inclusion complex formation studies, even in the solid state. Nowadays, as a result of the development of high-resolution instruments and of the two dimensional techniques, the quantitative data of the early years have been greatly improved. It is now possible to make quantitative measurements about thermodynamic and kinetic parameters of CD complexes.

In NMR spectroscopy analysis, moreover, cyclodextrins are mainly used as chiral NMR shift reagents. In many cases, the spectra of cyclodextrin inclusion complex of two enantiomers of a chiral compound differ in chemical shifts.[24] A ^{19}F-NMR study[25] of the formation of diastereomeric inclusion complexes between fluorinated amino acid derivatives and α-cyclodextrin in 10% D_2O solution shows that the chemical shifts of the (R) amino acids derivative-α-cyclodextrin inclusion complex are upfield relatively to those of their (S) enantiomer for deprotonated N-(p-fluorobenzoyl)valine, deprotonated α-(p-fluorophenyl)-glycine and N-acetyl-α-(p-fluorophenyl)glycine. The shift differences between the diastereoisomers formed with (R) and (S) enantiomers can be used for chiral analysis and optical purity determinations.

1.1.5.4 Enhancement of fluorescence.

Molecular fluorescence spectrophotometry has become established as a routine technique in many analytical applications. In many cases, spectrophotometry can yield a lower detection limit

and greater selectivity than molecular absorption spectrophotometry. However, although most compounds show strong fluorescence in organic solvents, the intensity is rather weak in water which acts as a quencher. Adding cyclodextrins, which form inclusion complexes with analyte molecules in aqueous solutions, can result in significant fluorescence enhancement.

The first utilization of cyclodextrins in fluorescence enhancement was performed by Kinoshita and co-workers, who examined the of effect cyclodextrins on the dansyl amino compounds.[26]

The inclusion of analyte molecules into the CD cavity can offer certain advantages:

- The cyclodextrin structure protects the fluorescing exciting state of the analyte from external quenchers;[27]

- As a consequence of inclusion complex formation, the rotation of the guest molecule is hindered, and the relaxation of the solvent molecules is considerably decreased. Both of these effects can result in a decrease in the vibrational deactivation;

- The cyclodextrin cavity behaves similarly to the organic solvent, affords an apolar surrounding for the included chromophore. This altered environment can provide favourable polarity for enhanced quantum efficiencies and hence the intensities of luminescence. The effective microenvironment of the cyclodextrin cavity is likely to be similar to that of such oxygenated solvents as dioxane, tert-amyl alcohol, or 1-octanol;[28]

- The cyclodextrin solution can improve the detection limit for hydrophobic analytes in aqueous solution by increasing their solubility or, for hydrophilic analytes, by increasing solubility of the water-insoluble fluorescent compounds into which the analytes are incorporated.

Inclusion complex formation within a cyclodextrin usually results in a higher fluorescent quantum yield. It has been found that the fluorescence intensities of many compounds, such as pyrene,[29] drugs, narcotics, hallucinogenics,[30] and polychlorinated biphenols[31] are significantly increased by the complex formation with cyclodextrins and their derivatives.

To evidence the importance of cyclodextrins in the field of analytical luminescence chemistry, an other important application of cyclodextrins is the development of fiber-optic cyclodextrin-based (FCD) sensors for the detection of a widely variety of organic compounds.[32] This FCD sensor uses laser excitation and fluorescence detection with β-cyclodextrin immobilizes at the tip of an optical fiber. The sensitivity of this sensors was 14 times greater than that of a bare optical fiber when measurements was made for pyrene with the sensor immersed in a buffer after a 10 min incubation period.

1.2 Mycotoxins: an overview

1.2.1 General.

Mycotoxins are toxic secondary metabolites produced by filamentous fungi, under suitable environmental conditions in a wide variety of food commodities. The number of raw food matrices recognized as susceptible to mycotoxin contamination is largely increased during the recent years, now including cereals, oleaginous seeds, coffee beans, vine fruits, cocoa beans, nuts, spices, fruits and vegetables. Fungal contamination can start at various stages of the food chain such as growth, harvest, shipping, and storage.

Since mycotoxin levels are generally not affected by cooking procedures and by the usually employed technological food processes, not only raw materials, but also food products can be contaminated. Cereal derivatives, roasted coffee, wine, beer, vine fruits, chocolate products and fruit juices are considered to be the most risky finished products.

The most ubiquitous toxigenic molds are some genera of *Aspergillus*, *Penicillium* and *Fusarium* and the most widespread mycotoxins derived are aflatoxins, ochratoxins A, fumonisins, trichothecenes, zearalenone, and patulin (Table 1.3). Specific conditions may influence mycotoxin biosynthesis, such as climate and geographical location of crops, cultivation practices, storage and type of substrate.

Mycotoxins display a variety of chemical structures (Table 1.4), accounting for their different biological effects. Depending on their nature, toxins may be carcinogenic, mutagenic, teratogenic, estrogenic, neurotoxic and immunotoxic when ingested by animals and humans. Ingestion occurs mainly via plant-based foods and the residues and metabolites present in animal-derived foods.

Some mycotoxins, such as aflatoxins, certain trichothecenes, fumonisines and ochratoxins have been associated with highly lethal episodic outbreaks of poisoning in animals and human populations.

In 1993, the World Health Organization – International Agency for Research on Cancer (WHO-IARC) evaluated the carcinogenic potential of aflatoxins, ochratoxin A, trichothecenes, zearalenone and fumonisines. Naturally occurring aflatoxins were classified as carcinogenic to humans (Group 1), while ochratoxin A and fumonisines B_1 were classified as possible carcinogen to humans (Group 2B). All of these carcinogenic compounds are DNA damaging agents, with the exception of fumonisines which may induce cancer by interfering with the transduction pathways. Trichothecenes and zearalenone were not classified as humans carcinogen (Group 3).

Table 1.3: The most important mycotoxigenic fungi, the produced mycotoxin and their common hosts.

		"in field" contamination	**Host**	**Mycotoxins**
Aspergillus	*flavus*	YES	maize	aflatoxins
	parasiticus	YES	maize	aflatoxins
	ochraceus	NO	dried fruits	ochratoxins
	sez. Nigri	YES	grapes	ochratoxins
Penicillium	*verrucosum*	NO	cereals	ochratoxins
	expasus	YES	apples	patulin
Fusarium	*culmorum*	YES	cereals	Trichothecenes, zearalenone
	graminearum	YES	cereals	Trichothecenes, zearalenone
	proliferatum	YES	cereals	fumonisines
	verticillioides	YES	cereals	fumonisines

Table 1.4: Fungi and their associated mycotoxins.

Fungi	Mycotoxins
Aspergillus flavus, A. parasiticus, *A. nomius*	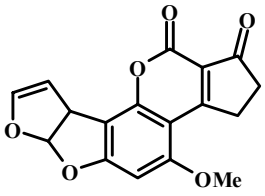 **AFLATOXIN B_1**
Penicillium verrucosum, *Aspergillus clavatus,* *A. niger*	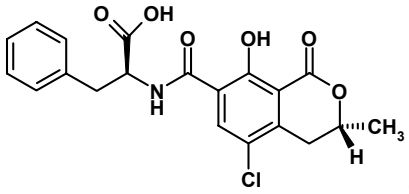 **OCHRATOXIN A**
Penicillium expansus, *P. urticae,* *Aspergillus clavatus,* *Byssochlamis nivea*	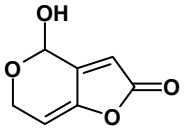 **PATULIN**
Fusarium sporotrichioides, *F. graminearum, F. culmorum,* *F. poe, F. roseum,* *F. tricinctum, F. acuminatim*	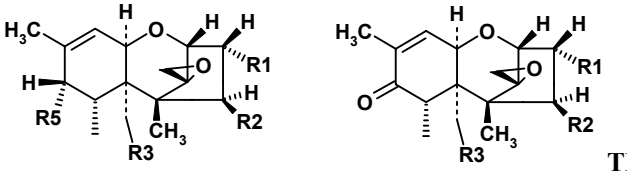 **TRICHOTHECENES**
Fusarium monoliforme *F. proliferatum*	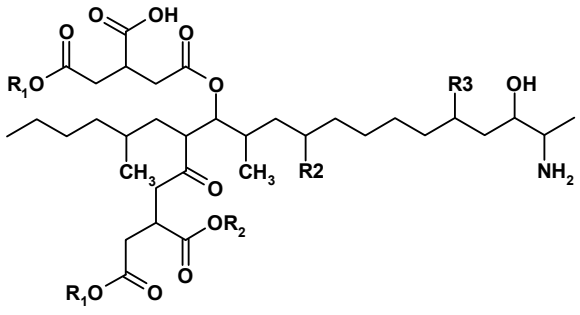 **FUMONISINS**
Fusarium graminearum, *F. culmorum, F. crookwellense*	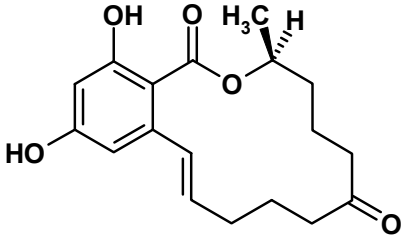 **ZEARALENONE**

1.2.2 Toxicology.

Mycotoxins can exert their toxic effects through three primary mechanisms:

- alteration of nutrient content, absorption and metabolism;
- changes of the endocrine and neuroendocrine function;
- suppression of the immuno system.

There are evidences indicative that many mycotoxins require metabolic activation in order to induce a toxic response. Only trichotecenes appear to posses directly toxic properties, probably associated with the presence of the epoxide group. Although primary metabolic activation might not be required, there remains the possibility of a genetic influence on their toxicity through the level of expression of secondary detoxifying metabolism. Recent studies have demonstrated the importance of secondary, conjugative metabolism in determining the extent of toxic responses to exposure to many toxins.[33]

1.2.2.1 DNA damage by mycotoxins.

Among mycotoxins, aflatoxins are the most potent genotoxic agents. AFB_1 has been demonstrated to be mutagenic, to produce chromosomial aberrations, unscheduled DNA synthesis and chromosomial strand breaks, as well as forming DNA-adducts in cells. Thus, AFB_1 was classified as a Group 1 carcinogen by IARC in 1993.

In particular, aflatoxins B_1 induces genotoxic effects by covalent binding to DNA via formation of an epoxidic ring on the unsaturated furan moiety: there is no doubt that the 8,9-epoxide formed by the cytochrome P450 is the critical metabolite for genotoxic damage. This metabolite may intercalate within the double-stranded DNA and may form an adduct with the N-7 atom of guanine residues via an SN_2 reaction (Figure 1.8).[34]

Also ochratoxin A has been classified as a Group 2B carcinogen by IARC in 1993. OTA, in particular, may be genotoxic and mutagenic, but there are only suggestions of carcinogenic effect in humans. By “in vivo” tests, it has been demonstrated that OTA induces DNA single-strand breaks. This mycotoxins can also form DNA-adducts in liver and kidney, but most of these adducts disappear within 5 days after administration. Recently, Dai et al. have for the first time isolated, synthesized and characterized the C8-guanine-specific DNA-adduct of ochratoxin A, which is responsible for the OTA induced oxidative stress and oxidative DNA damage (Figure 1.9).[35]

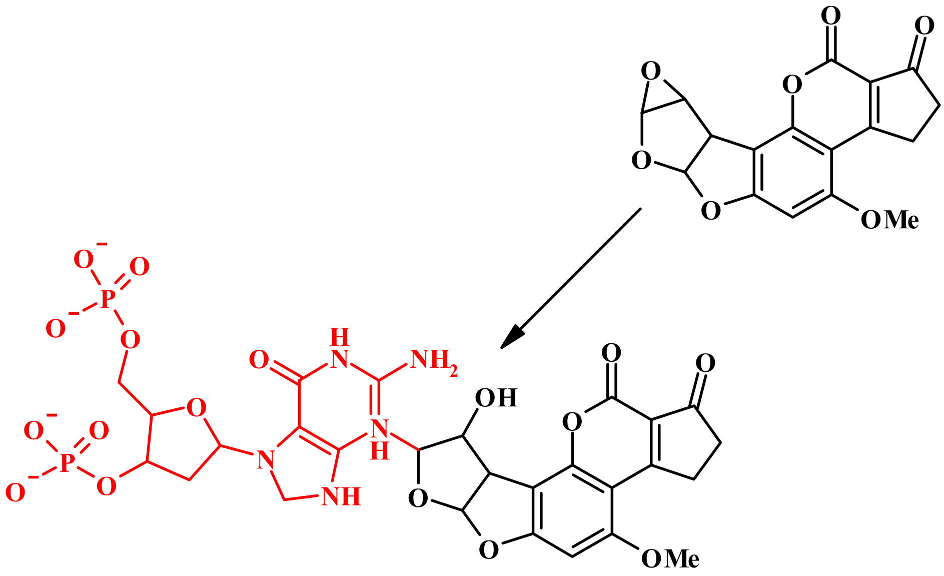

Figure 1.8: Structure of the AFB1-DNA adduct.

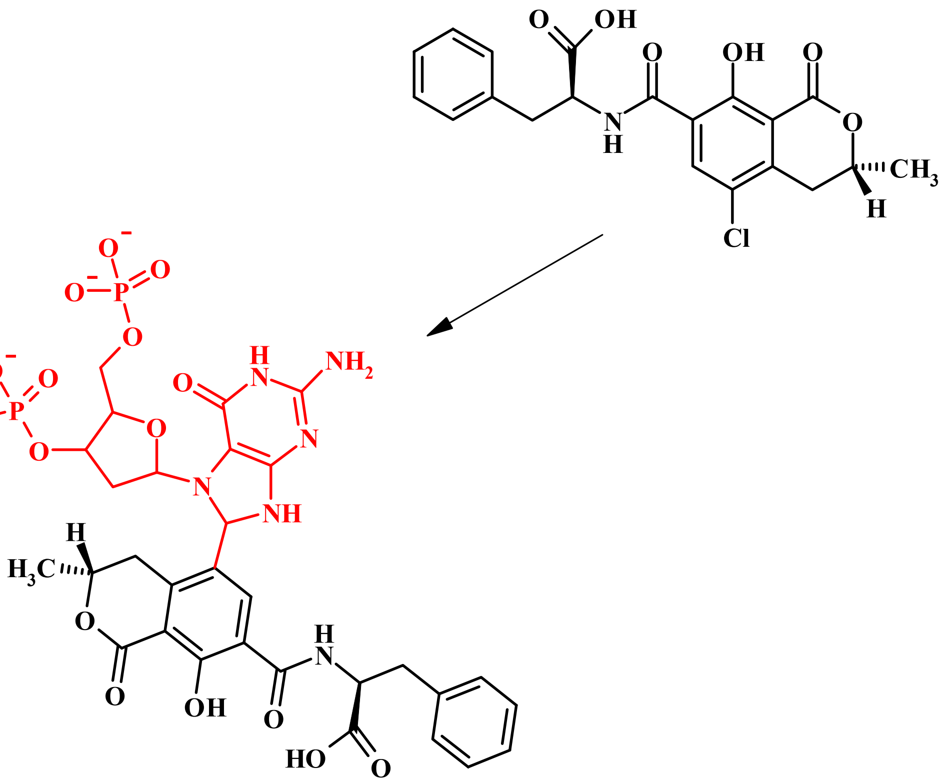

Figure 1.9: Structure of the OTA-DNA adduct.

Zearalenone has been not recognized as carcinogen, although it showed a positive DNA damaging effect in some "in vitro" tests. However, some DNA-adducts have been isolated in kidney and liver tissues after administration of doses of zearalenone or its estrogenic metabolites.[34]

1.2.2.2 Estrogenic effects.

Estrogenic mycotoxins are an important class of environmental estrogens although their contribution to the total environmental estrogen load has not been determined.

Mirocha et al.[36] reported the natural occurrence of a family of at least seven zearalenones in corn cultures of *Fusarium roseum*. Subsequent studies have identified numerous others naturally occurring members of the zearalenone family, some of which are shown in Figure 1.10 and in Table 1.5.

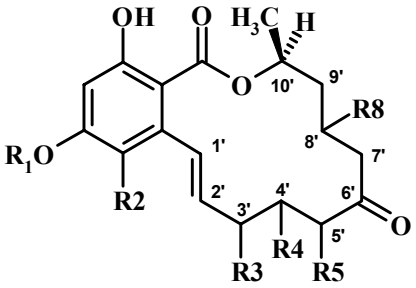

Figure 1.10: General structure of zearalenone derivatives.

Table 1.5: Zearalenone and its analogues.

Name	R_1	R_2	R_3	R_4	R_5	R_6	R_8
Zearalenone	H	H	H	H	H	-	H
α- or β-zearalenol	H	H	H	H	H	OH	H
3'-hydroxy-zearalenone	H	H	OH	H	H	-	H
8'-hydroxy-zearalenone	H	H	H	H	H	-	OH
5-formyl-zearalenone	H	CHO	H	H	H	-	H
LL-Z1641-1	CH_3	H	H	OH	OH	-	H
LL-Z1640-3	CH_3	H	H	OH	OH	OH	H

Zearalenone exhibits its physiological activity first by binding to the cytosolic estrogen receptor protein and then by translocation of the estrogen-receptor complex into the nuclei, for which it exhibits a high affinity. The affinity of zearalenone and its derivatives for the cytosolic estrogen receptor is greatly influenced by the 6'-OH and the double bond C-1'= C-2'. The α-epimer of zearalenol (α-ZOL) is much more active than the β-epimer (β-ZOL).[37]

1.2.3 Regulatory aspects.

Since the discovery of aflatoxins in 1960 and subsequent recognition that mycotoxins are of significant health concern to both humans and animals, regulations gradually developed for these natural contaminants in food and feed. In the early days of mycotoxin regulations, these measures focused mainly on aflatoxins. They were established by industrialized countries, and limits often had an advisory or guideline character. Over the years, however, the number of countries with known specific mycotoxin regulations has increased until to 100 in 2003.[38] (Up to now regulations have been set up not only for aflatoxins, but also for ochratoxins A, patulin, zearalenone and fumonisines B_1 and B_2 for many food and feed commodities and products).

Until the 1990s mycotoxin regulations were mostly a national concern. Gradually, several communities, for example EU (European Union), FDA (Food and Drug Administration), MERCOSUR (Mercado Cómun del Sur), Australia and New Zealand, harmonized their mycotoxin regulations, thereby overruling existing regulations. Current regulations are increasing based on scientific opinions of authoritative bodies, for example the European Food Safety Authority (EFSA) and the FAO/WHO Joint Expert Committee on Food Additives of the United Nations (JECFA). At the same time, requirements for adequate sampling and analytical methods put high demands on other professional organizations, for example AOAC International and the European Standardization Committee (CEN).

A variety of factors affects the promulgation of mycotoxin limits and regulations. These include:

- the availability of toxicological data of mycotoxins;
- the availability of exposure data of mycotoxins;
- knowledge of the distribution of mycotoxins concentration within commodity or product lots;
- the availability of analytical methods;
- legislation in others country with which trade contacts exist;
- the need for sufficient food supply.

In particular, the first two factors provide the information necessary for hazard assessment and exposure assessment, respectively, the main bases of risk assessment that is defined as the scientific evaluation of the probability of occurrence of know or potential adverse health effects resulting from human exposure to food-borne hazards. It is the primary scientific basis for promulgation of regulations. The third and fourth factors are important factors enabling practical enforcement of mycotoxin regulations, through adequate sampling and analysis and procedures. The last two

factors are merely socio-economic in nature but are equally important in the decision-making process to establish meaningful regulations and limits for mycotoxins in food and feed.

The hazard of mycotoxins to individuals is probably more or less the same all over the world, while exposure is not the same, because of different levels of contamination and dietary habits in the various parts of the world.

Exposure assessment is an important aspect of risk assessment, and reliable data on the occurrence of mycotoxins in different commodities and data on food intake are needed. Quantitative evaluation of intake of mycotoxins is quite difficult; to this aim, during its meetings, JECFA outlined the need of using validated analytical methods and application of analytical quality assurance to ensure that the results of surveys provide reliable assessment of intake.[39] Because most mycotoxin contamination is heterogeneously distributed, adequate sampling is another important consideration for obtaining information on levels of contaminations. In many countries, activities take place that contribute to the risk-assessment processes for mycotoxins. In the EU, for example, an important role is played by the European Food Safety Authority (EFSA), which makes use, where possible, of exposure and consumption data, generated by the European Scoop activities.

1.2.4 Methods of analysis of mycotoxins.

Analytical methods for mycotoxins are mainly based on thin-layer chromatography (TLC), high-performance liquid chromatography (HPLC), or enzyme-linked immunosorbent assay (ELISA). Other techniques such as gas chromatography (GC), gas-chromatography-mass spectrometry (GC/MS), liquid chromatography-mass spectrometry (LC/MS) and capillary electrophoresis (CE) are also at a well-developed stage, in some cases being the methods of choice for several mycotoxins. An important criteria of selection include the required limit of detection, the availability of sophisticated or simple instrumentations and the need for running a high number of analysis at low cost.

As for the cost of the analysis, the lowering of costs could be beneficial in many respects; in general terms, in order to achieve the most meaningful scenario of the presence of the toxins at the lowest cost, the best approach is considered to be the strategy of a balanced combination of screening (ELISA) and confirmatory tests (HPLC, LC/MS).

The basic principle of an ELISA assay is to use an enzyme to detect the binding of antigens (Ag) and antibodies (Ab). The enzyme converts a colourless substrate (chromogen) to a coloured product, indicating the presence of an Ag-Ab complex. There are commercially available tests for the determination of hormones, mycotoxins, microorganisms, drugs, tumour marker and pesticides.

In the most commonly used noncompetitive ELISA, the antibody, which is fixed on a solid support, may bind the antigen present in the sample in a specific way. When the solution containing the enzyme-conjugate is added to the ELISA plate, there is the formation of a coloured complex

between the enzymatic conjugate and the antigen-antibody complex and the absorbance of this complex is proportional to the concentration of the antigen.

In the competitive ELISA, the antigene in the sample will bind to an antibody that is firmly attached to a support. If the Ag-Ab binding occurs, it will inhibit the competitive binding of the same antigen linked to the enzymatic conjugate. Thus, if the sample does not contain antigens that react with the antibodies, the enzyme-labelled antibody would bind and a colour reaction would occur. The absorbance of the coloured complex is, in this case, inversely proportional to the concentration of the toxin in the sample.[40]

The mechanism of competitive and noncompetitive ELISA is reported in Figure 1.11.

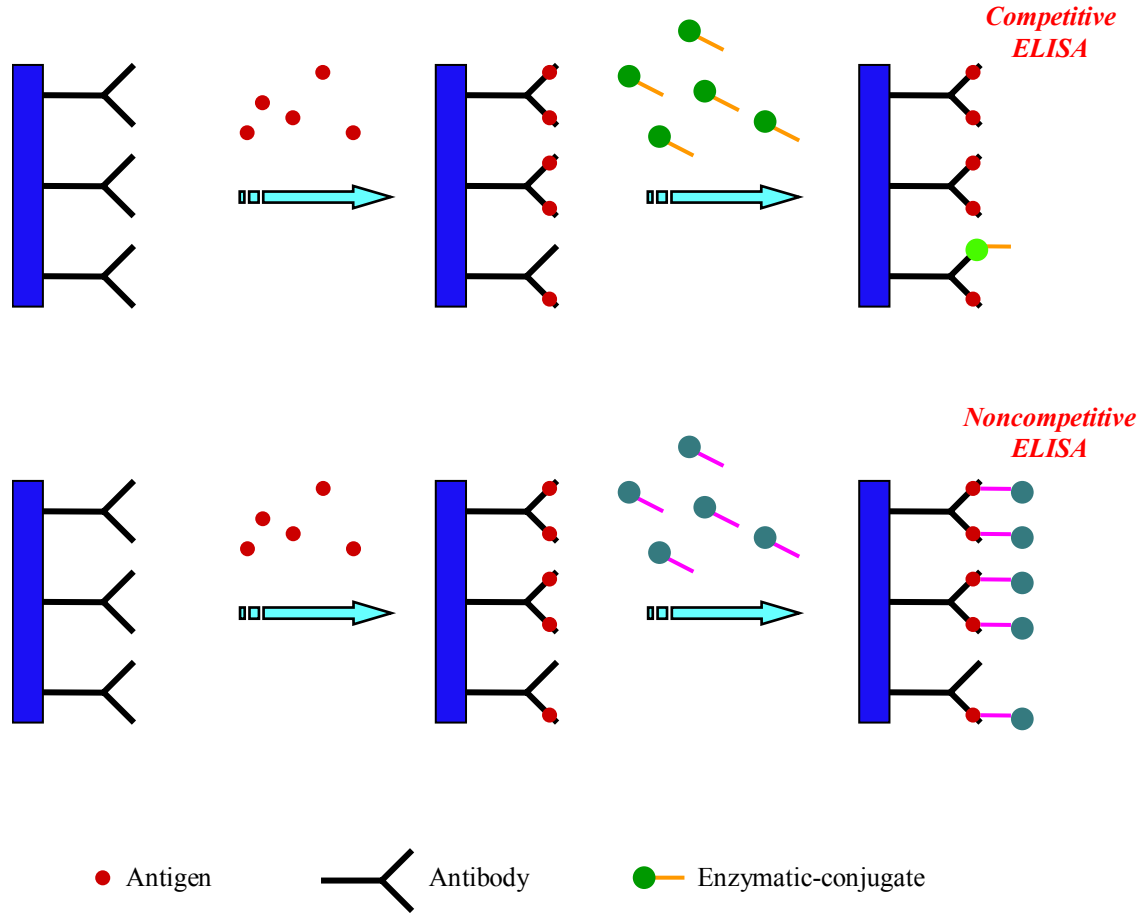

Figure 1.11: Mode of action of the competitive and noncompetitive ELISA test.

The analysis of different samples using ELISA tests are, however, very susceptible to the presence of interferents coming from the matrices and to the ability of the analysts. The uncertainty of the measurements obtained by ELISA is usually over the 20 %.

As reported above, the quantification of mycotoxins requires analytical methods able to guarantee high performance in terms of accuracy, reproducibility, ruggedness, sensibility and

specificity. Moreover, the enforcement of the existing legal limits involves the possibility to detect and quantify the contaminants also at very low concentrations (μg/Kg or ng/Kg).

The most important technique for the determination of mycotoxins is hence HPLC, because it is sensitive, reproducible, and versatile and requires relative not expensive equipments.

The fluorescence detector (FLD) is probably the most useful detector, because it is based on a spectroscopic property that can guarantee high sensitivity and high specificity. Moreover, several mycotoxins are naturally fluorescent, such as aflatoxins, ochratoxin A and zearalenone, and many others become fluorescent after a derivatization step (fumonisines).

The UV detection is commonly used for the analysis of patulin and the type B trichothecenes, in particular deoxyvalenol; however, this detection technique can't give good performance, because of the low specificy of the chromophores contained in mycotoxins and the high interferences due to the matrix.

Analytical methods for the determination of aflatoxins used to be HPLC coupled with post-column derivatization with iodine or bromine or pre-column derivatization with trifluoroacetic acid (TFA) and fluorescence detection. These derivatizing agents, however, present some serious drawbacks, such as the instrumental wear and the low stability. For this reason, the derivatization has been automatized by using an electrochemical system which promotes the halogenation of the furanic moiety of aflatoxins by the electrochemical oxidation of KBr to Br_2.[41] Moreover, Capeda et al. have proposed the use of cyclodextrin as post-column additive to enhance the natural low fluorescence of AFB_1 and AFG_1.[42,43]

Considering the importance of HPLC in the mycotoxins determination, during the last years the use of LC/MS methods has increased very rapidly, in particular due to the diffusion of the atmospheric pressure interfaces (APCI, ESI) and the relatively low prices for these instrumentations.

The methods commonly used for the analysis of mycotoxins involve the use of a single quadrupole mass spectrometer, although the triple quadrupole and ion trap mass spectrometer allow a definitive identification of the analyte by fragmentation and are more sensitive.

At the present, several LC/MS methods have been developed for the determination of mycotoxins which don't have a characteristic chromophoric or fluorophoric group; in particular, trichothecenes, fumonisins and zearalenone have been determined by LC/APCI-MS.[44]

A very recent review on the determination of mycotoxins by Mass Spectrometry has been reported by Sforza et al.[45]

[1] a) S. M. Roberts (ed.) *"Molecular Recognition–Chemical and Biochemical Problems"*, Royal Society of Chemistry, Cambridge, **1989**; b) J. M. Lehn, *"Supramolecular Chemistry"*, VCH, Weinheim, **1995**.

[2] E. Fisher, Ber. Dtsch. Chem. Ges., **1894**, 27, 2985.

[3] a) J. M. Lehn, *Angew. Chem. Int. Ed.* **1990**, 29, 1304; b) G. W. Gokel (ed.) *"Advances in Supramolecular Chemistry"*, JAI Press, Greenwich, CT, **1990**, vol. 1; c) F. Vögtle, *"Supramolecular Chemistry-An Introduction"*, Wiley, Chichester, **1993**.

[4] a) F. Vögtle and E. Weber (eds.), *"Host-Guest Complex Chemistry–Macrocyles"*, Springer, Berlin, Heidelberg, **1985**; b) *"Host-Guest Molecular Interaction–From Chemistry to Biology* (Ciba Foundation Symposium 158)*"*, Wiley, Chichester, **1991**; c) B. Dietrich, P. Viout and J. M. Lehn, *"Macrocyclic Chemistry* (*Aspects of Organic and Inorganic Supramolecular Chemistry*)*"*, VCH, Weinheim, **1993**.

[5] D. Hamilton, in *"Bioorganic Chemistry Frontiers"*, ed. H. Dugas., Springer, Berlin, Heidelberg, **1991**, vol. 2, p. 115.

[6] W. Saenger, J. Jacob, K. Gessler, T. Steiner, D. Hoffman, H. Sanbe, K. Koizumi, S. M. Smith, T. Tanaka, *Chem. Rev.* **1998**, 98, 1787.

[7] J. Szejtli, *Chem. Rev.* **1998**, 98, 1743.

[8] K. L. Larsen, H. Ueda, W. Zimmerman, 8th European Congress on Biotechnology. Budapest, 17-21 August, **1997**.

[9] a) K. H. Frömming, J. Szejtli, *"Cyclodextrin in Pharmacy"*; Kuwer: Dordrecht, **1994**, p. 224; b) D. Duchene, Ed *"Cyclodextrins and Their Industrial Uses"*; Edition de Santé: Paris, **1997**, p. 448; c) J. Szejtli, *J. Mater. Chem.* **1997**, 7, 575.

[10] Loftsson T, Brewster ME. Pharmaceutical applications of cyclodextrins: 1. Drug solubilisation and stabilization.

J Pharm Sci. **1996**;85:1017–25.

[11] Schneiderman E, Stalcup AM. Cyclodextrins: a versatile tool in separation science. *J Chromatogr B* **2000**;745, 83.

[12] G. Shmidt. Cyclodextrins glucanotrasferase production: yield enhancement by overexpression of cloned genes. *Trends Biotechnol*. **1989**, 7, 244-248.

[13] Y. Matsui, K. Mochida, *Bull. Chem. Soc. Jpn*. **1979**, 52, 2808-2814.

[14] H. A. Benesi, L. H. Hildebrand, *J. Am. Chem. Soc.* **1949**, 71, 2703.

[15] a) M. Suzuki, Y. Sasaki, *Chem. Pharm.Bull.* **1984**, 32, 832-838; b) I. M. Brereto, T. M. Spotswood, S. Lincoln, E. H. Williams, *J. Chem. Soc., Faraday Trans. 1*, **1984**, 80, 3147-3156 c) P. E. Hansen, H. D. Dettman, B. D. Sykes, *J. Magn. Reson.* **1985**, 62, 487-496; d) D. Greatbanks, R. Pickford, *Magn. Reson. Chem.* **1987**, 25, 208-215; e) S. E. Brown, J. H Coates, S. F. Lincoln, D. R. Coghlan, C. J. Easton, *J. Chem. Soc., Faraday Trans.* **1991**, 87, 2699-2703; f) E. Amato, F. Djedaini-Pilard, B. Perly, G. Scarlata, *J. Chem. Soc., Perkin Trans. 2*, **1992**, 2065-2069; g) A. F. Casy, *Trends Anal. Chem.* **1993**, 12, 185-189.

[16] a) V. I. Sokov, V. L. Bondareva, G. V. Shustov, *Metallorg. Khim.* **1991**, 4, 697-699 (in Russian); b) K. Kano, K. Yoshiyasu, H. Yasuoka, S. Hata, S. Hashimoto, *J. Chem. Soc., Perkin Trans. 2*, **1992**, 1265-1269; c) A. Ueno, Q. Chen, I. Suzuki, T. Osa, *Anal. Chem.* **1992**, 64, 1650-1655.

[17] a) H. Schönherr, M. W. J. Beulen, J. Huskens, F. C. J. M. van Veggel, D. N. Reynhoudt, G. J. Vancso, *J. Am. Chem. Soc.* **2000**, 122, 4963; b) S. Zapotoczny, T. Auletta, M. R. de Jong, H. Schönherr, J. Huskens, F. C. J. M. van Veggel, D. N. Reynhoudt, G. J. Vancso, *Langmuir*, **2002**, 18, 6988; c) T. Auletta, M. R. de Jong, A. Mulder, J. Huskens, F. C. J. M. van Veggel, D. N. Reynhoudt, S. Zou, S. Zapotoczny, H. Schönherr, G. J. Vancso, L. Kuipers, *J. Am. Chem. Soc.* **2004**, 126, 1577.

[18] F. Cramer, *Chem. Ber.* **1951**, 81, 851.

[19] a) Ikeda, K.; Vekama, K.; Otaqiri, M. *Chem. Pharm. Bull.* **1975**, 23, 201; b) M. Vikmon, A. Stadler-Szoke, J. Szejtli, J. Antibiot. 1985, 38, 1822.

[20] J. Szejtli, *Cyclodextrin Technology*, Kluwer Academy Publishers; Boston, **1988**.

[21] J. Szejtli, *Cyclodextrin Technology*, Kluwer; Dordrecht, **1988**.

[22] R. Corradini, A. Dossena, G. Galaverna, R. Marchelli, A. Panaglia, G. Sartori, *J. Org. Chem.* **1997**, 62, 6283-6289.

[23] a) P. V. Denmarco, A. L. Thakkar, *J. Chem. Soc. Chem. Commun.* **1970**, 2; b) A. L. Thakkar, P. V. Denmarco,

J. Pharm. Sci. **1971**, 60, 652.

[24] D. D. MacNicol, *Tetrahedron Lett.* **1975**, 38, 3325.

[25] S. E. Brown, J. H. Coates, S. F. Lincoln, D. Coghlan, C. J. Easton, *J. Chem. Soc. Faraday Trans.* **1991**, 87, 2699.

[26] T. Kinoshita

[27] a) K. Kano, I. Takenoshita, T. Ogawa, *J. Phys. Chem.* **1982**, 86, 1833; b) C. D. Tran, J. H. Fendler, *J. Phys. Chem.* **1984**, 88, 2167; c) N. J. Turro, G. S. Cox, X. Ki, *Photochem. Photobiol.* **1983**, 36, 149.

[28] a) H. Kondo, H. Nakatani, K. J. Hiromi, *Biochem. 1976*, 79, 393; b) K. W. Street, *J. Liq. Chromatogr.* **1987**, 10, 655.

[29] S. Hashimoto, J. K. Thomas, *J. Am. Chem. Soc.* **1985**, 107, 4655.

[30] L. J. Cline-Love, M. L. Grayeski, J. Noroski, R. Weinberger, *Anal. Chim. Acta*, **1985**, 170, 3.

[31] R. Temia, S. Scypinski, L. J. Cline-Love, *Environ. Sci. Technol.* **1985**, 19, 155.

[32] J. P. Alarie, T. Vo Dinh, *Talanta*, **1991**, 38, 529.

[33] G. E. Neal; *Toxicol. Letters*; **1995**, 82/83 861-867.

[34] J. S. Wang, J. D. Groopman, *Mutation Research*, **1999**, 424, 167-181.

[35] J. Dai, M. W. Wright, R. A. Manderville, *J. Am. Chem. Soc.* **2003**, 125, 3716-3717.h

[36] C. J. Mirocha, C. M. Christensen, G. H. Nelson, *Appl. Microbiol.* **1967**, 15, 497-503.

[37] W. T. Shier, *Revue Med. Vet.* **1998**, 149, 599-604.

[38] Food and Agricolture Organization (**2004**). Worldwide regulations for mycotoxins in food and feed in 2003. FAO Food and Nutrition Paper 81. Food and Agriculture Organization of the United Nations, Rome, Italy.

[39] World Health Organization (**2002**) Evaluation of certain mycotoxins in food. Fifty-sixth report of the Joint FAO/WHO Expert Committee on Food Additives, WHO Technical Report Series 906, World Health Organization, Geneva, Switzerland, p. 70.

[40] WEB FONTS: www.accessexcellence.org/AB/GC/antibodies.it.

[41] H. Joshua, *J. Chromatogr. A*, **1993**, 654, 247.

[42] A. Capeda, C. M. Franco, C. A. Fente, B. I. Vazquez, J. L. Rodriguez, P. Progno, G. Mahuzier, *J. Chromatogr. A*, **1996**, 721, 69-74.

[43] C. M. Franco, C. A. Fente, B. I. Vazquez, A. Capeda, G. Mahuzier, P. Prognon, *J. Chromatogr. A*, **1998**, 815, 21-29.

[44] J. Gilbert, *Nat. Toxins*, **2000**, 7, 347-352.

[45] S. Sforza, C. Dall'Asta, R. Marchelli, *Mass Spectrom. Rev.* **2006**, 25, 54-76.

Chapter 2

Aim of the Work

A great number of food matrices have been recognized as susceptible to mycotoxin contamination. The toxicological effects of these mycotoxins when ingested by animal and humans and the possibility to find them in finished products are causing great concern among producers and consumers. Thus, the availability of methods for screening foodstuffs is essential and has moved the scientific commnity in the direction of discovering and developing new convenient, reproducible and sensitive methods of detection and decontamination.

Since several mycotoxins (such as aflatoxins, ochratoxins, zearalenones, etc.) are naturally fluorescent, modified and unmodified cyclodextrins may be used as fluorescence enhancers on account of their ability to form inclusion complexes as with organic guests. Indeed, the inclusion of a mycotoxin (completely or partially) into the cyclodextrin cavity, can afford an apolar surrounding around the complexed chromophore and induce an increase of its fluorescence (Figure 2.1).

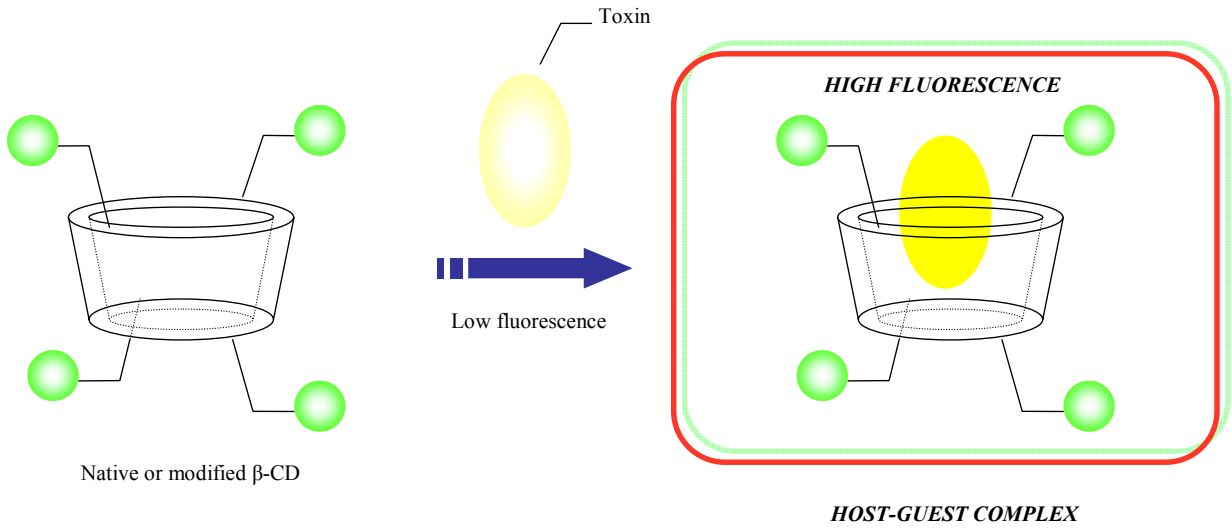

Figure 2.1: CDs as mycotoxins fluorescence enhancer.

The aim of this thesis is to study the interactions of mycotoxins (aflatoxins, ochratoxin A and zearalenone) with cyclodextrins in order to use them as receptors of mycotoxins for analytical purposes (in particular for fluorescence enhancement) but also eventually for detoxifying food and feed matrices.

In particular, the work reported in this Ph. D. thesis was developed according to the following lines:

- Study of the interactions between mycotoxins and cyclodextrins by molecular modelling: docking techniques and the HINT scoring function were used to rationalize the data previously obtained by spectroscopic methods regarding aflatoxins and a series of cyclodextrins and to predict the feasibility of inclusion for ochratoxin A.

- Synthesis of β-cyclodextrins modified also on the base of the results obtained with the molecular modelling, in order to obtaining a good receptor for the recognition of ochratoxin A. Since this toxin is potentially a mono or a di-anion, we planned to insert one, two or a number of positively charged groups, in particular the ammonium and guanidinium ions, on the upper or on the lower rim of the β-cyclodextrin.

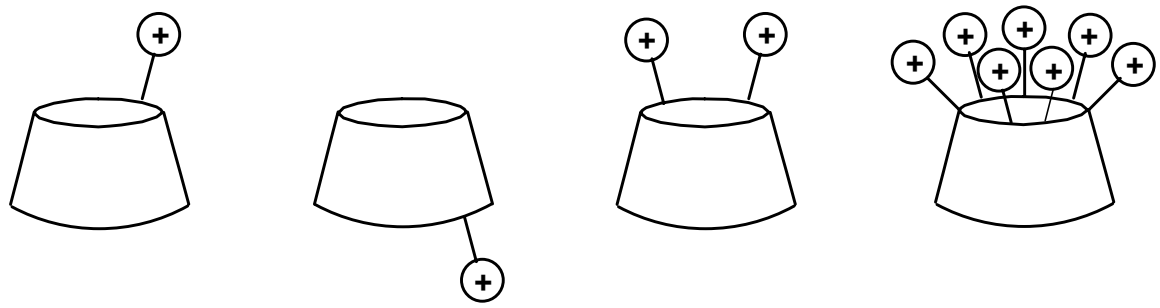

Figure 2.2: Design of different β-CD derivatives as ochratoxin A receptors.

- Spectroscopic studies of the complexation of ochratoxin A with the charged cyclodextrins.

- Spectroscopic studies of the complexation of zearalenone with β-cyclodextrin.

Chapter 3

Investigating CD-Mycotoxin Interactions using a "Natural" Force Field

3.1 General

Computational chemistry is a multidisciplinary area of science transcending traditional barriers separating biology, chemistry, physics and mathematics. Because theory can help to rationalize experimental observation, to provide information not amenable to experimentation, and even to make prediction concerning the outcome of future experiments, it is becoming more widely accepted by experimental scientists as a valuable tool for their studies.[1] One aspect of applied theory involves molecular simulations at the atomic level. This is sometimes called "molecular modeling", and it has been warmly embraced by chemical community and with good reasons; much can be derived from it.

The use of computational chemistry in the area of cyclodextrins have been rather limited so far. The reason is not a lack of interest but it is rather due to the fact that cyclodextrins are relatively large, flexible molecules which are usually studied experimentally in aqueous solution. This makes computation almost prohibitive, or forces to introduce so many assumptions and imposes so many restrictions as to become unrealistic. The size of cyclodextrins makes application of quantum mechanics difficult even when symmetry conditions are imposed. Because these macrocycles have many routable bonds, an enormous number of conformational states exist. So, even when computational expedient methods such as molecular mechanics are used, difficulties arise because one needs to perform a complete conformer search to locate all populated states at room temperature. Moreover, cyclodextrins are usually studied experimentally in aqueous media, an environment that until recently has been the bane of computational chemistry, creating a major hurdle that most computational chemists were not willing to approach.

Nevertheless, on account of the fact that availability of instruments able to carry out these calculation in a reasonable time period, at the end of 19th century, a significant increase of the computational studies occurred leading to a deeper understanding of the structure, dynamics and chemical behaviour of cyclodextrins.

3.2 Structure and objectives of the chapter

In this chapter a molecular simulation applied to cyclodextrin-mycotoxin interactions using a "natural" force-field is described. In particular, docking techniques and the HINT function (Idropathic Interactions) programme were used to simulate the interactions of aflatoxin B_1 (AFB_1)and ochratoxin A (OTA) with β- and γ-cyclodextrin. To this aim, after a brief description of the HINT scoring function and how the docking programs worked, the present chapter will be divided in two different parts, each one concerning the two mycotoxins. In the first part, since a model of inclusion of aflatoxins with cyclodextrins had been previously proposed by Dall'Asta et al.[2] on the base of spectroscopic techniques, the molecular modelling approach to the same mycotoxins was used in order to evaluate the docking techniques and the HINT function to explain cyclodextrin-mycotoxin interactions. A consistency between these two different studies can be considered as a test of this new modelling approach for explaining noncovalent interactions involved in inclusion phenomena. In the last part of this chapter, data obtained applying the "natural" force field to OTA are discussed. The exhaustive comprehension of the OTA-cyclodextrin inclusion mechanism may lead to the design of chemosensor devices for the more sensitive and accurate detection of OTA, even at very low concentrations, minimizing the risk of false negative/positive results which may be associated with ELISA tests. Moreover, chemosensors based on a luminescence response may be integrated into microarray systems, which could be applied for early detection of post-harvest contamination, providing an easy-to-use tool for mycotoxin analysis.

3.3 Computational approach

3.3.1 The "natural" HINT force field.

As it has been mentioned above, many computational studies of guest inclusion in cyclodextrins, which are well reviewed by Lipkowitz,[3] have been recently reported over the past several decades. The vast majority of these studies reported molecular dynamics simulations or molecular mechanical calculations, based on widely used Newtonian force fields.[4] Very recently, quantum chemistry calculations on AFB_1-β-cyclodextrin inclusion complex have also been reported.[5]

In this thesis, instead, we intended to propose a different approach to investigate the mode of AFB_1, and OTA inclusion into cyclodextrins. The analyses were carried out using two docking packages, GOLD[6] and Autodock[7] and the HINT program as a post-process scoring function.

HINT is a "natural" force field, based on experimentally determined $LogP_{octanol/water}$ values.[8] High HINT scores are indicative of a good interaction (negative ΔG^0), while low scores are

indicative of weak interactions between the examined molecules. HINT is normally applied to predict the ΔG^0 of binding for biological interactions such as protein-ligand, protein-protein, protein-DNA and protein-water.[8a, 9] Therefore, we believe that HINT could be extremely useful in computational studies of host-guest complexation. Indeed, because $LogP_{o/w}$ is derived from a salvation/desolvation experiment, HINT implicitly includes entropy contribution arising from water molecule displacement during complex formation, whereas the classical molecular mechanics approach usually omits, or only partially evaluates, salvation/desolvation events.[8b] It follows that HINT may be particularly suitable for the evaluation of entropically driven hydrophobic effects, which are among the main driving forces of cyclodextrin inclusion phenomena.[3, 10]

3.3.2 Docking studies.

β-cyclodextrin, γ-cyclodextrin, AFB_1, and OTA structures were taken from Cambridge Structural Database (CSD) and prepared for docking as will be described later in the experimental part of this chapter. Docking was performed using GOLD and AutoDock. Both programs allow full ligand flexibility but consider the host as rigid, therefore the cyclodextrin molecule geometry was maintained fixed in the crystal conformation reported in CSD. All the 50 docking poses generated by GOLD and the 100 generated by Autodock for each ligand were re-scored with HINT. Among the 50 solutions generated by GOLD for each mycotoxin-cyclodextrin complex, two were carefully analyzed. The solution with the best energy assigned by the ChemScore scoring function[11] included within the GOLD package (for convenience it will refers to it as a best ChemScore), and the one with the highest HINT score (best Hint/GOLD) was selected. Similarly, of the 100 solutions proposed by AutoDock, the one with the AutoDock best energy and the one with the highest HINT score were selected (it will refers to them as best AutoDock and best HINT/AutoDock, respectively).

A consensus approach, combining different docking tools and scoring functions based on different concepts, should allow for a more reliable analysis of the inclusion phenomena, overcoming errors and approximations of each single molecular modelling tool.

3.4 Studying of AFB_1-CD interactions

3.4.1 Previous fluorescence experiments.

Aflatoxins have a rigid, cyclic oxygenated structure with a high degree of conjugation which provides a low native fluorescence (Figure 3.1).[12]

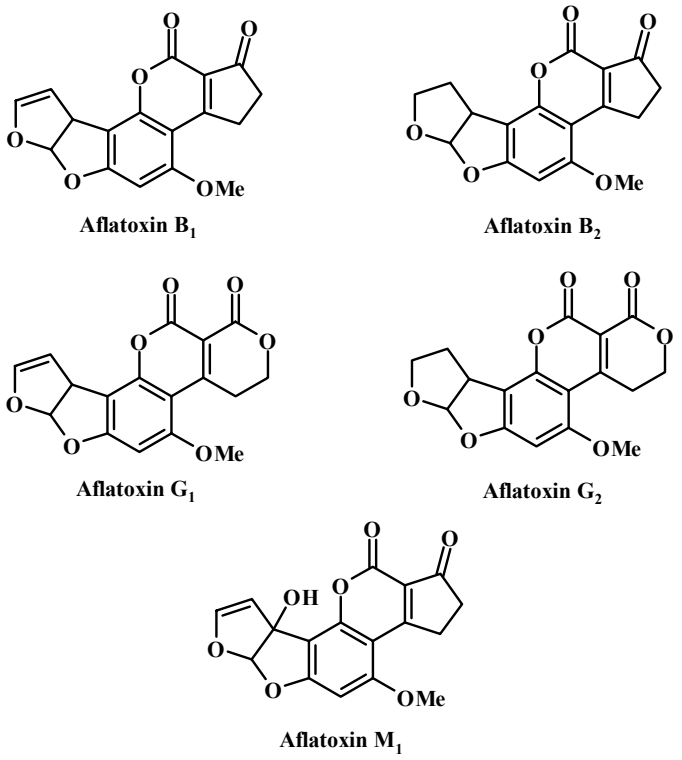

Figure 3.1: Structures of aflatoxins AFB_1, AFB_2, AFG_1, AFG_2 and AFM_1.

AFB_1 and AFB_2 are characterized by a blue fluorescence (λ_{ex} = 365 nm, λ_{em} = 440 nm), while AFG_1 and AFG_2 give a green fluorescence (λ_{ex} = 365 nm, λ_{em} = 460 nm) on account of a cyclopentenone ring versus an unsaturated δ-lactone ring in the structure. Differences are found also in the unsaturated or saturated terminal furan ring: the saturated derivatives, AFB_2 and AFG_2, have a higher fluorescence quantum yield than the unsaturated AFB_1 and AFG_1. Aflatoxin M_1 (AFM_1) is the 4-hydroxylated metabolite of AFB_1 produced by hepatic hydroxylation in mammalian species and it can be found in milk and dairy products.[13]

As reported in chapter 1, different analytical methods are currently used for AFs screening: immunoassay methods are well suited for a rapid, routine screening, although the detection of AFM_1 in milk in a range required by the European Union (50 ng/l) is affected by significant errors due to the low reproducibility and the sensitivity of the ELISA technique. Chromatographic methods, in particular reversed-phase liquid chromatography with fluorescence detection, are

currently the most commonly used methods of detection and are particularly suited for the analysis of complex matrices.

Native fluorescence of these toxins may be enhanced by the use of cyclodextrins since the inclusion of a fluorophore into the apolar cavity generally increases the fluorescence emission by protecting the toxin from the quenching effect exerted by water.[14] β-cyclodextrin, in particular, has been used as post-column additive[15] or directly dissolved in the chromatographic mobile phase.[16]

In order to evaluate which cyclodextrin induced the highest AF fluorescence enhancement, a spectroscopic screening of native cyclodextrins (α-CD, β-CD and γ-CD) and variously substituted cyclodextrins were carried out in aqueous solutions by the Parma group.[2, 16] Most of the tested cyclodextrins induced an enhancement in the fluorescence emission spectra of AFs and a blue shift in the emission maximum wavelength (from 440 nm to 435 nm), both phenomena suggesting a strong interaction between AF and cyclodextrins. In particular, a blue shifts of 3-6 nm in the emission maximum were similar to those recorded for AFs in media less polar than water, as methanol or ethanol, and were consistent with a lower polarity of the AF environment, thus suggesting an eventual inclusion phenomenon.

The AF fluorescence enhancements due to addition of cyclodextrins at a molar ratio AF:CD = $1:10^5$ are reported in Table 3.1.

Table 3.1: Fluorescence enhancements of AFs in the presence of CDs.(*) From ref. [2].

Cyclodextrin		$F_n = F/F_0$				
		AFB_1	**AFG_1**	**AFM_1**	**AFB_2**	**AFG_2**
N	α-CD	5.7 ± 0.1	6.5 ± 0.3	1.8 ± 0.6	1.0 ± 0.1	1.0 ± 0.1
	γ-CD	2.5 ±.0.3	1.7 ± 0.1	1.1 ± 0.1	1.05 ± 0.02	1.0 ± 0.2
	β-CD	11.6 ± 0.2	10.7 ± 0.2	1.7 ± 0.1	1.30 ± 0.03	1.06 ± 0.05
	TRIMEB	3.8 ± 0.7	2.4 ± 0.2	1.7 ± 0.1	1.1 ± 0.2	1.06 ± 0.06
	DIMEB	14.5 ± 0.5	21.0 ± 0.3	2.9 ± 0.1	1.32 ± 0.06	1.2 ± 0.1
	Hyp-β-CD	12.3 ± 0.4	8.1 ± 0.6	1.1 ± 0.1	0.98 ± 0.07	1.28 ± 0.02
	Hyp-γ-CD	1.5 ± 0.1	4.7 ± 0.5	2.5 ± 0.1	1.12 ± 0.02	1.0 ± 0.2
PC	MA-β-CD	7.5 ± 0.9	16.5 ± 0.7	3.6 ± 0.1	1.37 ± 0.04	1.11 ± 0.04
	TMA-β-CD	4.2 ± 0.2	12.1 ± 0.1	1.5 ± 0.1	1.13 ± 0.02	1.01 ± 0.01
NC	SBE-β-CD	6.5 ± 0.2	10.0 ± 0.6	1.1 ± 0.1	0.99 ± 0.03	1.15 ± 0.07
	S-β-CD	15.3 ± 0.5	3.4 ± 0.2	1.3 ± 0.2	1.4 ± 0.1	1.2 ± 0.1
	CM-β-CD	13.5 ± 0.4	8.3 ± 0.2	1.6 ± 0.04	1.26 ± 0.07	1.15 ± 0.07
	β-CD-Su	**27.4 ± 0.5**	**13.9 ± 0.5**	**3.01 ± 0.03**	**1.21 ± 0.05**	**1.2 ± 0.2**
	β-CD-Su (**)	**63.0 ± 0.2**	**53.9 ± 0.5**	**10.1 ± 0.1**	**2.0 ± 0.1**	**2.24 ± 0.03**
Z	ZW-β-CD	7.87 ± 0.1	17.4 ± 0.1	3.4 ± 0.2	1.4 ± 0.3	1.02 ± 0.02

(*) The entire names of the CDs are reported in the experimental section.

Conditions: molar ratio AF:CD = $1:10^5$, except (**) molar ratio AF:CD $1:10^6$; λ_{ex} = 365 nm for AFB_1, AFG_1, AFB_2, AFG_2 and λ_{ex} = 360 nm for AFM_1; $\lambda_{MAX\ (em)}$ = 425 nm for AFB_1, AFG_1, AFB_2 ,AFG_2 and $\lambda_{MAX\ (em)}$ = 435 nm for AFM_1; both excitation and emission slits were 15 nm. N = neutral CDs; PC = positively charged CDs; NC = negative charged CDs; Z = zwitterionic CDs.

The higher natural fluorescence intensity of saturated AFB_2 and AFG_2 is not greatly affected by cyclodextrins, whereas the lower natural fluorescence of AFB_1 and AFG_1 are greatly enhanced by the addition of the cyclodextrins (up to 60 times) and that of AFM_1 is increased up to 10 times under the same conditions. Only β-cyclodextrin seems to have an ideal cavity size to accommodate aflatoxins, while the α-cyclodextrins cavity is too small and the γ-cyclodextrin cavity seems to be too large and too flexible to give stable inclusion complexes. On the other hand, the functionalized cyclodextrins, especially the neutral 2-hydroxypropyl-β-CD (DIMEB) but in particular the negative charged succinyl-β-cyclodextrin (β-CD-Su) induce very significant fluorescent enhancement for AFB_1 and AFG_1.[2]

The emission spectra of AFB_1 in absence and in the presence of β-CD, DIMEB and β-CD-Su is reported in Figure 3.2 where the highest fluorescence increment was observed with β-CD-Su which can be used at high concentration.

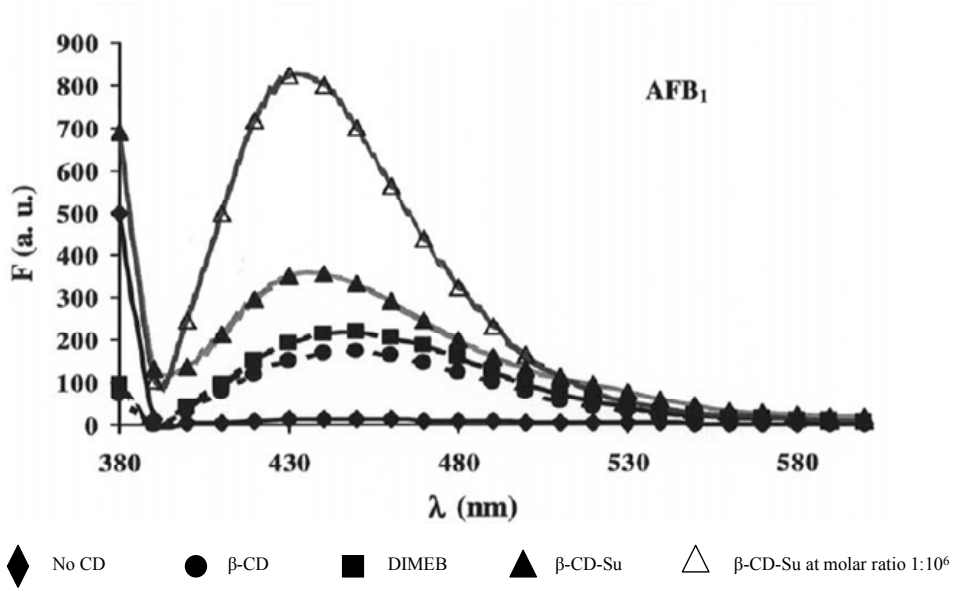

Figure 3.2: Emission spectra of AFB_1 in the absence and in the presence of CDs, molar ratio AF:CD = $1:10^5$ and β-CD-Su at a molar ratio AF:CD = $1:10^6$. From ref. [2].

Once obtained evidence for the fluorescence enhancement induced by cyclodextrins, an inclusion model was proposed on the basis of titration and competitive experiments with adamantanecarboxylic acid (ACA) and fluorescence quenching by KI.

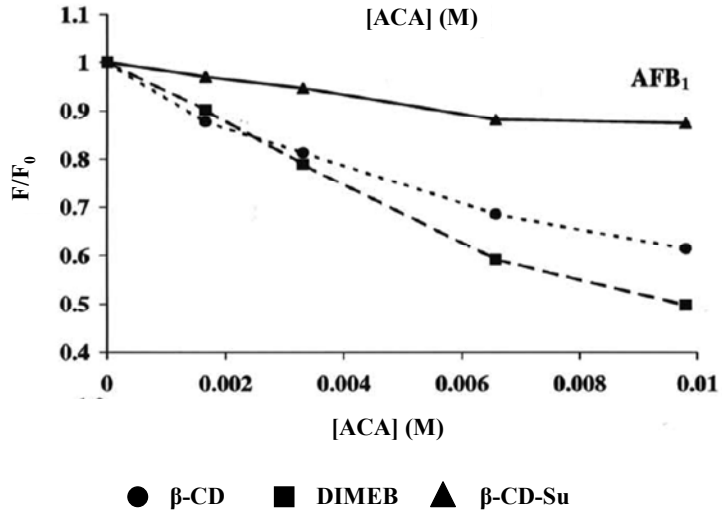

Figure 3.3: Variation of the fluorescence intensity of AFB_1 (10^{-7} M) in the presence of CDs (10^{-2} M) upon addition of ACA. From ref. [2].

As shown in Figure 3.3, addition of increasing amounts of ACA to the AFB_1-cyclodextrin aqueous mixtures caused a progressive decrease of the fluorescence intensity of AFB_1, consistently with an increasing exposure of the toxin structure to the water solution. In particular, in the presence of β-CD-Su, the ability of ACA to displace the guest from the cyclodextrin cavity was less efficient.

Fluorescence quenching experiments with KI were also performed; KI was chosen as quencher since it does not form inclusion complexes with the cyclodextrin cavity. If the AFB_1 is included in the cavity, then it should be protected from the action of the quencher.

The quenching efficiency was evaluated by the Stern-Volmer equation; the Stern-Volmer plots of AFB_1 quenching in the absence and in the presence of β-CD, DIMEB and β-CD-Su is reported in Figure 3.4.

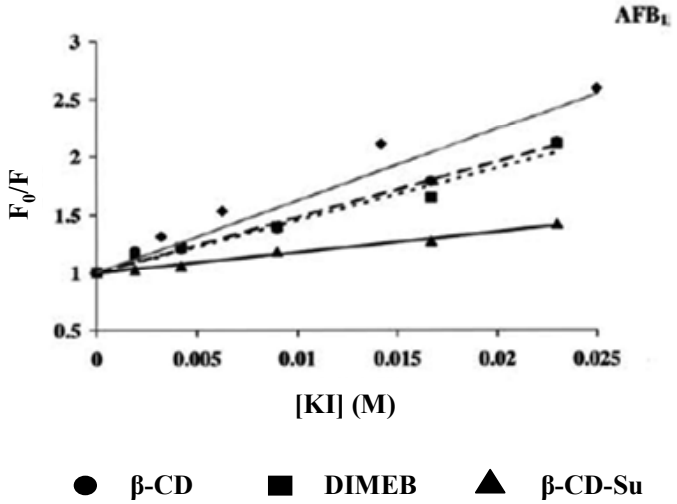

Figure 3.4: Quenching effect of KI on the fluorescent intensity of AFB_1 (10^{-7}). F_0 is the native fluorescence, F is the measured fluorescence.

The plot of F_0/F vs [KI] in the presence of cyclodextrins showed good regression coefficients and the same trend was observed, not only for AFB_1, but also for each others AFs (β-CD-Su>DIMEB>β-CD).

In conclusion, therefore, all data obtained by spectroscopic studies suggest that aflatoxins and cyclodextrins give rise to a host:guest inclusion complex. Although β-cyclodextrins resulted a good fluorescence enhancers, from the data obtained it seems that functional groups linked to the upper or lower rim of cyclodextrins greatly influence the intensity of fluorescence emission, favouring the inclusion of the AFs in the cavity. Moreover, the higher fluorescence enhancements observed in the presence of β-CD-Su might due to its higher solubility in water, so that it can be used at higher concentrations, thus increasing the amount of the complex.

3.4.2 Computational studies.

In this section the results obtained applying the docking packages (GOLD and AutoDock) and the HINT function to the AFs-cyclodextrin (β- and γ-cyclodextrin) interactions are reported to investigate the ability of this new modelling approach for studying noncovalent interactions generally involved in mycotoxins-cyclodextrin inclusion phenomena.

3.4.2.1 Predicted binding modes of AFB_1 in β-CD and in γ-CD.

In the case of AFB_1 in the presence of β-cyclodextrin, the four best solutions selected by the scoring functions described above exhibit the furan moiety of AFB_1 inserted inside the cyclodextrin cavity, with the coumarinic ring protruding into the solvent through the wider edge of the truncated cone (Figure 3.5).

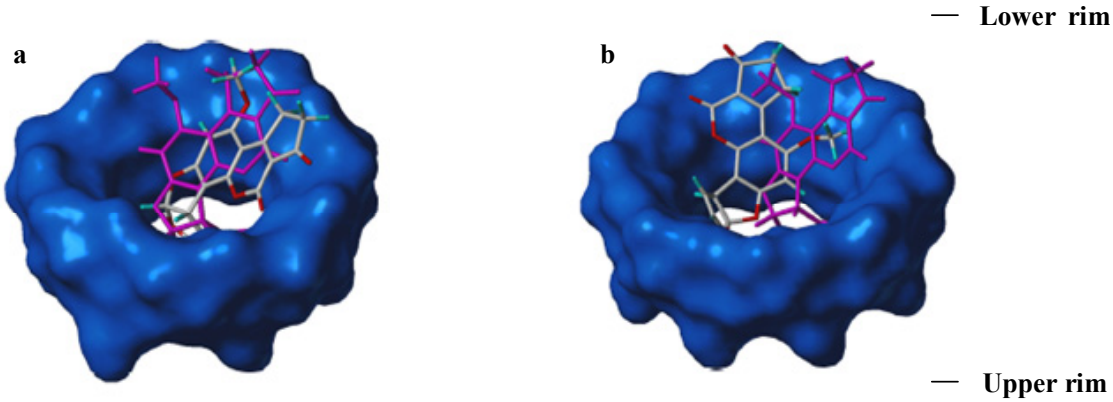

Figure 3.5: Illustration showing the predicted inclusion modes of AFB_1 in β- and in γ-cyclodextrins. The Connolly surface of the host (CD), built using Sybyl MOLCAD tools, is coloured blue, while guest molecule (mycotoxins) are represented in capped sticks. a) Best HINT/GOLD and best ChemScore (magenta) for AFB_1 in β-cyclodextin. b) Best HINT/AutoDock and best HINT/GOLD (magenta) for AFB_1 in γ-cyclodextrin.

As shown in Figure 3.5, the coumarin ring is bent towards the lower ring of the cavity, allowing for the hydrogen bonding between the AFB_1 carbonyl groups and the cyclodextrin secondary hydroxyl groups. Best AutoDock, best HINT/AutoDock and best HINT/Gold solutions do not display significant differences. On the other hand, the best ChemScore solutions, coloured in magenta, is rotated in comparison with the others. This difference is due to the formation of hydrogen bonds with different secondary hydroxyl groups, located on the cyclodextrin wider edge, but the predicted inclusion mode is the same, with the furan moiety of AFB_1 inserted in the cyclodextrin cavity. Therefore, the entrance of the mycotoxin from the lower rim is favoured not

only by a wider opening in comparison with the upper rim but also because of a greater number of hydroxyl groups located on the lower rim.

In the case of AFB_1 in the presence of γ-cyclodextrin, the best ChemScore and best HINT/GOLD solutions predicted an inclusion mechanism of the toxin in the cyclodextrin cavity analogous to the one proposed for the inclusion in the β-cyclodextrin. The furan moiety is located inside the cavity, while the coumarin ring and the cyclopentanone ring are more exposed to the solvent, allowing for hydrogen bonding between the carbonyl groups and the secondary hydroxyl groups located around the cyclodextrin lower rim (Figure 3.5 b, magenta). The best AutoDock and the best HINT/AutoDock solutions are very similar to each other, but show differences with the best ChemScore and the best HINT/GOLD. Their predicted binding mode also exhibits, in addition to the furan moiety, the coumarin phenyl ring and its methoxy group partially inserted inside the cavity (Figure 3.5 b).

The AutoDock and the ChemScore predicted free energy of binding (kcal mol^{-1}) and the HINT scores (the higher the HINT score the lower the predicted ΔG^0) for the best solutions selected by each program for AFB_1-β and γ-cyclodextrin complexes are reported in Table 3.2.

Table 3.2: HINT scores and predicted binding free energies (kcal mol^{-1}) calculated by ChemScore and AutoDock, relative to the best docking solutions selected for AFB_1-β-CD and AFB_1-γ-CD complexes.

	Best HINT/GOLD	**Best HINT/AutoDock**	**Best ChemScore**	**Best AutoDock**
AFB_1 β-CD	1496	979	-7.22	-6.98
AFB_1-γ-CD	1363	862	-6.21	-6.23

The calculation of the absolute binding free energies is very challenging, while the predicted free energy can be more properly used for the relative comparison between different binding poses of the same molecule ($\Delta\Delta G^0$). Furthermore, the HINT program is particularly suitable for the evaluation of the salvation/desolvation events, critical in inclusion phenomena. Therefore, discussion will focus mainly on HINT calculated free energies with particular attention to predicted $\Delta\Delta G^0$. Previous studies[8a] have reported that about 500 HINT score units correspond to a $\Delta\Delta G^0$ of 1 kcal mol^{-1} and this value has been shown to have general validity, being consistent with experimental findings in different heterogeneous systems.[8a, 9]

3.4.2.2 Post docking analysis.

Since water molecule displacement and hydrophobic interactions are probably the main driving forces for cyclodextrin inclusion phenomena (for more details, see chapter 1), a careful mapping of the hydrophobic-hydrophilic properties of the guest molecule has been performed using HINT. To this aim, Figure 3.6 shows the chemical structure and the HINT hydrophobic-polar contour map of AFB_1.

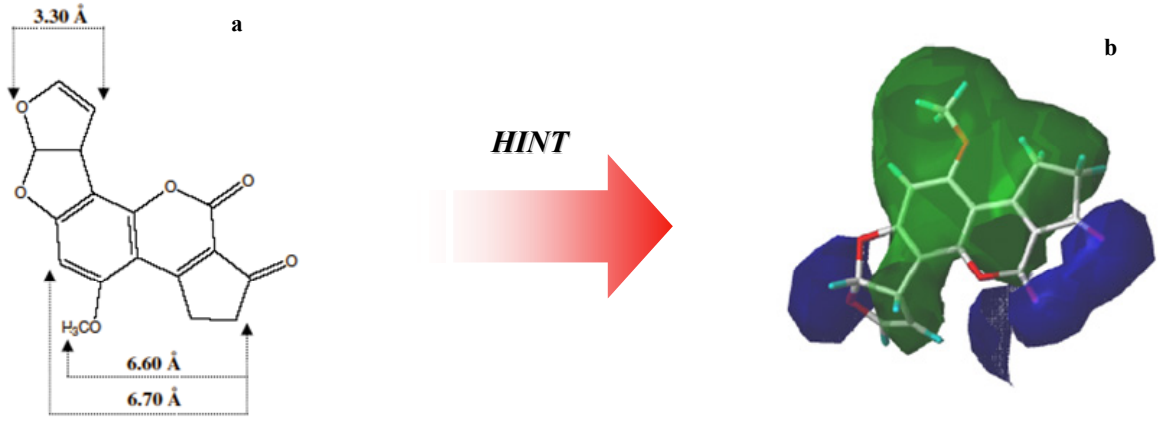

Figure 3.6: a) Chemical structure of AFB_1. The distances (atom centre to atom centre) between different extremities of the molecule are lighted. b) HINT hydrophobic-polar map of AFB_1. Hydrophobic regions are coloured green, while hydrophilic regions are coloured blue. The molecule is presented as capped stocks.

The region of AFB_1 exhibiting the hydrophobic character is constituted by the methoxy group and by the portion of the coumarinic and the cyclopentanone ring opposite to the carbonyl groups. However, the hydrophobic portion of the coumarinic and cyclopentanone rings cannot be included into the β-cyclodextrin cavity for steric reasons. As shown in Figure 3.6, indeed, the measured distances (centre atom to centre atom) between the extremities are beyond 6.40 Å and the additional increase in size given by van der Waals radius makes the inclusion of this part of AFB_1 inside the β-cyclodextrin impossible due to a cavity diameter of between 6.0 and 6.5 Å (Figure 3.7).[17]

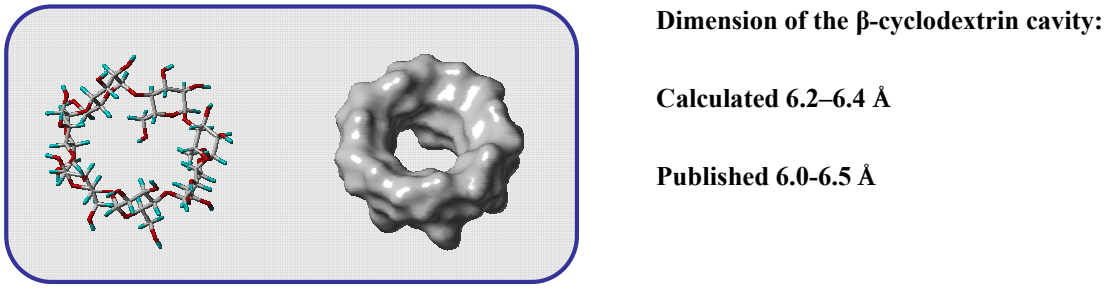

Figure 3.7: Cavity dimensions calculated for β-CD. The values are referred to the wider rim.

On the contrary, the furan moiety has a size that allows a good fitting into the cavity (the measured distance between the extremities is 3.30 Å) and it is also hydrophobic in the portion opposite to the oxygen atoms. These considerations support, therefore, the inclusion mechanism proposed by all the molecular modelling tools employed for AFB_1 inside the β-cyclodextrin. Furthermore, this mode of interaction is consistent with that previously proposed by Dall'Asta et al. using spectroscopic techniques[2] and with the observed enhancement of AFB_1 fluorescence in the presence of β-cyclodextrin.[16]

The situation, instead, is different in the case of inclusion of AFB_1 with the γ-cyclodestrin. γ-cyclodestrin exhibits a cavity diameter between 7.5 and 8.3 Å[17] which allows for a different way of binding for the mycotoxin, such as the one shown by the best AutoDock and the best HINT/AutoDock solutions. However, the assigned HINT score favours the HINT/GOLD best solutions (1363 for best HINT/GOLD vs 862 for best HINT/AutoDock). This difference of about 500 HINT score units corresponds to about -1 kcal mol^{-1}. Thus, among all the docking modes generated by GOLD and AutoDock, HINT considers the one with the furan moiety inserted into the γ-cyclodestrin cavity as the most energetically favourable, similar to that shown for the β-cyclodextrin.

The difference between the highest HINT score associated to the AFB_1 inclusion into the β-cyclodextrin (best HINT/GOLD) and the γ-cyclodextrin (best HINT/GOLD) is only 133 score units (~0.25 kcal mol^{-1}). AFB_1 inclusion into the β-cyclodextrin is predicted to be slightly more favourable than its inclusion in γ-cyclodextrin. This finding is in agreement with the free energy calculations made by AutoDock and ChemScore scoring functions, which did not predict $\Delta\Delta G^0$ beyond -1 kcal mol^{-1} (Table 3.2), but it seems to be in contrast with the experimental evidence which shows non significant enhancement of AFB_1 fluorescence in the presence of γ-cyclodextrin (see Table 3.3).

Table 3.3: Fluorescence enhancement recorded for AFB_1 with α-, β- and γ-cyclodextrin.

Complex	**F/F_0**
AFB_1-α-CD	5.7 ± 0.1
AFB_1-β-CD	11.6 ± 0.2
AFB_1-γ-CD	2.5 ± 0.3

The data are reported as F/F_0, where F_0 is the native fluorescence of the mycotoxin and F is the fluorescence obtained using the cyclodextrin (molar ratio: AF/CD = $1:10^5$).

It should be pointed out that calculated thermodynamic values may contain wide margins of error and this could explain disagreement between calculation and experimental data.[18]

In order to consider the inclusion phenomena under another point of view and, herein, to better rationalize all the results obtained by spectroscopic and computational studies, the analysis using the software GRID[19] has been performed to localize potential water sites within the complexes generated by docking. The GRID water probe did not identify energetically favourable water sites within the cyclodextrin cavity for the AFB_1-β-cyclodextrin complex, indicating that all the water molecules are displaced and the inclusion mechanism produces a perfect fit. On the contrary, the GRID analysis located water molecules in the cyclodextrin cavity of the AFB_1-γ-cyclodextrin complex. This funding suggests that AFB_1 inclusion into γ-cyclodextrin should be less energetically favoured than the inclusion into β-cyclodextrin, due to the fact that some water molecules are not displaced during ligand binding, because of the cavity's larger size. Therefore, it can be concluded that the γ-cyclodextrin cavity may not be able to protect included AFB_1 from the quenching effect exerted by water.

3.4.2.3 Circular dichroism experiments.

In order to obtain further evidence to validate the proposed inclusion model for the AFB_1-β-cyclodextrin complex, circular dichroism experiments were performed. The spectra were obtained for aqueous solutions of AFB_1, β-cyclodextrin and for AFB_1 + β-cyclodextrin. The results are reported in Figure 3.8.

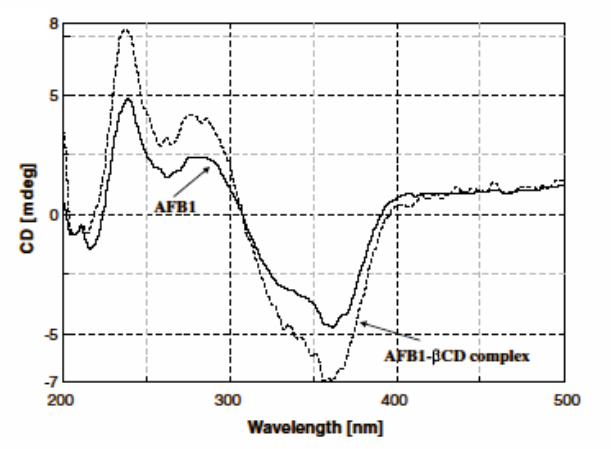

Figure 3.8: Comparison between the circular dichroism spectra recorded for AFB_1 and the inclusion complex AFB_1-β-CD at a molar ratio AF:CD =1:10^3.

Since the inclusion of the bifuranic system of AFB_1 into the β-cyclodextrin cavity allows for fluorescence enhancement due to the protection of the fluorophore from quenching, a variation in the circular dichroism spectrum would be expected.

As it can be seen from the spectra (the circular dichroism signal of the β-cyclodextrin was not significantly different from the baseline), both the bands in the circular dichroism spectrum

obtained for the complex were stronger than those observed for AFB_1 alone. These data suggest that the inclusion of the toxin in the β-cyclodextrin cavity involves the bifuranic systems, which is responsible for the absorption at 350-380 nm. These slight changes in the circular dichroism signal may be explained by several considerations. First, since the AFB_1-β-cyclodextrin binding constant is low (~10^{-3} M),[2] a strong interaction signal cannot be expected. Second, it was not possible to use the same molar ratio between the toxin and the cyclodextrin that was used in the fluorescence measurements (molar ratio: toxin/β-cyclodextrin $1:10^3$ instead to $1:10^5$) since the toxin concentration had to be increased in order to obtain good UV absorption, as required for the experiment and the cyclodextrin concentration could not be accordingly increased to the desired ratio for solubility reasons.

3.4.2.4 Conclusion about AFB_1-CD interactions.

In conclusion, we have tried to explain the inclusion mode of AFB_1 inside the β- and γ-cyclodextrins in the absence of available crystallographic and NMR structural data, using molecular modelling approaches imported from the field of protein-ligand docking. The proposed mode of inclusion is consistent with data previously reported on fluorescence enhancement for AFB_1 in the presence of β-cyclodextrin and supports the conclusions achieved by Dall'Asta et al.[2, 16] Moreover, since Log $P_{o/w}$ is derived from a solvation-desolvation experiment, the "natural" force field HINT, implicitly including entropic contributions arising from water displacement during complex formation, resulted to be extremely useful in the evaluation of entropically driven hydrophobic effects, which are among the main driving forces for cyclodextrin inclusion phenomena.

3.5 Computational studying of OTA-CD interactions

3.5.1 Preliminary fluorescence experiments.

Ochratoxin A (OTA) (Figure 3.9) is a mycotoxin produced by *Penicillium verrucosum*, *Aspergillus ochraceus* and other related species, which occurs in cereals, beans, ground nuts, spices, dried fruits and coffee beans.[20] OTA is nephrotoxic, hepatotoxic, immunosuppressive, teratogenic, and carcinogenic in several animal species and has been classified as a possible carcinogen for humans (Group 2B) by IARC.[21]

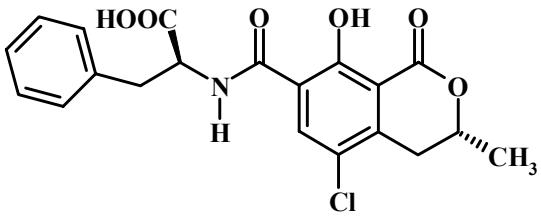

Figure 3.9: Chemical structure of ochratoxin A. Protonation constants: carboxylic group, $pK_a = 4.8$; phenol moiety, $pK_a = 7.1$.

The chemical properties of OTA are related to its structure: it is a derivative of isocoumarinic acid linked to L-phenylalanine through an amidic bond, with optical activity and natural fluorescence. The natural fluorescence is mainly due to the presence of the isocoumarinic moiety (the phenyl ring has a low fluorescence), and is enhanced by the presence of a rigid system due to the formation of an intramolecular hydrogen bond between the phenol moiety and the amidic carbonyl (α-form) or the esteric carbonyl group (β-form) (Figure 3.10).

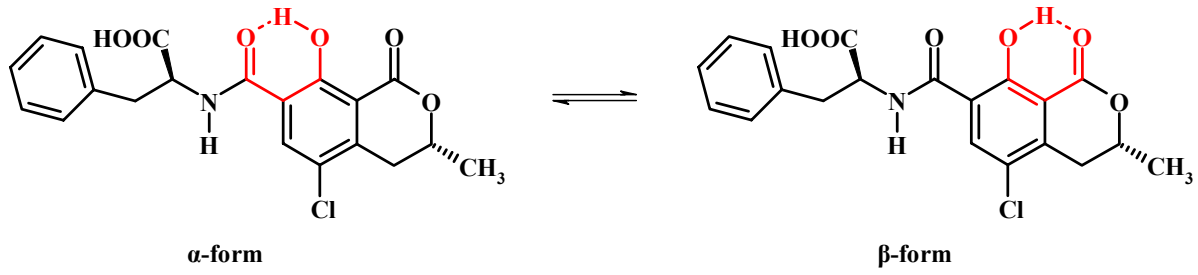

Figure 3.10: α- and β-form of OTA at acidic pH.

A preliminary study was performed to enhance the fluorescence of OTA using cyclodextrins since OTA could be included inside the cyclodextrin with its isocoumarinic portion as well as with the phenyl moiety. Therefore, α-, β- and γ-cyclodextrins were tested, in order to establish which

cyclodextrin gave the best enhancement of fluorescence (Table 3.4). Unfortunately none of theme gave a significant fluorescence enhancement when added to a neutral aqueous solution of the toxin.

Table 3.4: Fluorescence enhancement recorded for OTA with α-, β- and γ-CD at neutral pH.

Complex	F/F_0
OTA-α-CD	1.0 ± 0.1
OTA-β-CD	1.2 ± 0.2
OTA-γ-CD	1.0 ± 0.1

The data are reported as F/F_0, where F_0 is the native fluorescence of the mycotoxin and F is the fluorescence obtained using cyclodextrin (molar ratio: mycotoxin/CD, $1:10^5$).

Since fluorescence enhancement usually occurs when complexation inside the cyclodextrin protects the fluorophore from water quenching, the inclusion of the isocoumarinic portion, which is mostly responsible for OTA fluorescence, seems to be unlikely, based on spectroscopic data. For this reason, starting from these observations, the interaction between cyclodextrins (in particular β- and γ-cyclodextrin) and OTA was studied using molecular modelling.

3.5.2 Computational studies.

3.5.2.1 Predicted binding modes of OTA with β-CD and γ-CD.

The docking of OTA was carried out with the phenolic group in both the protonated and deprotonated forms, in agreement with its experimental pK_a of 7.1. The two forms did not display differences regarding the inclusion mechanism, while different binding free energies were predicted (Table 3.5 reports a mean ΔG^0 value).

Table 3.5: Hint scores and predicted binding free energies (kcal mol^{-1}) calculated by ChemScore and AutoDock, relative to the best docking solutions selected for different OTA-CD complexes.

	Best HINT/GOLD	Best HINT/AutoDock	Best ChemScore	Best AutoDock
OTA β-CD	3881	2553	-9.05	-5.77
OTA-γ-CD	1403	2292	-6.77	-5.50

When investigating the docking of OTA into β.cyclodextrin, different docking scoring combinations produced different predictions. The two suggested alternative modes of OTA inclusion into β-cyclodextrin are shown in Figure 3.11 a and b, respectively.

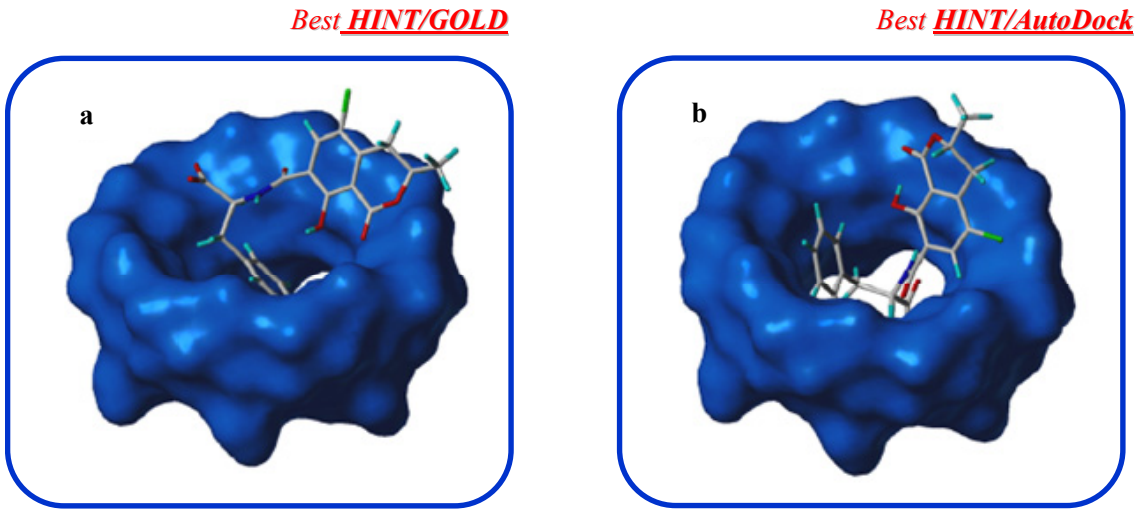

Figure 3.11: Illustration showing the predicted inclusion modes of OTA into the β-CD. The Connolly surface of the host (CD), built using Sybyl MOLCAD tools, is coloured blue, while the guest molecule (mycotoxin) is presented in capped sticks. a) Best HINT/GOLD for OTA in β-CD. b) Best HINT/AutoDock for OTA in β-CD.

The best ChemScore and the best HINT/GOLD (Figure 3.11 a) solutions show the phenyl ring of L-phenylalanine inserted inside the cyclodextrin cavity, while the carboxylic function and the isocoumarinic ring protrude into the solvent towards the wider opening. In this way the carboxylate on the phenylalanine residue and the phenol and ester carbonyl groups of the isocoumarinic ring can form hydrogen bonds with the secondary hydroxyl groups placed on the cyclodextrin lower rim.

The best AutoDock and the best HINT/AutoDock solutions (Figure 3.11 b), on the contrary, show the whole phenylalanine portion inserted inside the cyclodextrin cavity, with the carboxylate group exposed to the solvent through the narrower edge of the hollow truncated cone. However, once again the isocoumarinic ring is not placed within the cyclodextrin cavity, but is more exposed, allowing hydrogen bond formations between its carbonyl group and cyclodextrin secondary hydroxyl groups.

In the presence of γ-cyclodextrin, instead, best ChemScore, best HINT/GOLD and best HINT/AutoDock solutions are in agreement regarding the inclusion of OTA in this larger cyclodextrin.

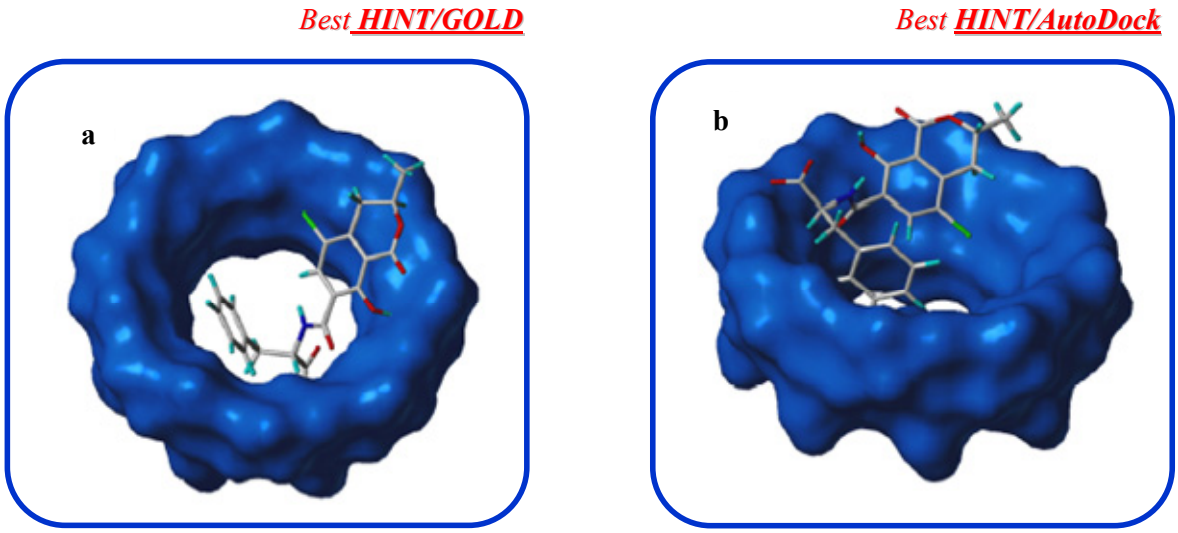

Figure 3.12: Illustration showing the predicted inclusion mechanism of OTA into γ-CD. The Connolly surface of the host (CD), built using Sybyl MOLCAD tools, is coloured blue, while guest molecule (mycotoxin) is presented with capped sticks. a) Best HINT/GOLD for OTA in γ-CD. b) Best HINT/AutoDock for OTA in γ-CD.

The predicted binding mode matches the one selected by AutoDock and HINT/AutoDock as best docking result for OTA inclusion in β-cyclodextrin. The phenylalanine portion is inserted inside the cyclodextrin cavity, with the exception of the carboxylate group, which is exposed to the solvent through the narrower opening of the γ-cyclodextrin. The isocoumarinic ring is exposed to the solvent, allowing for the hydrogen binding formation between its carbonyl group and the secondary hydroxyl groups located around the wider cyclodextrin opening (Figure 3.12 a). The best HINT/AutoDock solution shows, however, a very different behaviour (Figure 3.12 b). Only the phenylalanine phenyl group and, partially, the chlorine on the isocoumarinic ring are included inside the cyclodextrin cavity, while the entire molecule lies on the boundary of the cyclodextrin wider edge, allowing for hydrogen bond formation between OTA hydrophilic groups (carboxylate, carbonyl and phenol-OH) and the cyclodextrin hydroxyl groups.

3.5.2.2 Post-docking analysis.

Both of the two predicted mode of inclusion into β-cyclodextrin (Figure 3.11, a and b) can be explained at the light of the size and of the hydrophobic-polar balance of the OTA molecule (Figure 3.13).

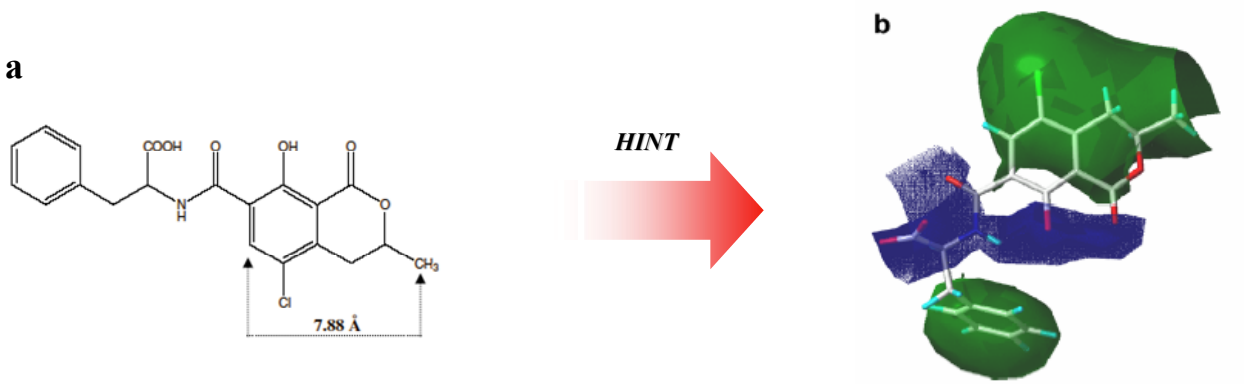

Figure 3.13: a) Chemically structure of OTA. The distances (atom centre to atom centre) between different extremities of the molecule are highlighted. b) HINT hydrophobic-polar contour map of OTA. Hydrophobic regions are coloured green, while hydrophilic regions are coloured blue. The OTA molecule is presented by capped sticks.

According to the HINT hydrophobic-polar contour map of OTA, it is possible to see that the entire hydrophobic portion of the isocoumarinic ring cannot be included into β-cyclodextrin for steric reasons. Indeed, the measured distance, centre atom to centre atom, between the aromatic hydrogen atom and a hydrogen belonging to the methyl group is of 7.88 Å (Figure 3.13 a). Therefore, the inclusion of the hydrophobic L-phenylalanine phenyl ring, which allows hydrogen bond formation between OTA hydrophilic groups and cyclodextrin secondary hydroxyl groups, seems to be realistic. Indeed, this predicted preferential inclusion mode exhibits a HINT score of 3881, against a score of 2553 assigned to the OTA conformation displaying the whole phenylalanine portion inserted inside the cyclodextrin cavity (corresponding to a $\Delta\Delta G^0$ of more than -2 kcal mol^{-1}). The lower predicted affinity for the latter solution may be due to the inclusion of the hydrophilic amidic portion of L-phenylalanine inside the hydrophobic cyclodextrin cavity, but also to a more difficult hydrogen bond formation between the OTA carboxylate group and the primary hydroxyl groups located around the narrower opening of the β-cyclodextrin cavity. These hydroxyl groups are not orientated toward the interior of the hole. The predicted $\Delta\Delta G^0$ between HINT best solutions for the OTA-β-cyclodextrin complex (best HINT/GOLD) and the AFB_1-β-cyclodextrin complex (best HINT/GOLD) is about -4.5 kcal mol^{-1}. This is consistent with a stronger binding of OTA than AFB_1 with the β-cyclodextrin, that can be justified by the higher number of hydrogen bonds formed by OTA and particularly by its negatively charged carboxylate group (which should contribute to stronger interaction with the cyclodextrin hydroxyl groups, due to the Coulombic reinforcement). This finding suggests that the experimentally observed lack of fluorescence enhancement for OTA in the presence of β-cyclodextrin is probably due to the nature

of the inclusion mechanism and not to weak binding. Indeed, the isocoumarinic ring responsible for OTA fluorescence is probably not included in the hydrophobic cavity and, thus, not protected by the quenching effect exerted by water.

Similarly, in the presence of γ-cyclodextrin, the predicted inclusion mechanism of OTA into the host is also not supportive for a possible fluorescence enhancement. Neither of the two alternative predicted modes of binding (best ChemScore, best AutoDock and best HINT/GOLD, shown in Figure 3.12 a and best HINT/AutoDock, shown in Figure 3.12 b) display the isocoumarinic ring inserted within the cyclodextrin cavity. Furthermore, it should be noticed that the calculated HINT scores are lower than those for OTA inclusion into β-cyclodextrin (Table 3.5). Therefore, the proposed model seems justified by the size of γ-cyclodextrin (diameter of 7.5-8.3 Å), which, although grater than β-cyclodextrin, is not wide enough to accommodate the isocoumarinic ring which bears a chlorine atom.

Also considering the water sites available inside the cavity by GRID analysis, no energetically favourable water sites within the β-cyclodextrin cavity were identified for the OTA-β-cyclodextrin complex, while the GRID water probe was able to detect different potential water sites within the cyclodextrin cavity of the OTA-γ-cyclodextrin complex. In a practical sense, herein, γ-cyclodextrin seems too small to include the isocoumarinic ring, but too large to produce a good fitting with the phenylalanine phenyl ring by displacement of all the water molecules.

3.5.2.3 Circular dichroism experiments.

As discussed above, molecular modelling simulations show that the complexation of OTA with β-cyclodextrin likely occurs through the inclusion of the phenylalanine residue and this model is in agreement with experimental fluorescence results: in the complex, the isocoumarinic nucleus is still exposed to solvent quenching, and thus, emission remains unchanged. Nonetheless, the inclusion of the phenyl ring should cause changes in the circular dichroism spectrum at 230-280 nm, which is the typical range of the phenylalanine UV absorption. For this reason, CD spectra could be an another test to verify the inclusion mechanism proposed by computational approach and fluorescence spectra.

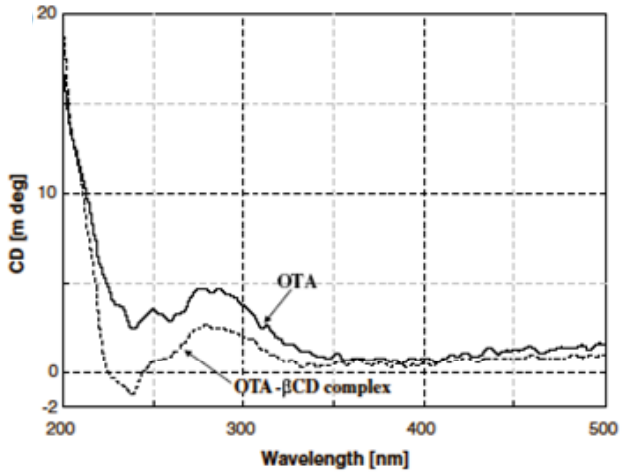

Figure 3.14: Comparison between the circular dichroism spectra recorded for OTA and the inclusion complex OTA-β-CD.

As shown in Figure 3.14, no significant differences exist between the signals of OTA alone and of OTA in the presence of the β-cyclodextrin. In particular, no differences are found in the range of the isocoumarinic moiety (330-380 nm), while only a small variation can be observed at 230-250 nm, where phenyl ring absorption occurs.

3.5.2.4 Conclusions about OTA-CD complexes.

The "natural" force field HINT has been applied to investigate the inclusion of OTA into β- and γ-cyclodextrins. According to the fluorescence spectra recorded for aqueous solutions of the toxin in the presence of β- and γ-cyclodextrin, no enhancement of fluorescence was detected. By the molecular modelling approach presented here, it is suggested for the first time that a binding between the phenylalanine portion of OTA and the cyclodextrin cavity may occur. In particular, the model obtained seems to be feasible since the predicted exclusion from the cavity of the isocoumarinic ring, the most fluorescence portion of the OTA structure, results the crucial factor for the lack of fluorescent enhancement. Moreover, the models here obtained may allow to design more specific cyclodextrins, opportunely functionalized in order to increase the affinity to the guest and allowing their use as chemosensors.

3.6 Experimental

The program Sybyl version 7.0 (Tripos, Inc., St. Louis, MO, USA; www.tripos.com), used in the present study, was installed on a FUEL Silicon Graphics workstation running o. s. IRIX 6.5. The program HINT 3.09 β test version was used as an add-on module within Sybyl. This version of HINT was developed by Prof. K. E. Kellog and can be obtained from eduSoft (eduSoft, LC, Ashland, VA, USA; www.edusoft-lc.com). The GOLD version 2.2 (CCDC, Cambridge, UK; www.ccdc.cam.ac.uk) and the AutoDock version 3.0 (SCRIPPS, La Jolla, CA, USA; www.scripps.edu) programs were installed on a dual Pentium processor, running o. s. Linux Red Hat Enterprise 3.0.

3.6.1 Reagents.

AFs and OTA standards were purchased from SIGMA. Doubly distilled water was produced using an Alpha-Q System Millipore. α-, β- and γ-CD were purchased from ACROS (Carlo Erba, Italy). Working solutions of mycotoxins (10^{-7} M) and of mycotoxins with cyclodextrins (10^{-2} M) were prepared by dissolving the proper amount of powder standard and cyclodextrin in water. These solutions are stable at −4 ◦C for a month. Decontamination of waste solutions and glassware was performed with sodium hypochlorite (10% aqueous solution) for 12 h.

3.6.2 Spectroscopic experiments.

Fluorescence spectra were recorded on a Perkin-Elmer LS55 instrument in a 0.2 x 1.0 cm quartz cell. The excitation wavelengths were 365 and 380 nm for AFB_1 and OTA, respectively. The emission scan was performed in the range 400-600 nm. Both emission and excitation slits were set at 15 nm. Each spectrum was recorded in triplicate. Circular dichroism spectra were recorded on a JASCO J-715 spectropolarimeter equipped with Peltier thermostat (measurements done at 25 °C): acquisition range 200-500 nm, accumulations 3, band width 1.0 nm, response 1s, scan speed 100 nm/min, quartz cells (0.1 x 1.0 cm) were used. All spectra were treated with the noise reduction software included in the program J-700 for Windows Standard Analysis, version 1.33.00.

3.6.3 Host and guest preparation for docking.

The three dimensional coordinates of β-cyclodextrin, γ-cyclodextrin, AFB_1 and OTA were taken from CSD and imported into the molecular modelling program Sybyl.

All structures were checked for chemically consistent atom and bond type assignment. Hydrogen atoms were added using Sybyl Build/Edit menu tools. To avoid steric clashes, added hydrogen atoms were energy-minimized using the Powell algorithm, with a convergence gradient of 0.5 kcal mol^{-1} for 1500 cycles. This procedure affected only non-experimentally detected hydrogen atoms.

3.6.4 Gold.

The CDs and the ligands were prepared for docking using Sybyl. All hydrogen atoms were added to the CDs and to the ligands and all water molecules were removed from the target structure. The input files for docking were generated in .mol2 format. We used a radius of 15.0 Å from the centre of the CD cavity to direct site location. For each of the genetic algorithm runs, a maximum number of 100,000 operations were performed on a population of 100 individuals with a selection pressure of 1.1. Operator weights for crossover, mutation and migration were set at 95, 95 and 10, respectively, as recommended by the software authors. The number of islands was set to 5 and the niche size was set to 2. 50 GA runs were performed in each docking experiment. The ChemScore fitness function, implemented in GOLD, was used to identify the better binding mode. ChemScore is an empirical scoring function.[22] The overall binding free energy is composed of several free energy terms (hydrogen bonding, hydrophobic interactions, entropic changes, etc.) and the coefficients of each term in the sum are derived from fitting to know experimental binding energies.

3.6.5 AutoDock.

The CDs were treated using the united atom approximation. Only polar hydrogens were added to the structure and atomic charges were then calculated using the Gasteiger method.[23] All water molecules were removed from the target structure. 60 x 60 x 60 Å affinity grids, centred on the CD cavity with 0.375 Å spacing, were calculated by use of Autogrid 3.0,[7] for each of the following atom types: C, A (aromatic C), N, O, S, H and Cl.

Only polar hydrogens were added to the ligands (AFB_1 and OTA) and Gasteiger charges were assigned. The rotatable bonds were selected via AutoTors.[7]

Lamarckian genetic algorithm (LGA) was selected for ligand conformational searching. LGA adds local minimization to the genetic algorithm, enabling modification of the gene population. The

following dockings parameters were used: trials of 100 dockings, population size of 100, random starting position and conformation, translation step ranges of 1.0 Å, rotation step ranges of 1.0 Å, elitism of 1, mutation rate of 0.02, crossover rate of 0.8, local search rate of 0.06 and 250,000 energy evaluations.

3.6.6 Hydropathic analysis.

HINT (Hydropathic Interactions) software was used as a post-process scoring function. All the 50 docking poses generated by GOLD and the 100 generated by AutoDock for each ligand were re-scored with HINT and the solution exhibiting the highest HINT score (the higher the HINT score, the lower the negative binding free energy variation), was selected as the best docking model for HINT. HINT first calculates Log $P_{o/w}$ (partition constant for 1-octanol/water) for each component of the complexes. The Log $P_{o/w}$ of a molecule is the sum of all hydrophobic atomic constants, **a**, for that molecule. HINT assigns to each interacting atom a partial Log $P_{o/w}$ value $\mathbf{a_i}$ and a Solvent Accessible Surface $\mathbf{S_i}$. For both CDs and ligands the partition were performed using the calculated method, an adaptation of the CLOG-P method of Leo.[24] The "essential" option was chosen to perform molecule partition. With this approach only polar hydrogens are treated explicitly.

Genetic algorithms fulfil the role of global search particularly well, but are not always suited for local optimisation.[7] To allow a more accurate evaluation of the binding free energy, a local optimisation of the ligand and the CD rotatable bonds, based on the HINT score, was performed after docking. This optimisation generally affected hydroxyl groups on the CDs.

3.6.7 Grid.

The GRID program (www.moldiscovery.com) was used to propose water molecules sites within host-guest complexes generated by docking. The standard water probe was applied over the region of interest, that is, a box measuring 15 x 15 x 15 Å centred on the ligand within the CD cavity. The grid spacing was set to 0.33 Å.

List of abbreviations used for CDs:

DIMEB: heptakis (2,6-di-O-Methyl)-β-cyclodextrin;
TRIMEB : heptakis (2,3,6-tri-O-Methyl)- β-cyclodextrin;
Hyp-β-CD: (2-hydroxypropyl)-β-cyclodextrin;
Hyp-γ-CD: (2-hydroxypropyl)-γ-cyclodextrin;
MA-β-cyclodextrin: 6-amino-6-deoxy-β-cyclodextrin
TMA-β-cyclodextrin: O-(2-hydroxy-3-thimethyl-ammonio-n-propyl)-β-cyclodextrin;
SBE-β-cyclodextrin: tetra (6-O-(sulfo-n-butyl))-β-cyclodextrin (substitution degree n = 4);
S-β-cyclodextrin: sulphated-β-cyclodextrin (randomly substituted, substitution degree n = 7-10);
CM-β-CD: carboxymethyl-β-cyclodextrin;
β-CD-Su: succinyl-β-cyclodextrin (randomly substituted, substitution degree n = 4-6);
ZW-β-CD: mono (6-δ-(glutamylamino-6-deoxy)-β-cyclodextrin.

Acknowledgments:

The docking experiments and the HINT program were performed under the supervision of Prof. Pietro Cozzini, Department of Biochemistry and Molecular Biology, University of Parma.

Communication:

The content of this chapter has been the object of a publication:
A. Amadasi, C. Dall'Asta, G. Ingletto, R. Pela, R. Marchelli and P. Cozzini; *Bioorg. Med. Chem.* **2007**, 15, 4585-4594.

[1] See the cover story: Computational Chemistry Becoming a "Must-Have" *Tool. Chem. Eng. News*, **1997**, May 12.

[2] C. Dall'Asta, R. Corradini, G. Ingletto, G. Galaverna, R. Marchelli, *J. Incl. Phenom. Macr. Chem.* **2003**, 45, 247.

[3] K. B. Lipkowitz, *Chem. Rev*. **1998**, 98, 1829.

[4] a) K. L. Yap, X. Liu, J. C. Thenmozhiyal, P. C. Ho, *Eur. J. Pharm. Sci*. **2005**, 25, 49; b) Y. Zheng, I. S. Haworth, Z. Zuo, M. S. Chow, A. H. Chow, *J. Pharm. Sci*. **2005**, 94, 1079.

[5] G. Ramirez-Galizia, R. Garduno-Juarez, M. G. Vargas, *Photochem. Photobiol. Sci*. **2006**, 6, 110.

[6] G. Jones, P. Willet, R. C. Glen, A. R. Leach, R. Taylor, *J. Mol. Biol*. **1997**, 267, 727.

[7] G. M. Morris, D. L. Goodsell, R. S. Halliday, R. Huey, W. E. Hart, R. K. Belew, A. J. Olson, *J. Comput. Chem*. **1998**, 19, 1639.

[8] a) P. Cozzini, M. Fornabaio, A. Marabutti, D. J. Abraham, G. E. Kellog, A. Mozzarelli, *J. Med. Chem*. **2002**, 45, 2469: b) G. E. Kellog, D. J. Abraham, *Eur. J. Med. Chem*. **2000**, 35, 651.

[9] a) F. Spyrakis, M. Fornabaio, P. Cozzini, A. Mozzarelli, D. J. Abraham, G. E. Kellog, *J. Am .Chem. Soc*. **2004**, 126, 11764; b) M. Fornabaio, F. Spyrakis, A. Mozzarelli, P. Cozzini, D. J. Abraham, G. E. Kellog, *J. Med. Chem*. **2004**, 47, 4507; c) D. J. Cashman, J. N. Scarsdale, G. E. Kellog, *Nucl. Acids Res*. **2003**, 31, 4410; d) J. C. Burnett, P. Botti, D. J. Abraham, G. E. Kellog, *Proteins*, **2001**, 42, 355; e) A. Amadasi, F. Spyrakis, P. Cozzini, D. J. Abraham, G. E. Kellog, A. Mozzarelli, *J. Mol. Biol*. **2006**, 358, 289; f) F. Spyrakis, P. Cozzini, C. Bertoli, A. Marabotti, G. E. Kellog, A. Mozzarelli, *BMC Struct. Biol*. **2007**, 7, 4.

[10] A. R. Katritzki, D. C. Fara, H. Yang, M. Karelson, T. Suzuki, V. P. Solov'ev, A. Vernek, *J. Chem. Inf. Comput. Sci*. **2004**, 44, 529.

[11] M. D. Eldridge, C. W. Murray, T. R. Auton, G. V. Paolini, R. P. Mee, *J. Comp. Aided Mol. Des*. **1997**, 11, 425.

[12] . Holcomb, D. M. Wilson, M. W. Truksess, H. C. Thompson, *J. Chromatogr*. **1992**, 624, 341.

[13] W. E. Steiner, K. Brunshweiler, E. Leimbacher, R. Schnaider, *J. Agric. Food Chem*. **1992**, 40, 2453.

[14] M. L. Vasquez, A. Capeda, P. Prognon, G. Mahuzier, J. Blais. *Anal Chim. Acta*, **1991**, 255, 343.

[15] a) C. M. Franco, C. A. Fente, B. I. Vazquez, A. Capeda, G. Mahuzier, P. Prognon, *J. Chromatogr. A*, **1998**, 815, 21-29; b) O. J. Francis, J. P. Kirschenheuter, G. M. Ware, A. S. Carman, S. S. Kuan, *J. Assoc. Off. Anal. Chem*. **1988**, 7, 725; c) A. Capeda, C. M. Franco, C. A. Fente, B. I. Vazquez, J. L. Rodriguez, P. Progno, G. Mahuzier, *J. Chromatogr. A*, **1996**, 721, 69-74.

[16] E. Chiavaro, C. Dall'Asta, G. Galaverna, A. Biancardi, E. Gamberelli, A. Dossena, R. Marchelli, *J. Chromatogr. A*, **2001**, 937, 31.

[17] T. Loftsson, M. E. Brewster, *J. Pharm. Sci*. **1996**, 85, 1017.

[18] M. Kontoyanni, L. M. McClellan, G. S. Sokol, *J. Med. Chem*. **2004**, 47, 558.

[19] P. J. Goodford, *J. Med. Chem*. **1985**, 28, 849.

[20] The third FAO/WHO/UNEP International Conference on Mycotoxins; MYC-CONF/99/5c, **1999**.

[21] a) W. T. Shier, A. C: Shier, W. Xie, C. J. Mirocha, *Toxicon*, **2001**, 39, 1435; b) H. S. Hussein, J. M. Brasel, *Toxicol*, **2001**, 167, 101.

[22] M. D. Eldridge, C. W. Murray, T. R. Auton, G. V. Paolini, R. P. Mee, *J. Comp. Aided Mol. Des*. **1997**, 11, 425.

[23] J. Gasteiger, M. Marsili, *Tetrahedron*, **1980**, 36, 3219.

[24] C. Hansch, A. J. Leo, In Substituent Constants for Correlation Analysis in Chemistry and Biology; Wiley: New York, N. Y. **1979**.

Charter 4

Synthesis of Positively Charged β-CD as OTA Receptors

4.1 General

The modification of cyclodextrins offers both enormous opportunities and challenges for chemists. Opportunities are provided by the fact that, through modifications, cyclodextrins can provide new molecules that can have different abilities ranging from enzyme-like activity[1] and receptor-like binding[2] to aesthetically pleasing molecules. Challenges are provided by the presence of the hydrophobic cavity and a large number of hydroxyl groups.[3] Since each hydroxyl group present at the 2-, 3- and 6-positions could be able to compete for the reagent, selective modification are extremely difficult. Moreover, the hydrophobic cavity often has a tendency to interfere with the plan of the chemist by complexing with the reagent to direct the reaction to unexpected place.[4]

Cyclodextrins are modified for a variety of reasons ranging from achieving solubility in a desired solvent to investigating the mechanism of enzyme-catalyzed reactions. The strategy for modifications depends on the purpose of the final product. For example, if a highly water soluble cyclodextrin is desired for application in a drug formulation, then a random conversion of hydroxyl groups to sulphate groups can be easily achieved and the product will have the desired solubility in water.[5] Similarly, if a cyclodextrin with a high solubility in organic solvent is desired, one can easily convert the hydroxyl groups to silyl ethers in a random fashion.[6] However, in both cases, the final product is not homogeneous and cannot be subjected to rigorous characterization. On the other hand, if an enzyme mechanism is to be investigated using cyclodextrin derivatives, then these compounds need to be homogeneous with a structure that is well characterized. Thus, several factors such as the number of substituents, the regiochemistry of the substitution, and the stereochemical changes that have taken place during the synthesis have to be established before the mechanistic information about the artificial enzyme can be reliably derived.

4.2 Methods for modifying CDs: an overview

4.2.1 Categories for synthetic strategies.

Methods for the selective modification of cyclodextrins can be divided into three categories: 1) the "clever" method, where the chemistry of cyclodextrin is exploited to get the desired product by the shortest route; 2) the "long" method, where a series of protection and deprotection steps have taken place in order to selectively reach the position which would otherwise not be selectively accessible; 3) the "sledgehammer" method, where cyclodextrin is indiscriminately reacted to give a mixture of products and then the desired product is painstakingly separated out from other isomers and homologues by chromatographic methods.

An example from the first category is the synthesis of 2-tosyl-β-cyclodextrin by reacting cyclodextrin with *m*-nitrophenyl tosylate.[4] In this synthesis, on account of the complexation property of the cyclodextrin, it is possible to direct the tosyl group to the secondary side. This avoid the natural tendency of cyclodextrin to react on its primary side and predominantly gives cyclodextrins substituted at the 2-position.

An example of the second category is the alkylation of the primary side,[7] which involves in sequence 1) protection of the primary side with silyl groups, 2) protection of the secondary side with acetyl groups, 3) desilylation of the primary side, 4) reaction of the primary hydroxyl group with an appropriate alkyl halide, and finally 5) deprotection of the secondary side to give the desired product. In this strategy, each reaction is carefully chosen to give a high yield and the product should be easily separated and purified. However, the overall yield of the final product is often very small.

An example of the third category is the ditosylation of the secondary side of cyclodextrins.[8] In this case, tosyl chloride is reacted with the cyclodextrin to give a mixture of products; this mixture is separated using reverse phase HPLC.

Given the choice among the three categories, one would always choose the first strategy because it is most productive and less time-consuming; however, a method in the first category is not always available when a modified cyclodextrin of a specific structure is needed.

4.2.2 Chemistry involved in methods for modification of CDs.

It is important to understand the various chemical factors that are involved in different methods of modification of cyclodextrins to be able to apply them for synthesis that have not yet been attempted. Two primary factors need to be considered in the chemistry of cyclodextrins for their modification, the nucleophilicity of the hydroxyl groups and the ability of cyclodextrins to form complexes with the reagents used. All modifications of cyclodextrins take place at the hydroxyl

groups. Since hydroxyl groups are nucleophilic, the initial reaction, which directs the regioselectivity and the extent of modification (mono, di, tri, etc.) of all subsequent reactions, is an electrophilic attack on these positions.

Of the three types of hydroxyl groups present in cyclodextrins, those at the 6-position are the most basic (and often most nucleophilic), those at the 2-position are the most acidic, and those at the 3-position are the most inaccessible.[9] Thus, under normal circumstances, an electrophilic reagent attacks the 6-position (**I** in Figure 4.1).

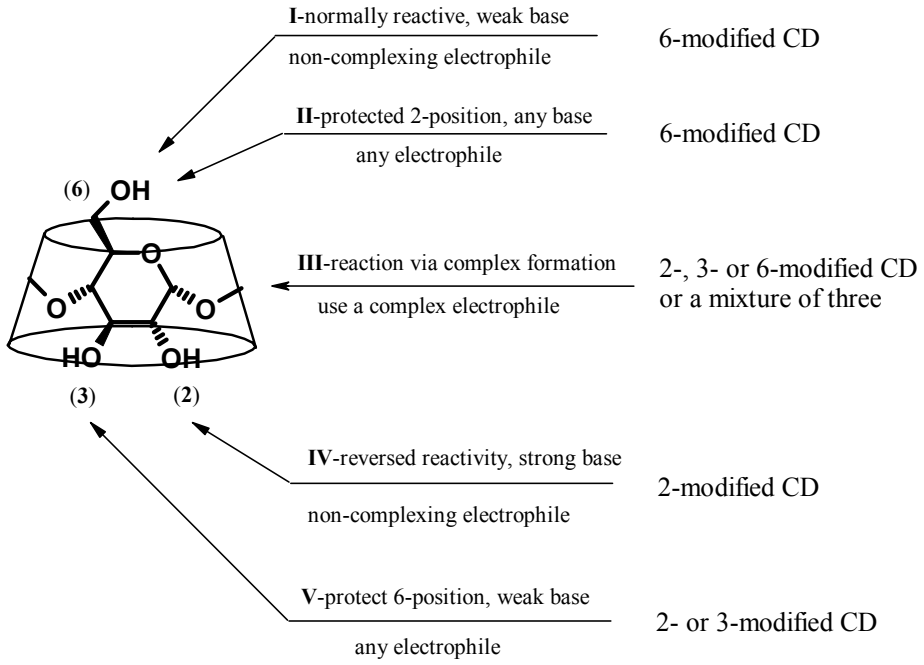

Figure 4.1: Overview of the methods for modification of cyclodextrins.[10]

It is important to recognize that more reactive reagents will attack the hydroxyl groups less selectively. Thus, more reactive reagents will not only react with hydroxyl groups at the 6-positions but also with those on the secondary side; whereas, less reactive reagents will react more selectively with the 6-position hydroxyl groups. An example of this is the less reactive reagent tert-butyldimethylsilyl chloride (TBDMSCl) will react selectively with the hydroxyl groups at the 6-positions,[11] while the more reactive reagent trimethylsilyl chloride (TMSCl) will react with all the hydroxyl groups indiscriminately.[12] Since the hydroxyl groups at the 2-position are the most acidic, they will be the first to be deprotonated.[13] The oxyanion thus formed is more nucleophilic than the protonated hydroxyl groups at the 6-positions (**IV** in Figure 4.1). However, this situation is complicated by proton transfers between these two positions which can lead to a product mixture consisting of modifications at the 2- as well as at the 6-positions.

An interesting factor affecting the chemistry of the hydroxyl groups is provided by the ability of cyclodextrins to form complexes (**III** in Figure 4.1). If the electrophilic reagent forms a complex with the cyclodextrin, then the orientation of the reagent within the complex introduces an additional factor in determining the nature of the product.[4] If the complex formed is very strong,

then the predominant product formed will be dictated by the orientation of the reagent within the complex. On the other hand, if the complex is weak, then the product formation will be directed by the relative nucleophilicities of the hydroxyl groups. It is also important to note that both solvents and the size of the cyclodextrin cavity play an important role in determining the strength and the orientation of the complex between the reagent and the cyclodextrin, as well as in affecting the product of the reaction. Even the most inaccessible hydroxyl groups at the 3-position can be modified using this property of cyclodextrins,[14] although a more generally strategy followed to produce 3-substituted cyclodextrin derivatives is based on the initially selective protection of the hydroxyls at the 2- and the 6-position.

A strategy used to avoid complications due to binding of the reagent and thus obtaining products which are not expected by their normal nucleophilicity, is to protect the hydroxyl groups and direct the incoming reagent exclusively to the other free hydroxyl groups. For example, if one protects the 2-position of the cyclodextrin, it is possible to direct the incoming electrophile to the 6-position (**II** in Figure 4.1). A specific example of this is the peralkylation of the primary side of the cyclodextrin in which the secondary side is first protected by esterification and then the primary side is reacted with alkyl halides.[11] Similarly, protection of the primary side enables one to direct the incoming electrophile exclusively to the hydroxyl groups at the 2-position (V in Figure 4.1). Pertosylation of this side has been achieved using this strategy,[15] and TBDMS is the most popular protecting group since it is easy to attach and easy to remove.[11, 16]

Generally, mono-, di-, tri- and permodifications refers to modification at respectively one, two, three and all hydroxyl groups at one site (either the 2-, 3- or 6-positions) of cyclodextrins. It is important to note that of the four types of modifications mentioned above, only di- and trimodifications give positional isomers. As shown in Figure 4.2 both α- and β-cyclodextrins give three (AB, AC and AD) disubstituted isomers. On the other hand, α- and β-cyclodextrins have respectively four (ABC, ABD, ABE and ACE) and five (ABC, ABD, ABE, ABF and ACE) trisubstituted positional isomers at the upper rim.

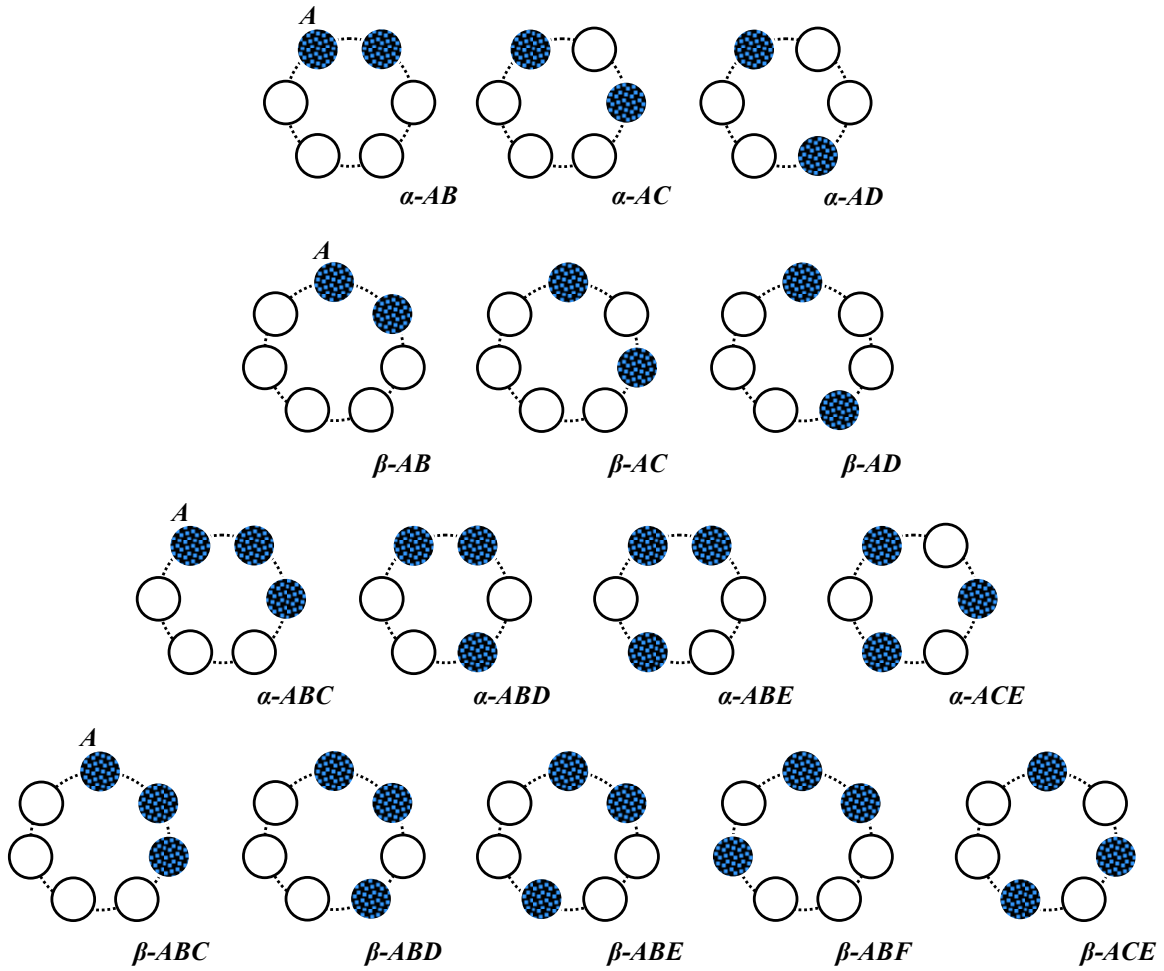

Figure 4.2: Possible positional isomers of di- and trimodified α- and β-CDs. From ref. [10].

Although the poly-functionalized cyclodextrin derivatives are very important in organic chemistry, their synthesis are quite difficult, in particular because of the formation of a mixture of different products that have to be separated by tedious chromatographic techniques as RP-HPLC. Statistical calculations suggest that disubstitution can produce 33 regioisomers in the case of β-cyclodextrins,[17] which indicates the enormous complexity of this process. Use of an oversized reagent like mesitylenesulfonyl chloride is not effective in limiting the number of substitution on the primary face to two or three.[18] As in sulfonation reactions in general,[19] these can also be plagued by substitution on the secondary side and exchange (of the sulfonates) with chloride ions present in the medium to further lower the yield of the final product. Toluenesulfonyl[20] or mesitylenesulfonyl[21] chlorides react with α-, β- or γ-cyclodextrin in pyridine and generate a mixture of bis(sulfonates) in a low yield which are then separated by HPLC. Reaction of tosyl chloride with cyclodextrins is reported to give a mixture of di-O-6[22], di-O-2[14] or di-O-3[23] derivatives along with other products. Despite all these difficulties, a variety of disulfonates are reported in the literature.[24]

A particular efficient method to obtain disubstituted sulfonates of cyclodextrins is by reaction of arenedisulfonyl chlorides with cyclodextrins to give AB, AC and AD isomers.[25] Although these disulfonyl chlorides give a mixture of regioisomers, they show distinct regiospecificity based on

their structure (Figure 4.3). An elegant method to control the regiospecificity to produce AB, AC or AD isomers by the use of the geometry has been described.[26]

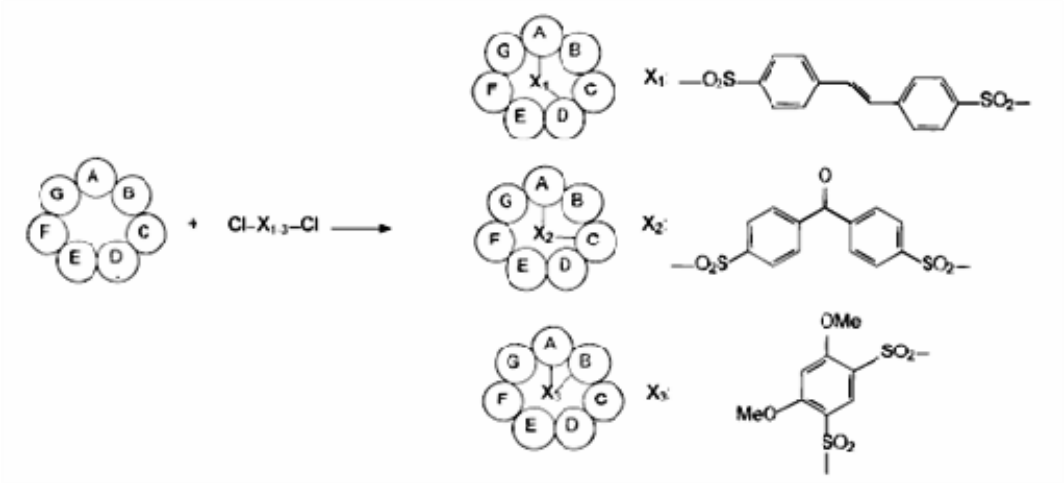

Figure 4.3: Use of the geometry of reagents to direct the regiospecificity in disubstitution of CDs. From ref. [10].

4.3 Structure and objectives of the chapter

The molecular modelling studies reported in the former chapter showed that the interaction of ochratoxin A with the β-cyclodextrin occurs by insertion of the phenyl ring of the toxin inside the cavity, but that the complex is poorly stable. It was also possible to note that the carboxyl group was preferentially located near the lower rim. On the other hand, the ochratoxin A molecule can be present as monoanion, when the carboxyl group is deprotonated ($pK_a = 4.8$) or as dianion when also the phenol group is deprotonated (pKa = 7.1).

In this chapter we report the synthesis of several modified β-cyclodextrins bearing one or more positively charged groups; in fact, within a general project about molecular recognition, there have been designed modified β-cyclodextrins in order to build up good sensors for ochratoxin A (OTA). In particular, on the base of the mode of OTA inclusion into the β-cyclodextrin cavity and considering the shape, the hydrophobicity and the negative charges potentially present on the toxin molecule, according to pH value, we decided to synthesize several derivatives of the β-cyclodextrin bearing one or more positively charged groups at either position 6 of the upper rim and at position 2 of the lower rim, in order to improve the complexation. Ammonium or guanidinium groups were chosen as positively charged groups (Figure 4.4).

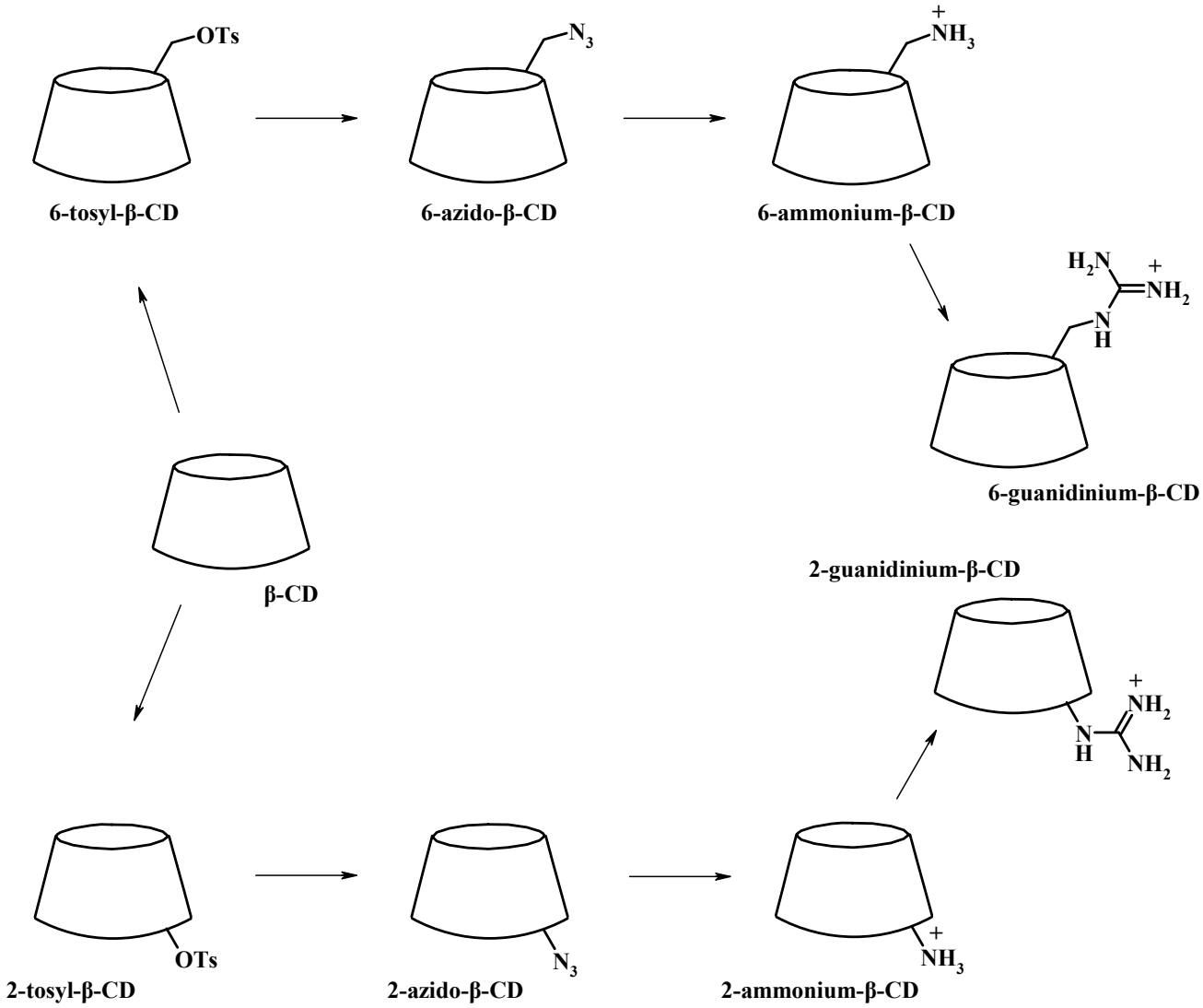

Figure 4.4: General scheme of the synthesis of β-CD derivatives bearing one positively charged group at position 6 and at position 2.

Independently from which rim of the β-cyclodextrin we wish to modify, the first important step is the tosylation of the hydroxyl groups. Therefore, the first part of the synthetic procedure will be singly described: there will get information about the synthesis of the tosylate derivatives at position 2 and at the position 6, from which is possible to obtain both the mono- and the three (AB, AC and AD) disubstituted isomers. In particular, an investigation on the discrimination of 2A,2X-dideoxy-2A,2X-ditosyl-β-cyclodextrin applying the ESI-MS spectrometry and 1D and 2D NMR spectroscopy will be also reported.

In the remainder part of the chapter, the synthesis of the guanidinium derivatives obtained from the relative tosylate products will are given.

4.4 Tosylation of β-CD at the 2-position

As explained above, the secondary side is more crowded than the primary side due to the presence of secondary hydroxyl groups. Moreover, hydrogen bonding between hydroxyl groups at the 2- and 3-positions makes them rigid and less flexible as compared to C-6 hydroxyl groups. All these factors make the secondary side less reactive and harder to selectively functionalize than the primary face.

For these reasons, regioselective sulfonation of the lower rim, as well as of the upper rim, is considered as a key step for the modification of the β-cyclodextrin structure, since the tosylate group linked on a cyclodextrin edge could be rapidly substituted *via* a SN_2 reaction with many other nucleophiles, allowing thus the possibility to obtain many different cyclodextrin derivatives.

A general scheme of the reaction between β-cyclodextrin and tosyl chloride, giving both mono-substituted and di-substituted cyclodextrins at position 2, is given in Figure 4.5.

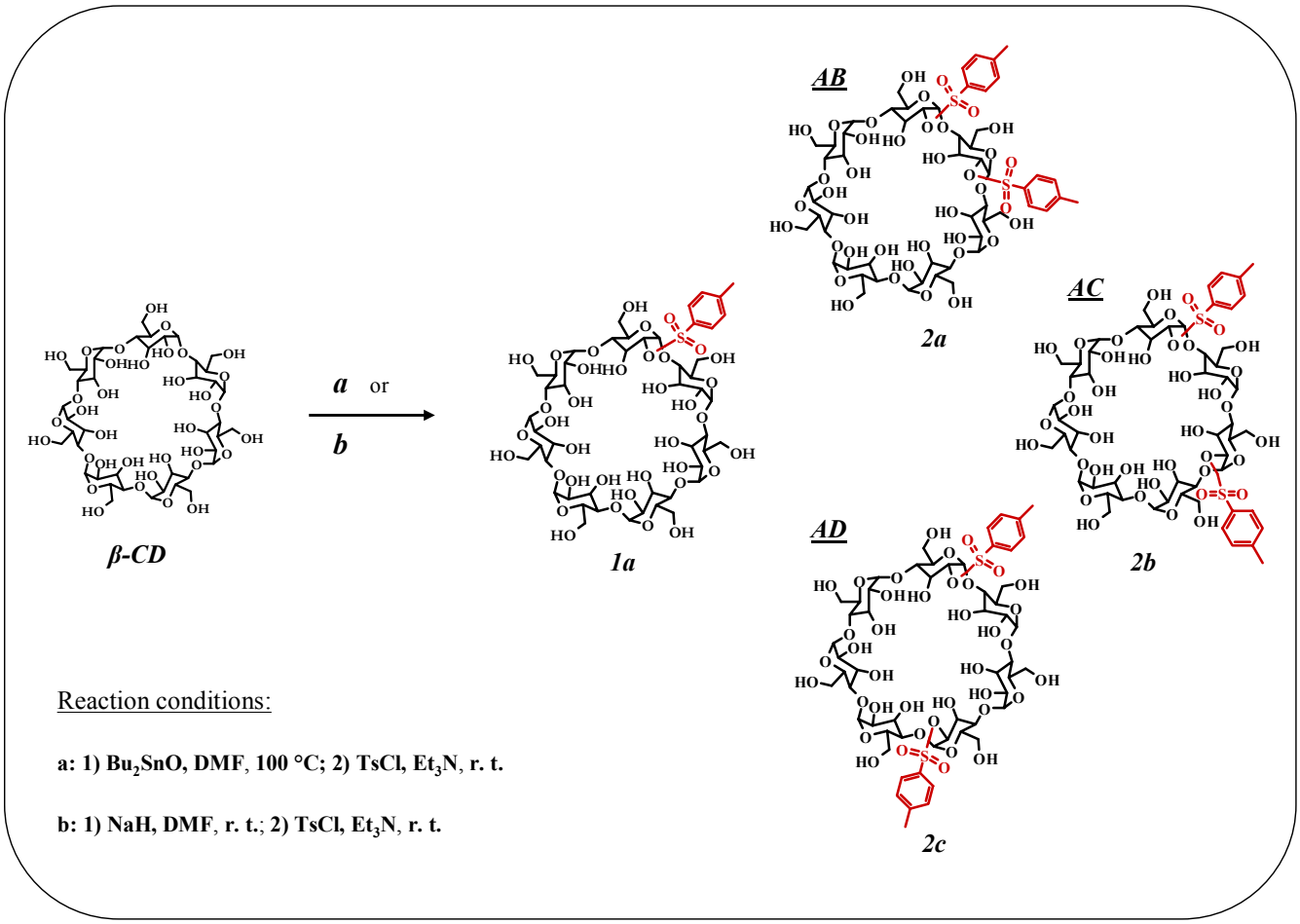

Figure 4.5: General scheme of the tosylation of the β-CD at the 2-position in the presence of TsCl.

4.4.1 Tosylation of hydroxyl groups at the 2-position of β-CD by using organotin compounds.

Since regioselective acylation or sulfonation of carbohydrates has been developed by using of organotin compounds, in order to promote the sulfonation of β-cyclodextrin at the position 2, di-*n*-butyltin oxide, which is known to react with 1,2-diols forming five membered dibutylstannylidene derivatives,[27] has been used. Since alkyltin alkoxide is more nucleophilic than the original OH-group, di-*n*-butyltin could promote the selective activation of vicinal diol systems in polyhydroxy compounds like cyclodextrins.

Here, the results obtained by applying this synthetic methodology to the sulfonation of β-cyclodextrin will be described. Figure 4.6 shows the mechanism with which the reaction produces the mono-substituted product (yield: 10%); with analogous mechanisms, the three (AB, AC and AD) di-substituted isomers can be generated by the same reaction, but only in traces (yield: 1%).

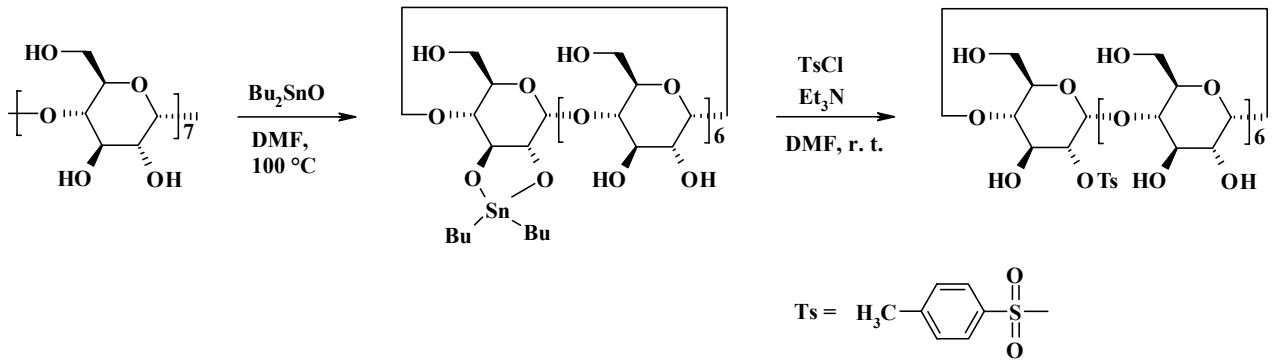

Figure 4.6: Reaction of β-CD with TsCl using Bu_2SnO as activating agent.

^{1}H- and ^{13}C-NMR spectra of the different products separated from the mixture reaction by reversed-phase liquid chromatography showed the total absence of 3-substitutd products. In particular, as explained by Breslow,[4] from the ^{13}C-NMR spectra of the mono-tosyl derivative, it is possible to note a large downfield chemical shift of C-2 and a small upfield chemical shift of C-3. Moreover, no change of the chemical shift of C-6 of the substituted glucose unit with respect to unsubstituted glucose units clearly indicate that the substituent is at the 2-position of the cyclodextrin (Figure 4.7).

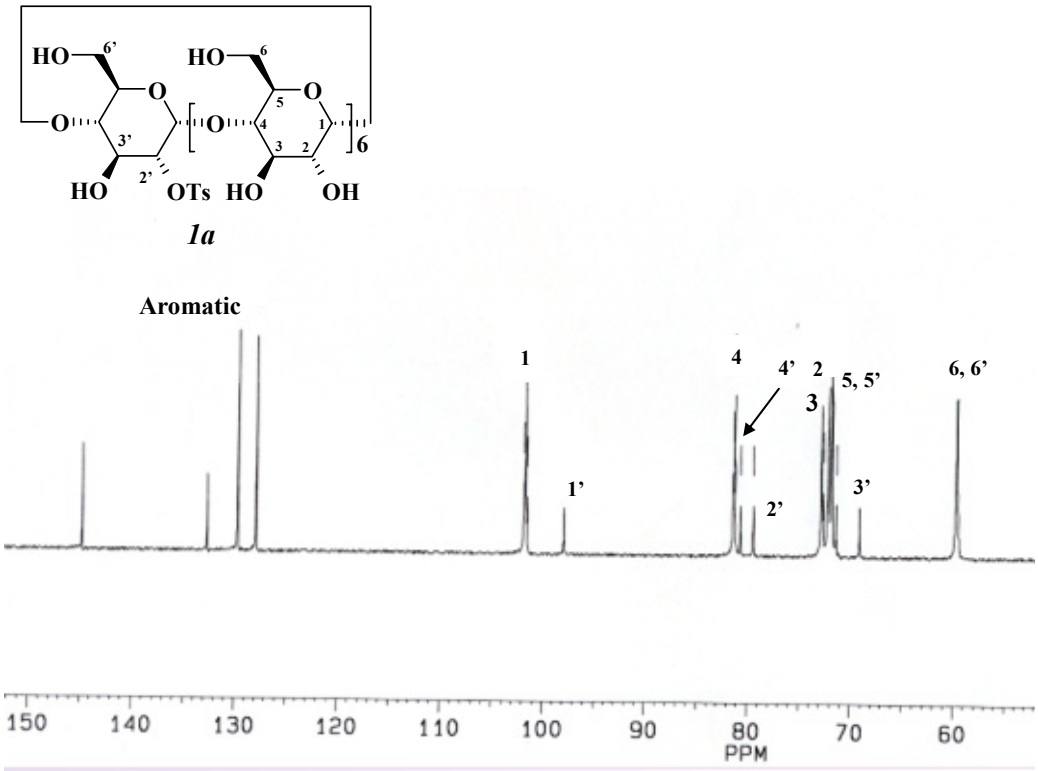

Figure 4.7: ^{13}C-NMR spectrum of 2-tosyl-2-deoxy-β-CD-

As shown in Figure 4.6, the reaction proceeds through the formation of a dibutylstannyl alkoxide derivatives that subsequently attack the tosyl chloride to form the 2 sulfonated compound. The products obtained suggest the selective formation of the dibutylstannylidene derivatives, which is a consequence of the greater thermodynamic stability of the cyclic 2-stanna-1,3-dioxolane structure relative to acyclic alkoxytin derivatives. Szmant et al.[28] reported the selective preparation of C-2 tosylates of methyl α-D-glucopyranoside derivatives *via* cyclic tin intermediates (Figure 4.8).

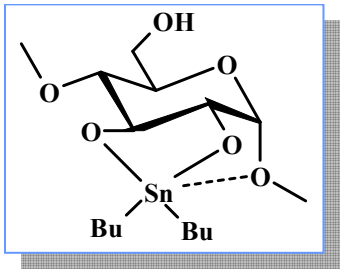

Figure 4.8: Cyclic tin intermediates responsible of the selectivity observed in the tosylation at C-2 oxygen.

The Authors suggested the formation of a coordination bond between tin and the C-1 anomeric oxygen, as shown in Figure 4.8. This coordination bond, which seems to be important for the selective tosylation at the C-2 oxygen, can be formed in the case of cyclodextrins. Another reason

for the selectivity is that C-2 hydroxyl groups of the cyclodextrins are intrinsically reactive than C-3 hydroxyl towards electrophiles.

However, the low yields with which the tosyl derivatives were obtained suggested to change the synthetic strategy to perform the tosylation at the lower rim. For this reason, a more convenient method for functionalization at the 2-position involving deprotonation of cyclodextrin by sodium hydride has been taken into account.

4.4.2 Tosylation of hydroxyl groups at the 2-position via cyclodextrin oxyanion formation.

An alternative strategy for the synthesis of 2-tosyl derivatives is based on the different acidity showed by the three types of cyclodextrin hydroxyl groups (OH-2, 3 and 6). Among them the hydroxyl groups at the 3-position are the least reactive and resist functionalization and this has been attributed to the hydrogen bonds formed between the protons of the hydroxyl groups at the 3-position and the oxygen atoms of the hydroxyl groups at the 2-position.[29] The hydroxyl groups at the 6-position are most reactive towards electrophilic reagents because they are primary hydroxyl groups and their pK_a can be compared with other primary hydroxyl groups (pK_a = 15-16). The hydroxyl groups at the 2-position, instead, are the most acidic of the three hydroxyl groups with a pKa of 12.1, and this has been attributed to the hydrogen bond between the hydroxyl groups at 2- and at 3-position described above which can stabilize the oxyanion. This can also be attributed in part to the proximity of this hydroxyl group to the electron withdrawing acetal functionality. The most acidic hydroxyl group in an unsubstituted methyl glucoside is known to be the one at the 2-position with pKa of 12.35.[30] The carbohydrate oxyanions are known to attack electrophilic reagents and to give derivatives functionalized at the 2-position for this reason.[31] Thus, it is not surprising that the oxyanions of cyclodextrin attack electrophiles in a similar manner providing a convenient method for functionalizing them at the 2-position.

The scheme of the reaction used is shown in Figure 4.9.[13]

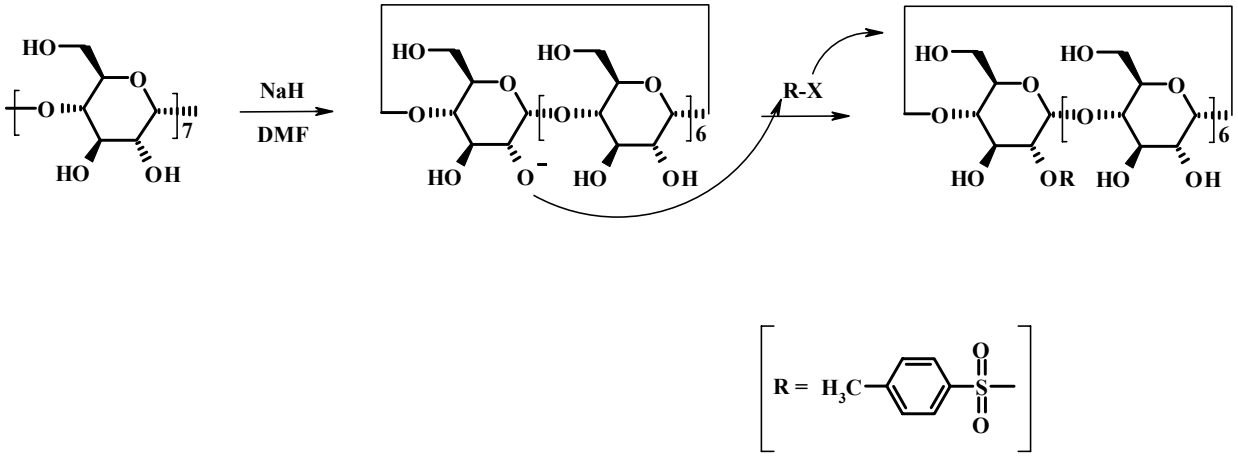

Figure 4.9: Tosylation of β-CD in the presence of NaH. From ref. [13]

As described in the previous paragraph, the precipitate (containing unreacted β-cyclodextrin and mono- and di-derivatives) obtained adding the reaction mixture to a great excess of acetone was purified by RP-HPLC (Figure 4.10). After the separation step the mono- and di-tosylated derivatives were obtained in amounts higher than that obtained using dibutyltin oxide. Using the same equivalents of sodium hydride and tosyl chloride as the amount of β-cyclodextrin, the yield of the 2-tosyl-2-deoxy-β-cyclodextrin was 25 %, while the yield of the three disubstituted isomers were 3 % for the AC and AD derivatives and 5 % for the AB derivative.

With the aim of increasing the yield of the di-substituted isomers, several reaction conditions were investigated. The equivalents of sodium hydride and tosyl chloride added to the solution of β-cyclodextrin were doubled and triplicated, but unfortunately without meaningful effects.

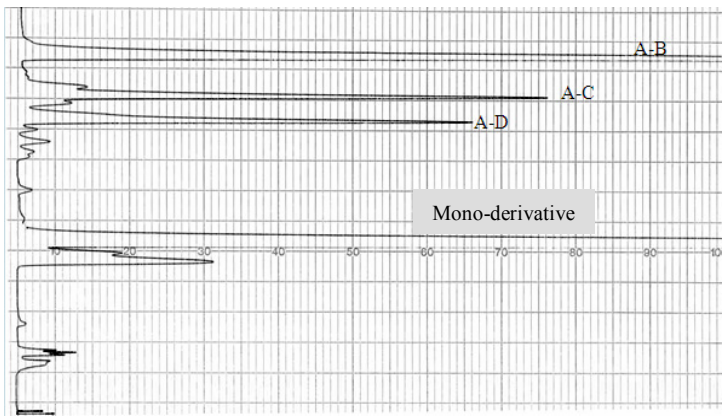

Figure 4.10: Chromatographic separation of the tosyl derivatives obtained by reaction of β-CD and TsCl in the presence of NaH. Chromatographic conditions: Water Spherisorb ® 10μm ODS2 20x250mm column; mobile phase water-methanol, from water-methanol 72:28 to methanol; flow rate 15 ml/min; column temperature 25 °C; UV detector (λ_{abs} = 260 nm).

Confirmation of the structures of the tosyl derivatives was then obtained by ESI-MS and ^{1}H- and ^{13}C-NMR. In particular, the structure of the 2-tosyl-2-deoxy-β-cyclodextrin, was confirmed by the presence in the ^{1}H-NMR spectra of signals in the region of the aromatic protons and by typical large downfield shift of C2' and upfield shift of C-3' in the ^{13}C-NMR spectra, consistent with the know shift effects of C-2 tosylation (Figure 4.11).

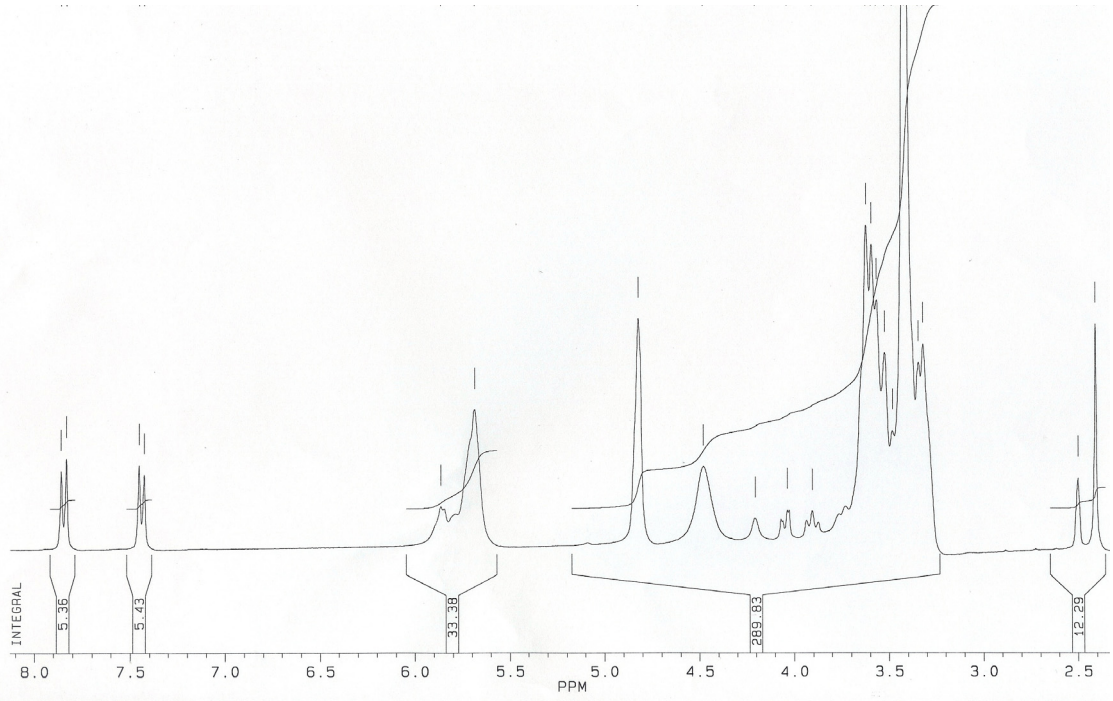

Figure 4.11: ^{1}H-NMR spectrum of the 2-tosyl-2-deoxy-β-CD (300 MHz, DMSO-d_6).

The elution order showed in Figure 4.10, clarified by subsequent characterization, was in agreement with the polarity order of the different derivatives. Naturally, being the more polar compound, the mono-tosylate product eluted as first, while the elution order of the di-tosylate showed a dependence on the relative position of the two substituents on the rim of the cyclodextrin structures. The characterization of the three ditosyl isomers was obtained by the use of different techniques such as the ESI-MS spectrometry and NMR spectroscopy. The identifications are described below.

4.5 Characterization of 2A, 2X-ditosyl-β-CDs.

Despite of the difficulties for the syntheses and purifications, the three ditosyl regioisomers 2A,2X (X = B, C, D) of a β-cyclodextrin are among the most important intermediates in the preparation of a wide range of homo- and hetero-difunctionalized cyclodextrin, that could be interesting in developing artificial receptors in the field of molecular recognition. However, the exact characterization is still based on the results reported in the 1989 by Fujita et al.[8] where the structure of each compound was assigned on the basis of its conversion into a known product or *via* hydrolysis with Taka amylase A.

Once prepared the three regioisomers AB, AC and AD following the procedure reported by D'Souza et al.,[13] they were characterized by ESI-MS spectrometry and 1D and 2D NMR spectroscopy.

4.5.1 ESI-MS spectrometry analysis of 2A, 2X-ditosyl-β-CD.

In order to identify the cyclodextrin regioisomers, an ESI-MS method, previous developed by Sforza et al.[32] for determining the analogues 6,6'-ditosylate β-cyclodextrins, was used. The method is based on an applied cone-induced fragmentation in the presence of a two-fold excess of sodium chloride. On the basis of the fragmentation observed for the unsubstituted β-cyclodextrin, it has been shown by a statistical analysis that different fragmentation patterns are expected for the three different isomers (AB, AC and AD) of a 2,2'-disubstituted β-cyclodextrin. According to this model, the different isomers showed different fragmentation patterns, allowing for the correct assignment by fast and easy mass spectral analysis.

4.5.1.1 β-CD fragmentation.

The mass spectrum was collected by the direct infusion of a 100 μM NaCl:β-cyclodextrin 2:1 solution in doubly distilled water. Given the high affinity of the cyclodextrin molecule for the sodium ion, the presence of the sodium chloride favors the formation of the sodiated ions, thus the spectrum is dominated by the sodiated molecular ion (1157 Da). Moreover, a simple fragmentation pattern generating a series of peaks always with a difference of 162 Da (1157/995/833/671/509/347 m/z) can be observed. This molecular mass corresponds to the monomeric residue of the β-cyclodextrin (a dehydrated glucose molecule) and this may be interpreted by assuming that every fragmentation event takes place at the acetal conjunction and may occur via the complexation of sodium by the two acetal oxygens and subsequent sodium-assisted fragmentation (Figure 4.12 a).

Thus, the first fragmentation event has the effect to open the cyclodextrin ring (and therefore it is not visible in the mass spectrum since the opened sodiated cyclodextrin still has a molecular mass of 1157 m/z), whereas the subsequent fragmentations generate sodiated fragments characterized by the following molecular masses: 995 (6 monomeric units), 833 (5 monomeric units), 671 (4 monomeric units), 509 (3 monomeric units), 347 (2 monomeric units), as schematically shown in Figure 4.12 b.

It is important to notice that the fragmentation events can occur almost randomly at every acetal junction of the opened cyclodextrin since all the possible fragmentation peaks (2, 3, 4, 5 and 6 monomeric units) are present in the spectrum.

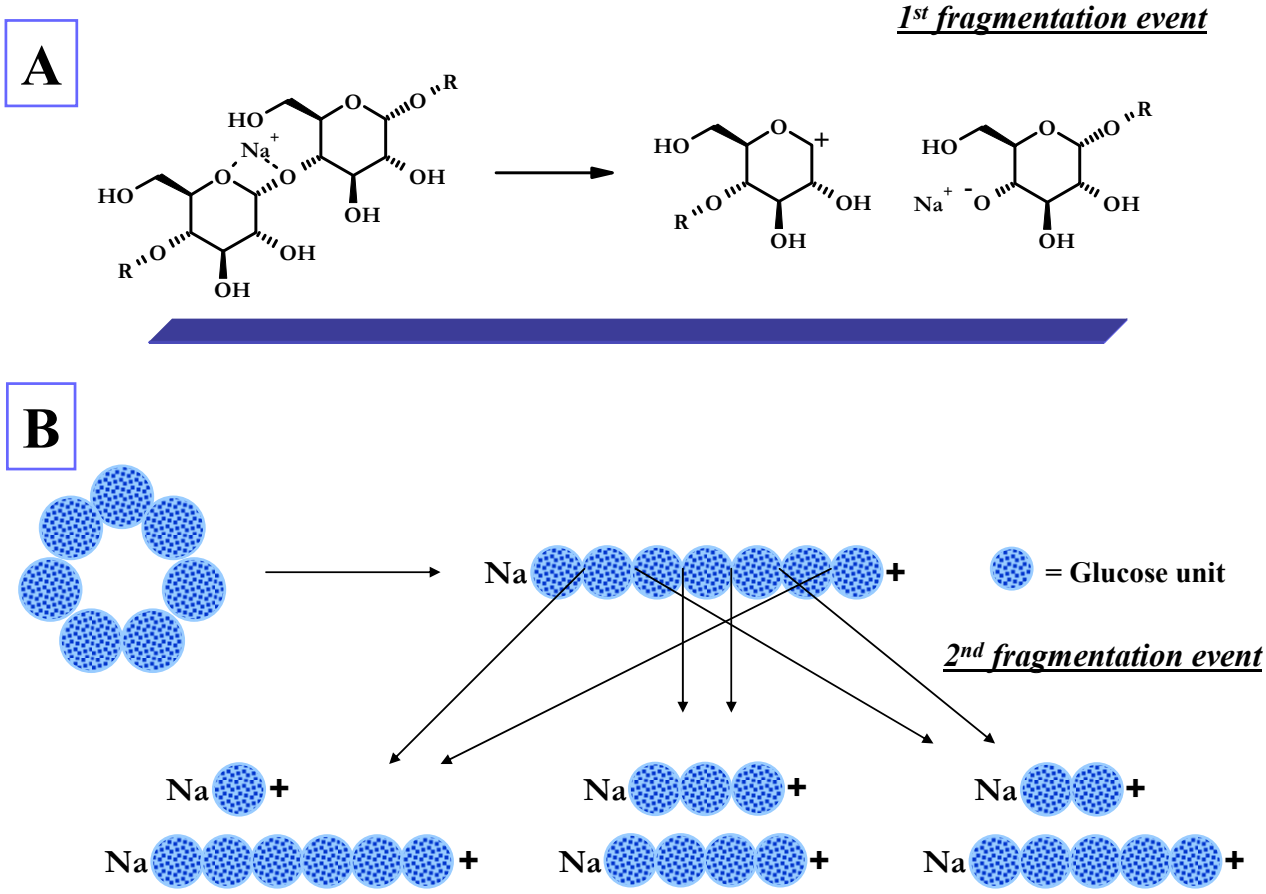

Figure 4.12: a) Hypothetical mechanism of β-CD fragmentation at the acetalic junction and b) generation of the β-CD fragments through a two-fragmentation random process. Every circle represents a glucose moiety.

4.5.1.2 Identification by fragmentation: the case of ditosyl- β-CDs.

Assuming that a disubstituted β-cyclodextrin will follow the same mechanism of fragnmentation reported above, it is immediately evident that the fragmentation pattern will be more complicated. In fact, every fragment characterized by a given number of monomeric units will contain two, one or no substituted glucose units, thus generating three different mass peaks.

The key feature for the correct identification of the regioisomers relies on the fact that the relative intensity of these three peaks is expected to be different for the AB, AC and AD disubstituted cyclodextrins. The reason for this behaviour is exemplified in Figure 4.13, in the case of the generation of the four-unit fragments.

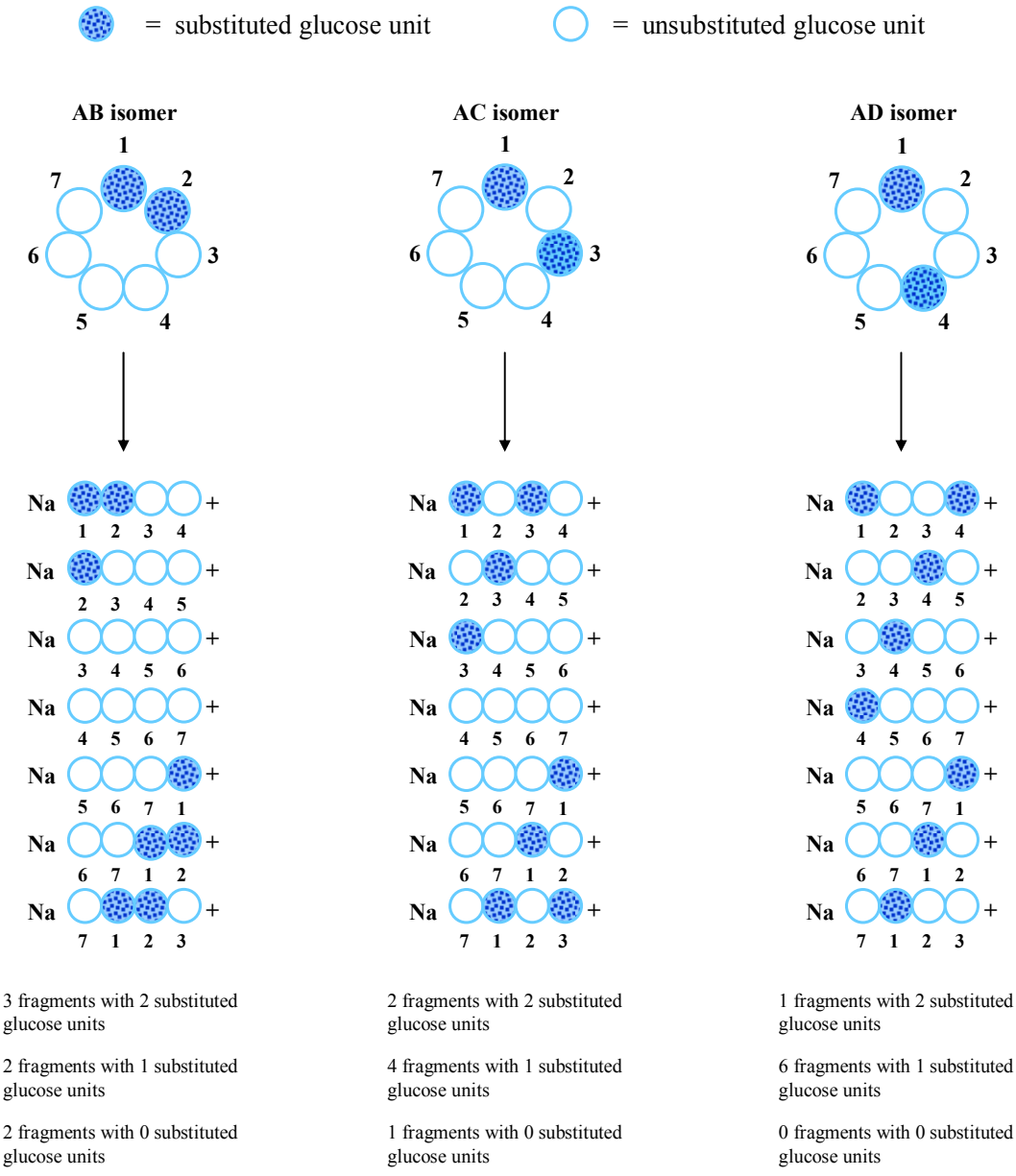

Figure 4.13: Four-monomeric unit fragments generated by the two-fragmentation random process in the case of a disubstituted β-CD. Every circle represents a glucose moiety.

By considering all the possible points of fragmentation, there are seven different possibilities for generating four-unit fragments. In the case of the AB isomer, three fragments out of seven will have two substituted glucose moieties, two out of seven will have one substituted glucose moiety and two out of seven will have unsubstituted glucose moieties. In the case of the AC isomer, on the other side, two fragments out of seven will have two substituted glucose moieties, four out of seven will have one substituted glucose moiety and one out of seven will have unsubstituted glucoses. Finally, in the case of the AD isomer, one fragment out of seven will have two substituted glucose moieties, six out of seven will have one substituted glucose moiety and no fragment with unsubstituted glucose moieties will be generated. The case of the four unit fragments can be extended to every fragment characterized by a defined number of monomeric units, as shown in Table 4.1.

Table 4.1: Expected distribution of the unsubstituted, monosubstituted and disubstituted peaks for every fragments characterised by a defined number of monomeric units in the case of AB, AC and AD regioisomers, given a random fragmentation at the acetal junction.

	AB isomer					**AC isomer**					**AD isomer**				
Fragments	2	3	4	5	6	2	3	4	5	6	2	3	4	5	6
unsubstituted	4/7	3/7	2/7	1/7	0/7	3/7	2/7	1/7	0/7	0/7	3/7	1/7	0/7	0/7	0/7
Monosubstituted	2/7	3/7	2/7	2/7	2/7	4/7	4/7	4/7	4/7	2/7	4/7	6/7	6/7	4/7	2/7
Disubstituted	1/7	2/7	3/7	4/7	5/7	0/7	1/7	2/7	3/7	5/7	0/7	0/7	1/7	3/7	5/7

Thus, if the fragmentation mechanism of disubstituted cyclodextrins is that which was previously proposed, it would be possible to distinguish between the three regioisomers simply by evaluating the relative intensity of the di-, mono- and unsubstituted fragments in every group characterized by the same number of monomeric units. This, indeed, was observed from the ESI spectra of the three pure isomers, previously separated by preparative HPLC (details will are given in the experimental section), which were obtained in the same condition reported above (50 μM CD in the presence of 100 μM NaCl). The spectra are showed in Figure 4.14

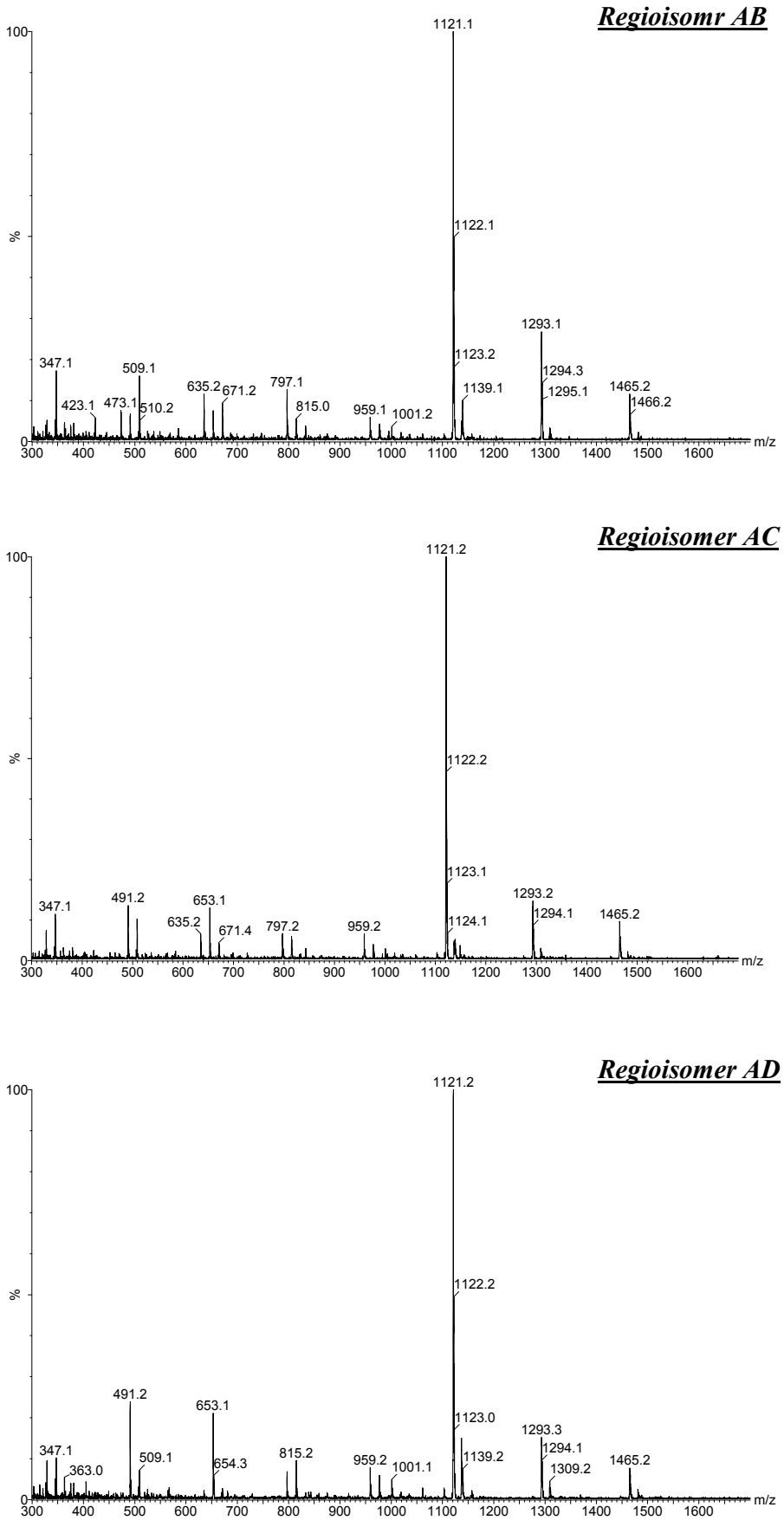

Figure 4.14: The mass spectra of the ditosyl-β-CDs synthesized after HPLC purifications.

In all cases the sodiated molecular ion is the dominating peak. Many signals are present in the spectra. The two most intense, with m/z of 1293 and 1121, derive from two consecutive loses of 172 Da, which correspond to the molecular mass of p-toluenesulphonic acid. This is consistent with the character of leaving group of the tosyl substituents and it means that the first two events of fragmentation are the losses of the substituents leading to dehydratated glucose units (possibly a 3,6-dehydro compound). Therefore, in order to correctly calculate the expected molecular masses of the fragments in every group defined by the number of the monomeric units, the disubstituted, the monosubstituted and the unsubstituted peaks should be expected to differ by 18 Da, since the disubstituted will actually have two dehydratated units, the monosubstituted will have one dehydratated unit and the unsubstituted will have no deydratated units. Although many peaks are present in the spectra, the most abundant fragments observed have m/z ratios exactly corresponding to those calculated. The other fragmentation peaks observed may probably be due to the different fragmentation reaction in the gas-phase, which may be triggered by the formation of dehydratated glucose moieties.

As described before, a statistical analysis was performed in order to define every regioisomer: for every compound the relative percentages of the unsubstituted, monosubstituted and disubstituted peaks were correlated to the expected number of fragments (out of seven).

A quick identification of the three regioisomers was therefore achieved by checking in the spectra showed in Figure 4.15 the peaks having four glucose units and two, one or no dehydratated group (m/z 635, 653 and 671, respectively). In fact, the ratios between these peaks were found to be characteristic for every regioisomer, consistent with the proposed mode of fragmentation, the 635 peak being higher in the AB isomer, the 671 peak being higher in the AD isomer and the 653 peaks being higher in the AC isomer.

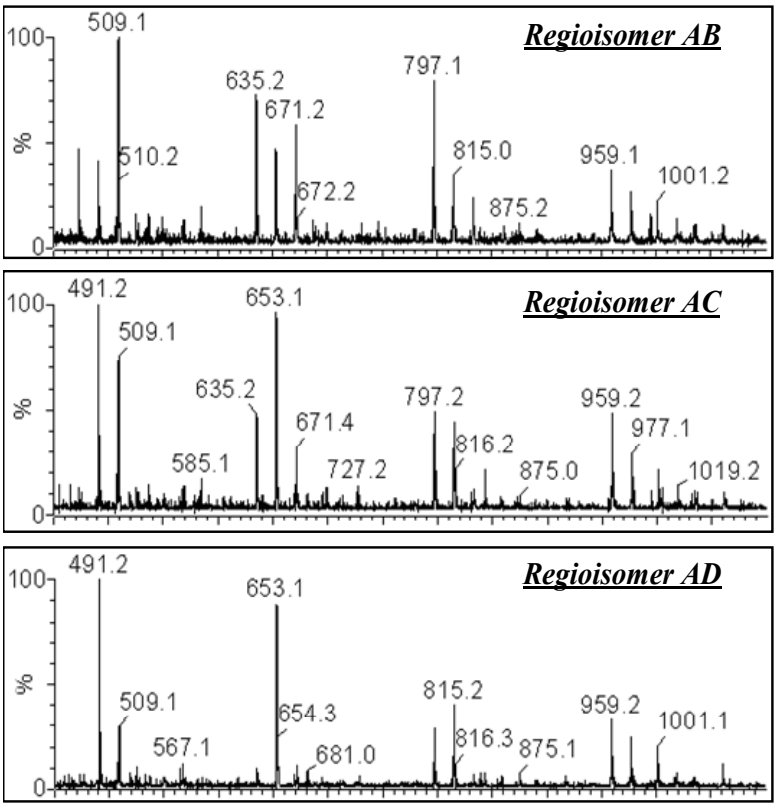

Isomers	AB	AC	AD
No substituted	2/7	1/7	0/7
Mono-substituted	2/7	4/7	6/7
Di-substituted	**3/7**	**2/7**	**1/7**

Fragments:

671 m/z (no substituted)
653 m/z (mono-substituted)
635 m/z (di-substituted)

Figure 4.15: The spectra of the ditosyl-β-CD synthesized as a mixture after isolation by HPLC with several signals identified as diagnostic peaks.

4.5.1.3 Conclusion.

The data collected by studying the in-source fragmentation in ESI mass spectra in the presence of a twofold excess of sodium chloride support the fragmentation mechanism previously proposed by Sforza[32] and consisting with the fact that unsubstituted and disubstituted β-cyclodextrins mainly randomly break at the acetal junctions, giving rise to different polyglucose sodiated fragments.

The results obtained are important from a theoretical point of view since they explain the main fragmentation mode of substituted β-cyclodextrins in ESI mass spectrometry, and even more important, from a practical one, by making available a very rapid procedure for the correct identification of disubstituted β-cyclodextrin regioisomers. Moreover, data obtained show the great versatility of the method, since it is independent both by the type of substituents than by the position at which the substituents are linked in the cyclodextrin structure.

4.5.2 NMR spectroscopic analysis of 2A, 2X-ditosyl-β-CD.

In order to obtain information about the ditosylation in 2A,2B-, 2A,2C- and 2A,2D-dideoxy-β-cyclodextrin, a series of 1D (^{1}H and ^{13}C) and 2D (TOCSY and ROESY) NMR experiments were performed. The coupling of mono and bidimensional NMR experiments allowed to obtain an unambiguously assignment of the exact position of the sulfonylated glucosides in the ditosyl 2A,2B- and 2A,2C-dideoxy-β-cyclodextrin structures.

4.5.2.1 1D NMR analysis.

The ^{1}H (600 MHz) NMR spectra of the 2A,2B-ditosyl-2A,2B-dideoxy-β-cyclodextrin, measured at 25 °C in dimethyl solfoxide (DMSO-d_6), is shown in Figure 4.16.

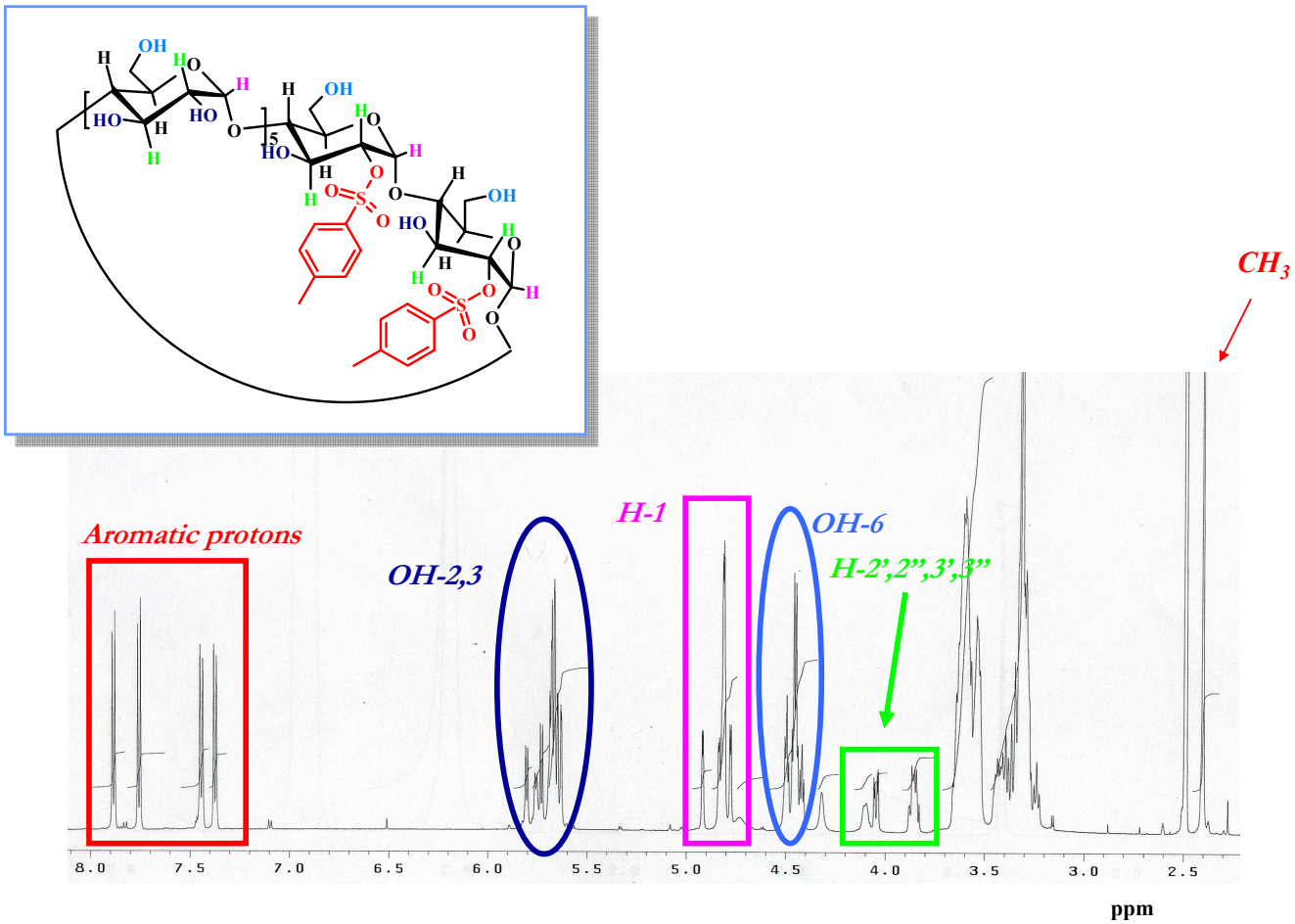

Figure 4.16: ^{1}H-NMR spectra of the 2A,2B-ditosyl-2A,2B-dideoxy-β-CD in DMSO-d_6. 600 MHz.

Based on $^{1}H,^{1}H$ TOCSY NMR spectra, it is possible to recognize signals relative to the hydrogens of the hydroxyl groups (OH-2, 3 and 6), the characteristic anomeric protons and signals

corresponding to the H-2 and H-3 of the substituted glucosidic units (indicated in Figure 4.16 as H-2', 2'' and H-3', 3''). Moreover, it was easy to recognize signals relative to the aromatic protons of the two tosyl moieties; these signals, as it will demonstrate after, were crucial for obtaining important details on the position occupied by the substituents in the regioisomer structure.

The ^{1}H-NMR spectra of the three ditosyl regioisomers are reported below.

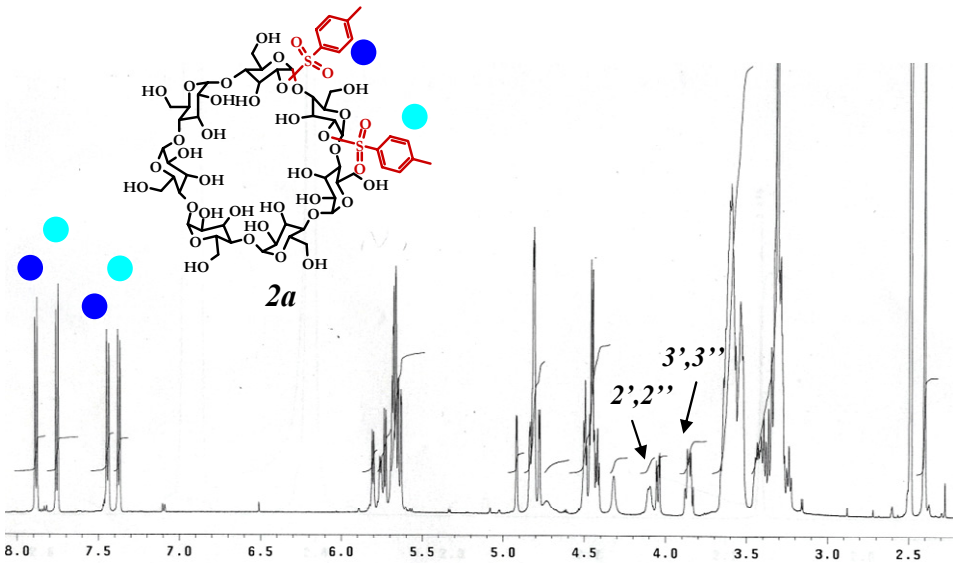

Figure 4.17: ^{1}H-NMR spectrum of 2A,2B-ditosyl-2A,2B-dideoxy-β-CD in DMSO-d_6 at 25 °C (600 MHz).

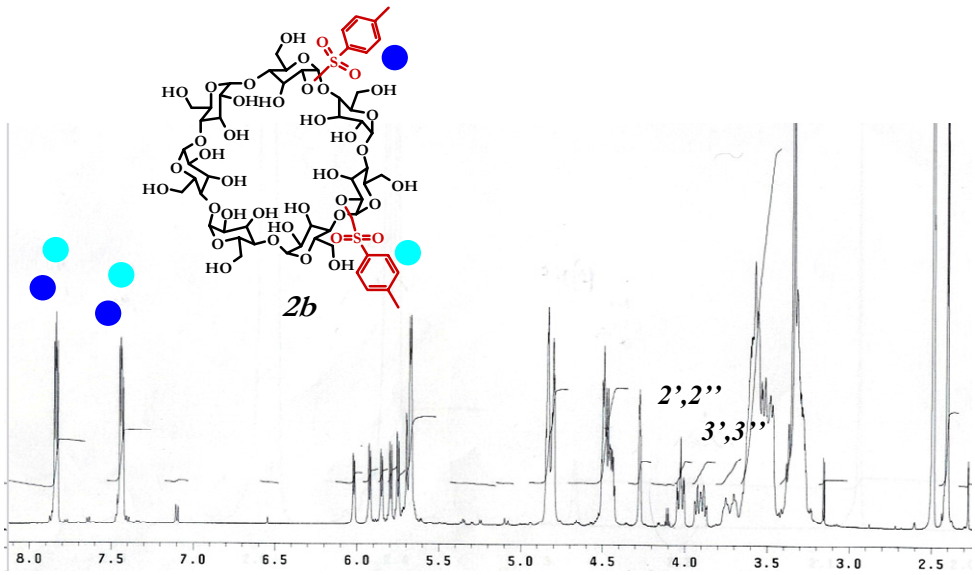

Figure 4.18: ^{1}H-NMR spectrum of 2A,2C-ditosyl-2A,2C-dideoxy-β-CD in DMSO-d_6 at 25 °C (600 MHz).

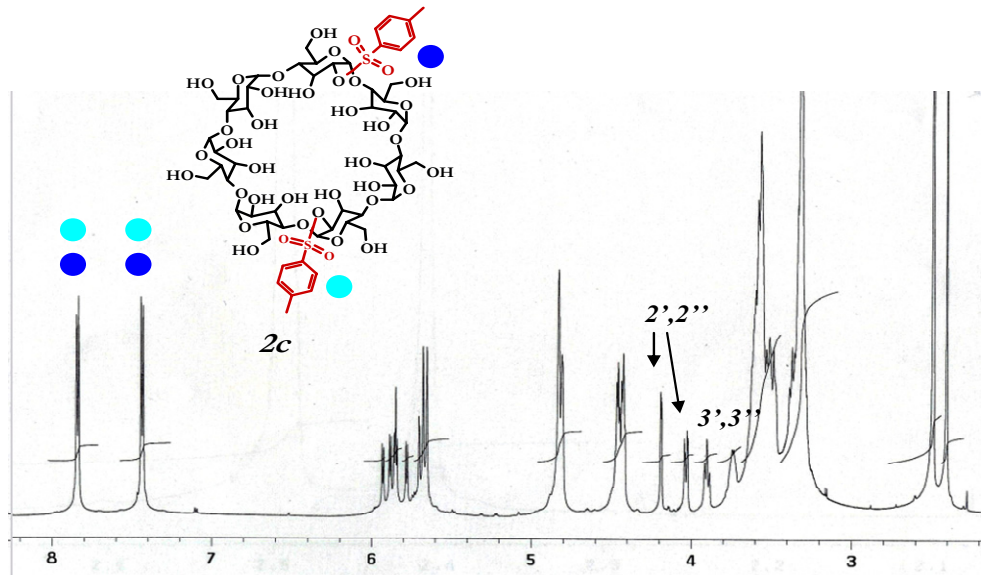

Figure 4.19: ^{1}H-NMR spectrum of 2A,2D-ditosyl-2A,2D-dideoxy-β-CD in DMSO-d_6 at 25 °C (600 MHz).

From the ^{1}H-NMR spectra of the AB, AC and AD ditosyl derivatives it is important to note that, in all cases, they presented downfield shifts of two H-2 (2', 2'') as compared with those of β-cyclodextrin. Moreover, all ^{13}C-NMR (see in the experimental section) showed large downfield shifts for two C-2, small upfield shifts for two C-3 and two C-1 as compared with those for β-cyclodextrin. These results indicated the occurrence of double 2-*O*-tosylsulfonylation in the ***2a-c*** compounds. In particular, important information about the relative position of the two tosyl groups in the cyclodextrin structures were deducted simply by observing the behaviour of the aromatic proton signals. In fact, in the case of the AB isomer, where the two aromatic rings are linked to two adjacent glucosidic units, the chemical environments of the aromatic protons of each phenyl ring are different (causing the presence of four doublets in the aromatic region of the ^{1}H-NMR spectra), while in the case of the AD isomers, the chemical environments of the aromatic protons of each phenyl ring are similar (causing the presence of only two doublets in the aromatic region of the ^{1}H-NMR spectra) since the two aromatic rings are linked to two glucosidic units located, in the cyclodextrin structure, one opposite to the other.

For the same reasons, also in the ^{13}C-NMR spectra of the three regioisomers, relative to the methyl carbons of the two tosyl groups, two distinct signals were detected for the AB derivative while only one signal was observed for the AD isomer, confirming the hypothesis that the chemical environments for the two aromatic rings tend to become identical when they are located at opposite sites of the lower rim.

4.5.2.2 2D NMR analysis.

In order to verify the exact positions of the two tosyl groups in the bitosylated structures, TOCSY and ROESY NMR spectra for the AB and AC derivatives were performed.

In the case of the 2A,2B-ditosyl-2A,2B-dideoxy-β-cyclodextrin (compound ***2a***) the aim of this analysis can be explained simply observing the structure of the compound (Figure 4.20).

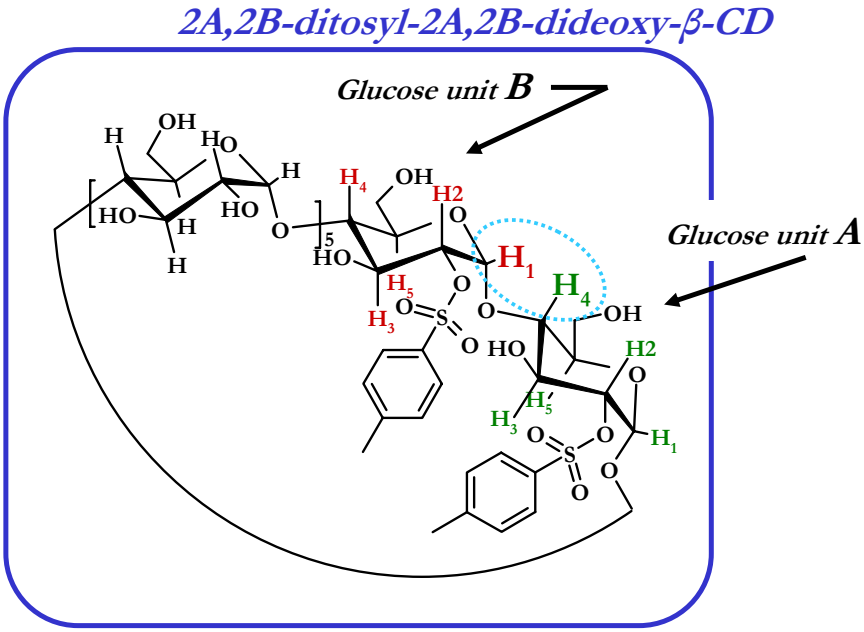

Figure 4.20: Structure of the 2A,2B-ditosyl-2A,2B-dideoxy-β-CD (*2a*).

As it can be seen in Figure 4.20, due to the presence of the two substituents on adjacent glucose units, the NMR signals of the H-1 hydrogen relative to the glucosidic units A and B may be clearly separated from those of the other nuclei, and therefore, starting from them, it is possible to assign the entire proton signals in the same units by searching the (H^A-1)-(H^A-X) and (H^B-1)-(H^B-X) correlations by performing several TOCSY experiments with different mixing times. Once to obtain the (H^A-1)-(H^A-4) correlation peak for the unit A and the (H^B-1)-(H^B-4) correlation peak for the unit B, a ROESY spectra, showing the (H^A-4)-(H^B-1) correlation island (as outlined in Figure 4.20) could provide reliable information about the exact regioisomery of the compound.

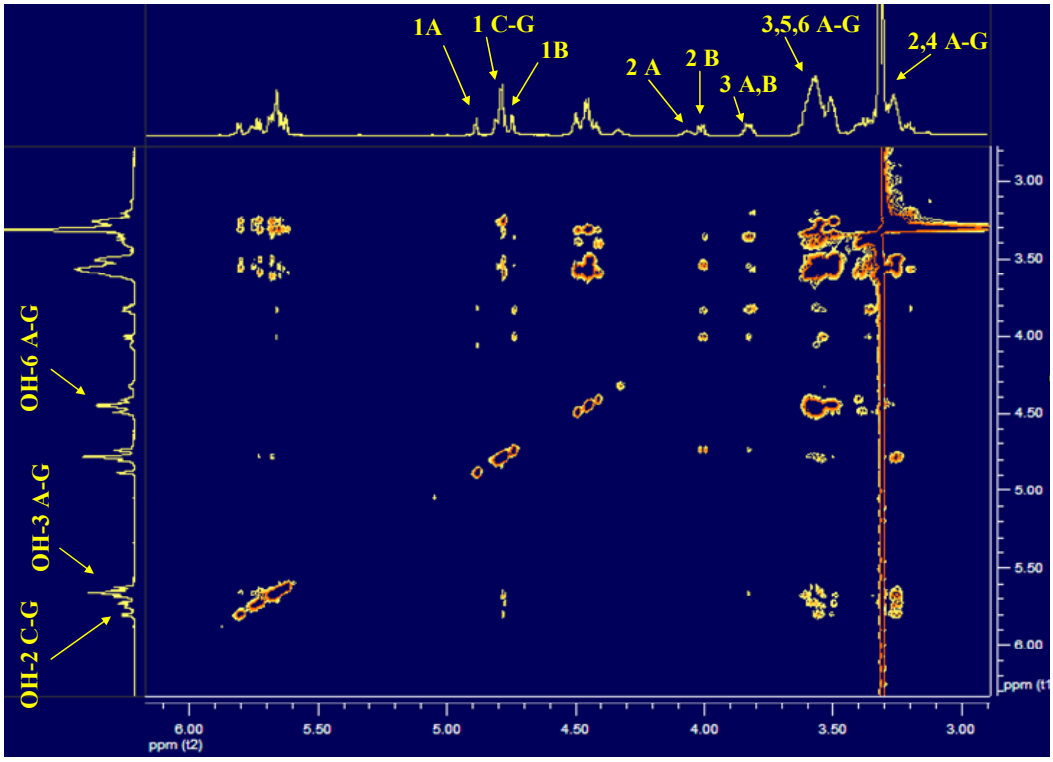

Figure 4.21: TOCSY NMR spectrum of the carbohydrate part of compound *2a* in DMSO-d_6 solution. Mixing time: 160 ms.

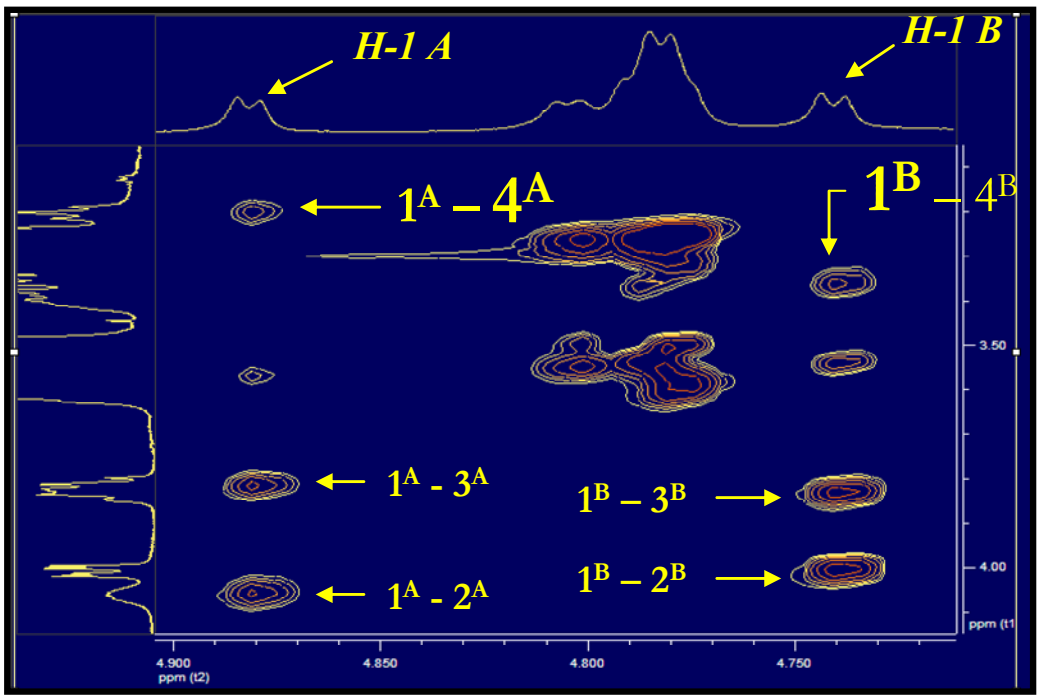

Figure 4.22: TOCSY spectrum of *2a*. Determination of the (H^A-1)-(H^A-4) and (H^B-1)-(H^B-4) correlation peaks.

As shown in Figure 4.22, one doublet at δ 4.88 and one doublet at δ 4.74 were observed respectively for the H-1 protons of the units initially attributed to A and B. The (H^A-1)-(H^A-4) and (H^B-1)-(H^B-4) correlation areas were those desired to verify the AB regioisomery by a ROESY spectra. In fact, as shown in Figure 4.23, the key (H^A-4)-(H^B-1) correlation peak was found, allowing to assign the AB disubstitution to the compound ***2a*** and confirming the results previous obtained by the ESI-MS method.

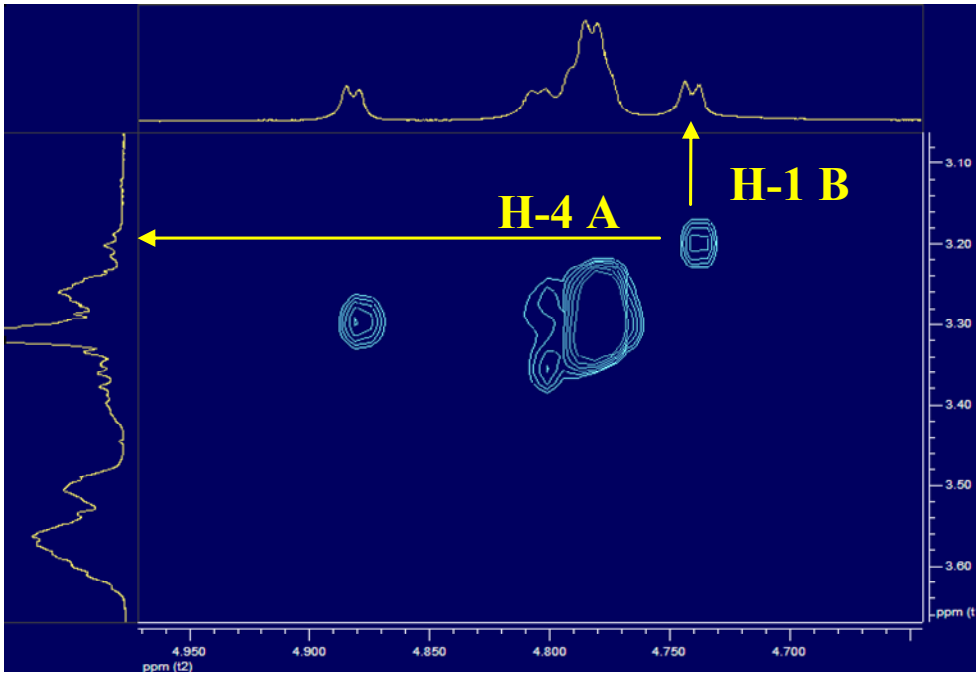

Figure 4.23: ROESY spectrum of *2a* showing the (H^A-4)-(H^B-1) correlation peak.

In contrast with what observed for compound ***2a***, the characterization of the 2A,2C-ditosyl-2A,2C-dideoxy-β-cyclodextrin (compound ***2b***) by 2D NMR spectra was much difficult to obtain, since, the two substituted units (units A and C) are not strictly linked one to the other but they are now bound to the same unsubstituted unit (unit B) that lies between the units A and C, as shown in Figure 4.24.

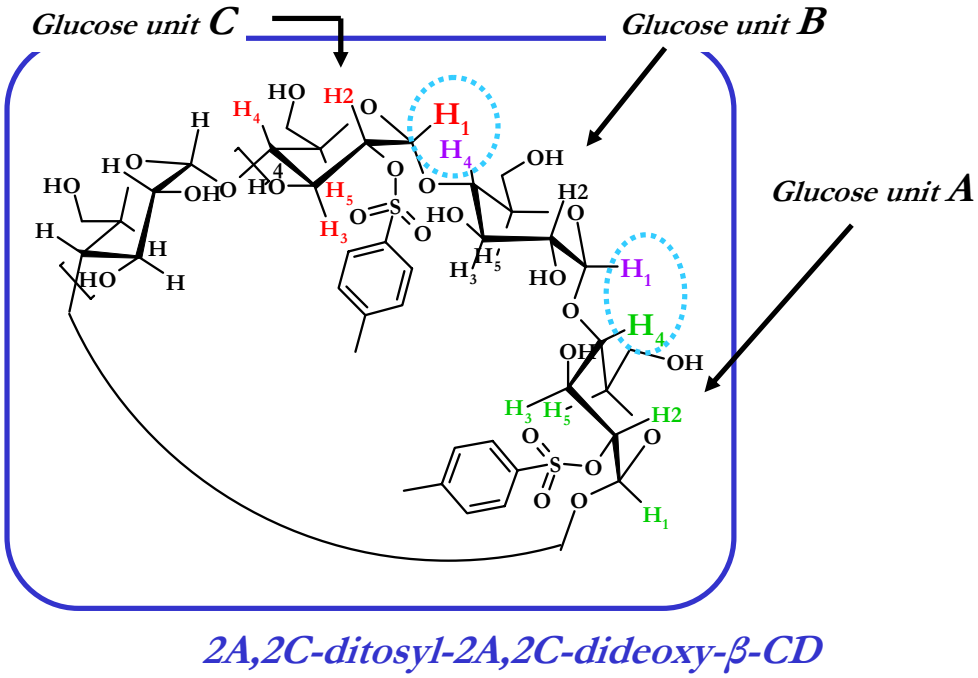

Figure 4.24: Structure of 2A,2C-ditosyl-2A,2C-dideoxy-β-CD (*2b*).

Due to the presence of an unsubstituted glucosidic unit between the units A and C, the key correlation peaks that could unambiguously characterize this compound are (H^A-4)-(H^B-1) and (H^B-4)-(H^C-1). Also in the ^{1}H-NMR spectra of compound ***2b***, as well as in the analogous spectra of the ditosyl AB, signals relative to the H-2 and H-3 of the substituted units are clearly separated from those of the other nuclei allowing to recognize the H-1 signals relative to the same units (H^A-1 and H^C-1) (see Figure 4.25and Figure 4.26).

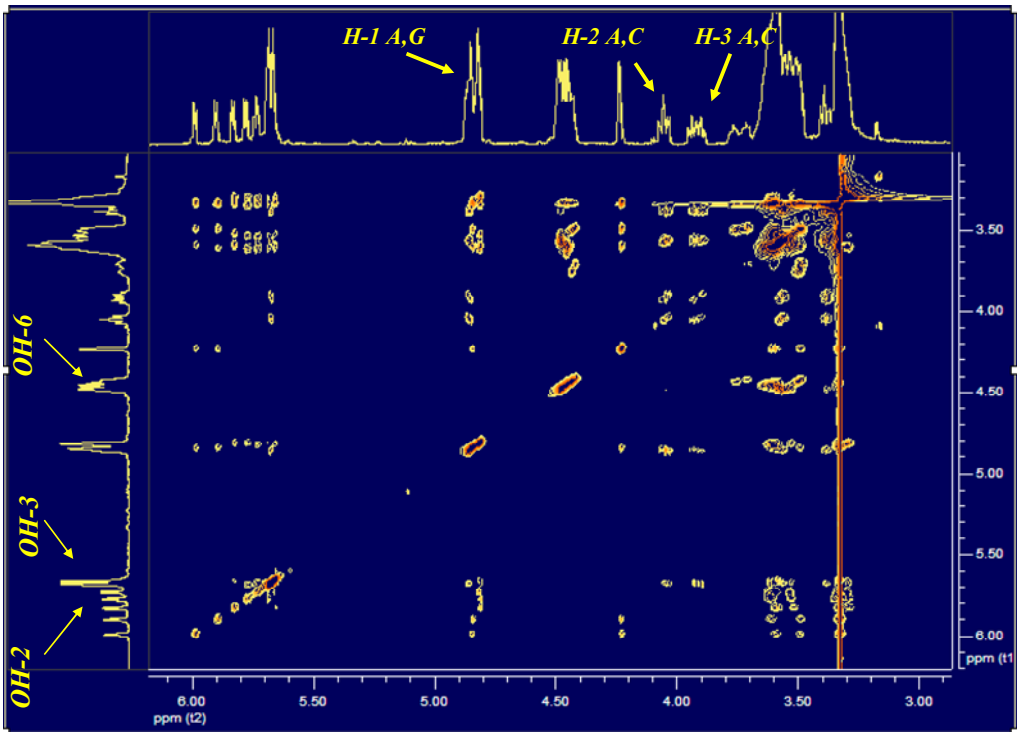

Figure 4.25: TOCSY NMR spectrum of the carbohydrate part of compound *2b* in DMSO-d_6 solution. Mixing time: 160 ms.

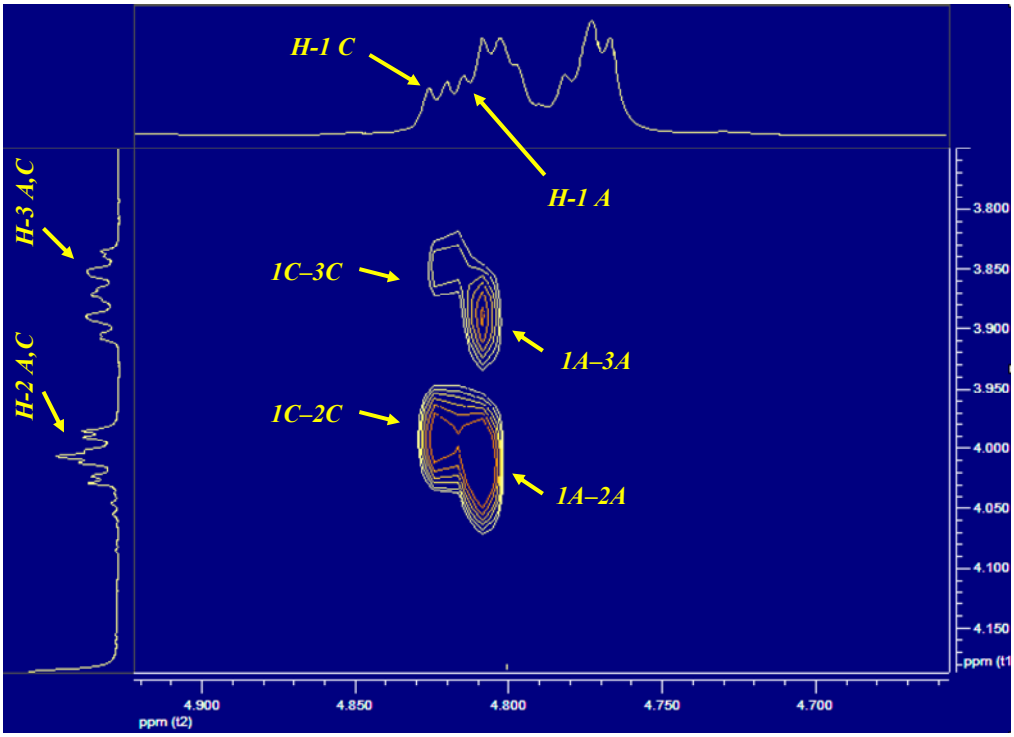

Figure 4.26: TOCSY NMR spectrum of *2b*. (H-1)-(H-2) and (H-1)-(H-3) correlation peaks for the substituted units A and C.

By the well separated OH-2 signal, then it was possible to recognize signals relative to H-1 and H-4 of the unsubstituted unit B (see Figure 4.27 and Figure 4.28) that are important, as explained before, for searching the two (H^A-4)-(H^B-1) and (H^B-4)-(H^C-1) key correlation islands needed to verify a disubstitution with an AC regioisomery by ROESY NMR spectroscopy.

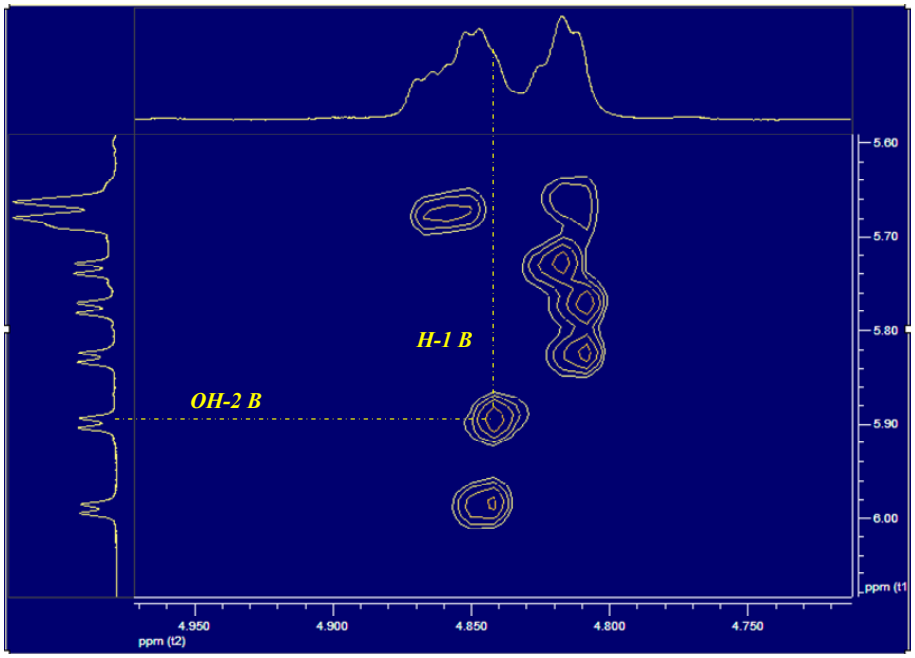

Figure 4.27: TOCSY spectrum of *2b*. (OH-2)-(H-1) correlation for the glucosidic unit B.

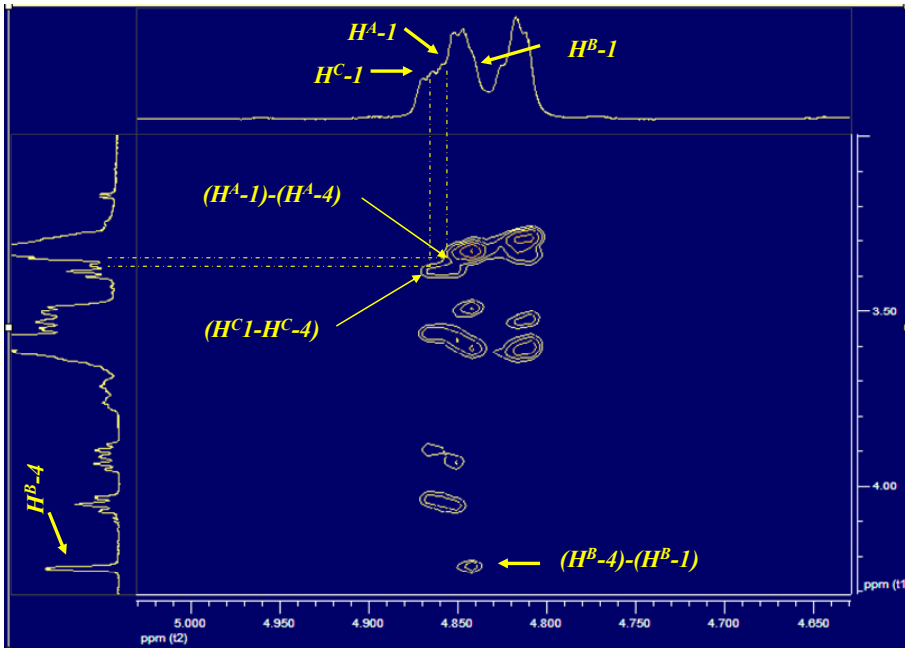

Figure 4.28: TOCSY spectrum of *2b*. (H-1)-(H-4) correlations for the unit A, B and C.

Finally, by the ROESY spectrum, the two key correlations characterizing the AC di-substitution were found, as shown in Figure 4.29 and in Figure 4.30.

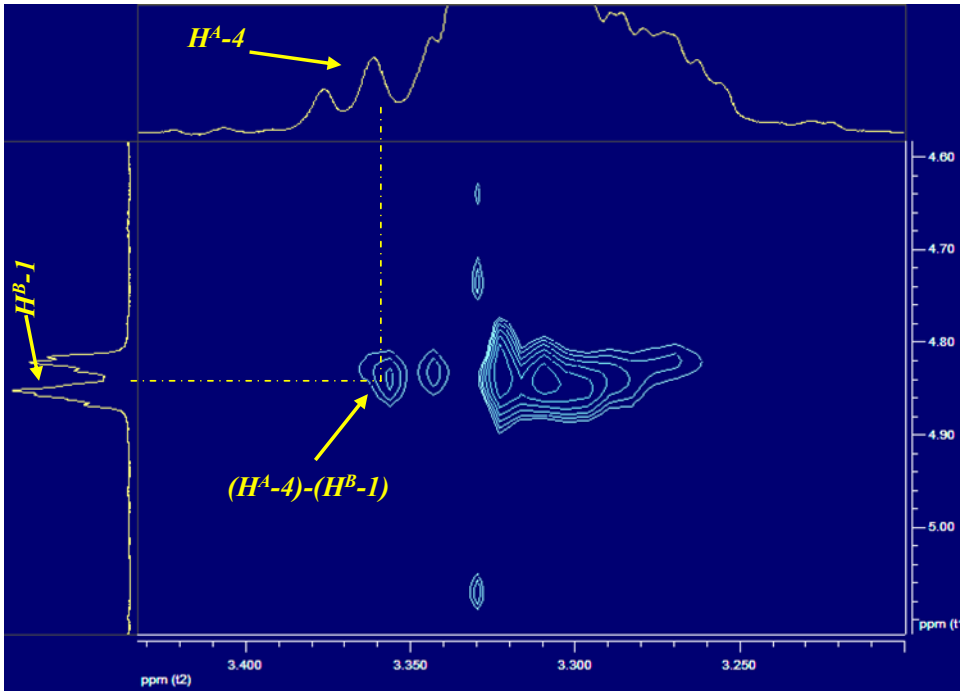

Figure 4.29: Section of the ROESY spectrum of *2b* showing the (H^A-4)-(H^B-1) correlation peak.

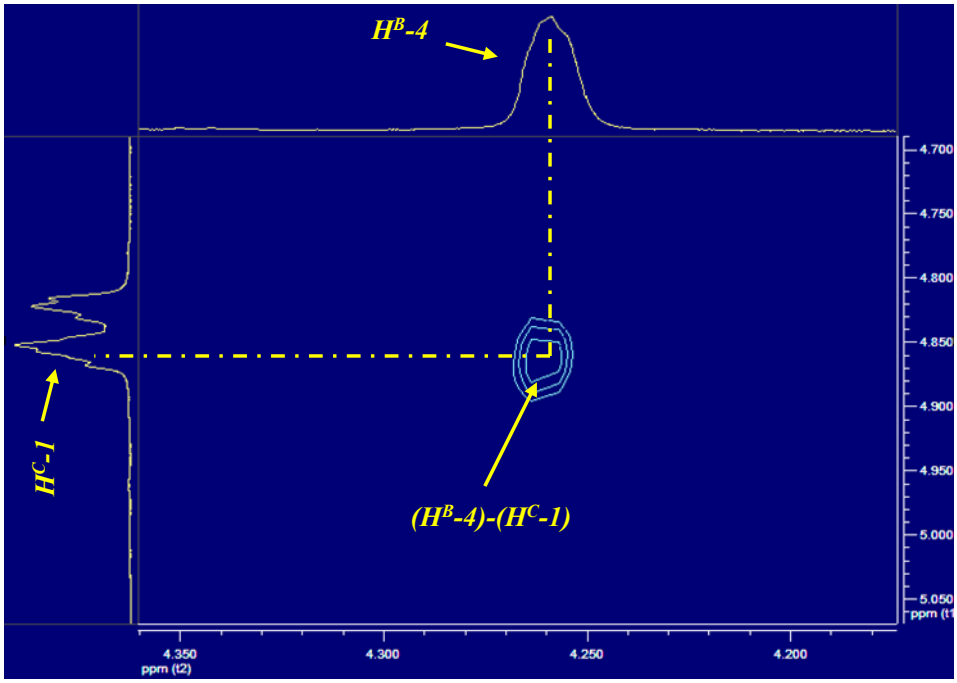

Figure 4.30: Section of the ROESY spectrum of *2b* showing the (H^B-4)-(H^C-1) correlation peak.

In contrast with what observed for compounds ***2a*** and ***2b***, the characterization of the 2A,2D-ditosyl-2A,2D-dideoxy- β-cyclodextrin (***2c***) by 2D analysis was not obtained. Indeed, the presence of two unsubstituted units (B and C) between the two sulfunylated units (A and D) did not allow to obtain data with which to get information about the regiochemistry of the disubstitution, since it was not possible to recognize exactly signals relative to all hydrogens contained in the glucose units A, B, C and D.

However, the exact characterizations of the ditosyl A,B- and A,C-dideoxy-β-cyclodextrin obtained as described above, allow confirming that the ^{1}H-NMR spectrum showing two doublets in the aromatic region is relative to the A,D regioisomer.

4.5.2.3 Conclusion.

Results obtained by 2D NMR analysis performed through TOCSY and ROESY experiments allowed to obtain the exact characterization of the 2A,2X-ditosyl-2A,2X-dideoxy-β-cyclodextrin, confirming results previously obtained by using the ESI-MS spectrometry.

The discrimination of the three regioisomers performed by using 2D NMR techniques allow to get, now, information about the regioisomery of the three ditosyl cyclodextrin derivatives simply recording rapid ^{1}H-NMR spectra.

Moreover, coupling of TOCSY and ROESY experiments showed to the discrimination of the three regioisomers can be considered, in general, as powerful tool for a clear recognition homo- and hetero-difunctionalized β-cyclodextrin.

4.6 Synthesis of 2-guanidinium-2-(S)-β-CD.

In order to insert a positive charge at the lower rim, the guanidinium ion was chosen on the basis of its pK_a value (≈ 13), which allows to have a positively charged cyclodextrin derivative also at pH values equal to 9 or 10.

Since the introduction of the guanidinium functional group can be obtained by a nucleophilic attack of an amino group toward an appropriate guanidilating reagent, guanidinium-containing β-cyclodextrin ***6a*** has been prepared *via* the known amino derivative ***5a*** using the guanylating agent 1H-pyrazolecarboxyamidine hydrochloride *7*.[33] The overall synthetic scheme followed to prepare the desired target is shown in Figure 4.31.

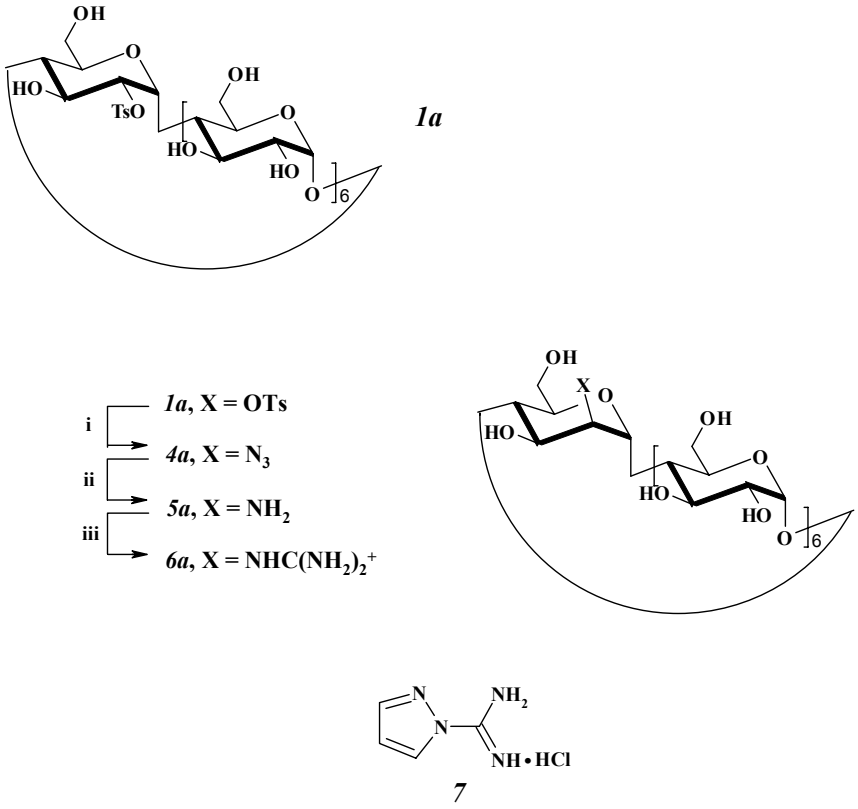

i: NaN_3, H_2O (90%); **ii**: 1) TPP, DMF, 2) H_2O (90%); **iii**: *7*, $(i\text{-}Pr)_2NEt$, DMF (40%).

Figure 4.31: Synthetic procedures followed for the synthesis of *6a*.

First of all, the tosylate derivative was converted into the azido derivative *via* nucleophilic substitution of the tosyl group by the sodium azide in water. The reaction was chemoselective since it gave only ***4a*** as the unique product, but proceeding by a SN2 mechanism, it caused inversion of the configuration at the C-2 of the substituted unit providing thus a mannosidic unit. In order to avoid this conversion, the tosyl group was first substituted with KI, but no good results were obtained, mainly because of steric hindrance. The disapparence of the typical signals of the

aromatic protons observed by the ^{1}H-NMR spectrum confirmed the substitution with the azido group.

The reduction of the azido group to the amino group was obtained by the Staudinger reaction. The mechanism with which ***4a*** was converted in to ***5a*** is shown in Figure 4.32.

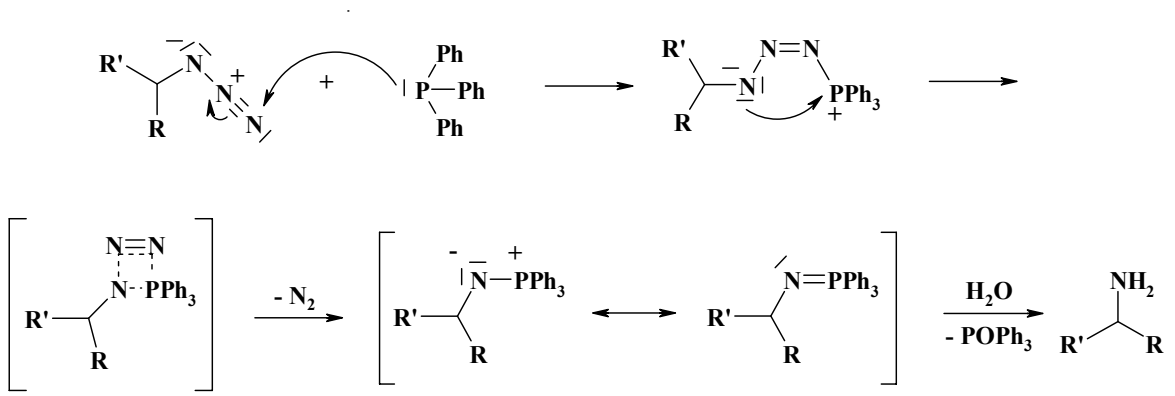

Figure 4.32: Mechanism of the Staudinger reaction.

Among the advantages presented by the reaction, the selectivity of the triphenylphosphine towards the azido group, no drastic reaction conditions were requested, high yields were obtained and a facile separation of the triphenylphosphineoxyde from the amino cyclodextrin products was achieved by washing the precipitate, obtained by adding the reaction mixture drop wise to a great excess of acetone, with acetone. In particular, the scheme of the reaction followed in the case of 2-azido-2(S)-β-cyclodextrin is shown in Figure 4.33.

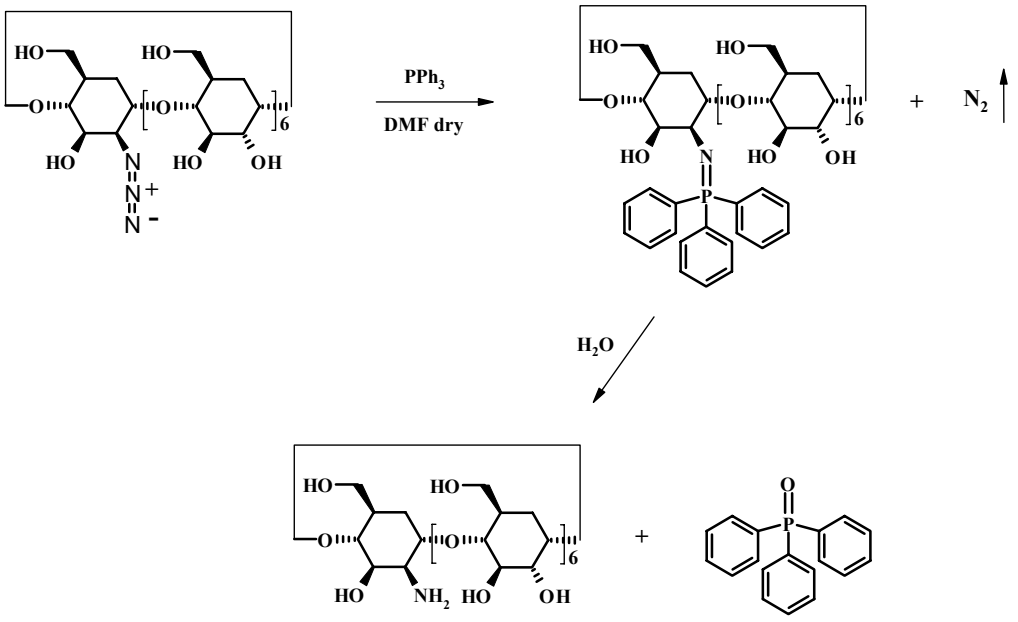

Figure 4.33: Reduction of the azido derivative *4a*.

Finally, the guanidilation was performed using the guanidilating agent ***7*** in the presence of the 2-amino-2(S)-β-cyclodextrin and (i-Pr)NEt as base and using DMF as solvent. The purification of the product was performed by ion-excange chromatography using sephadex C-25 as stationary phase. The yield of the reaction was not so high (40 %) probably because of the loss of part of the product during the purification step.

4.7 Tosylation of β-CD at the 6-position

The sulfonylation of the β-cyclodextrin at the 6-position with tosyl chloride has been performed following the procedure reported by Takahashi et al.[34] The scheme of reaction is shown in Figure 4.34.

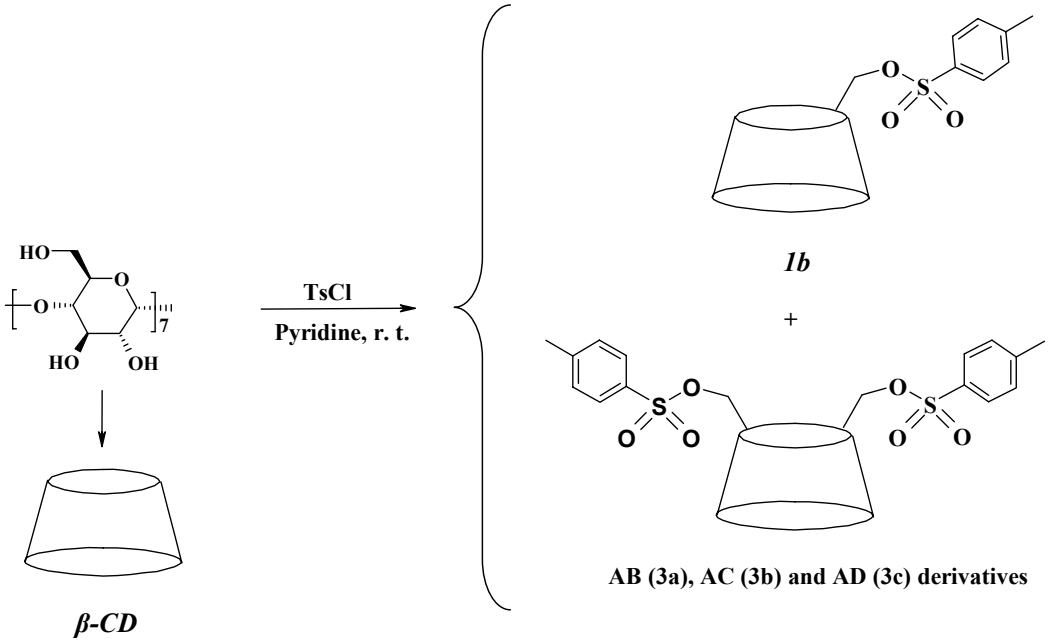

Figure 4.34: Tosylation of β-CD with TsCl in pyridine.

As shown in the figure, this kind of reaction is chemoselective towards the nucleophilic attack of the OH-6 to the tosyl chloride but, as for the tosylation at the 2-position, produces a mixture of mono and bitosylated species. Mono and ditosylated compounds were then purified by RP-HPLC; the yield of the 6-tosyl-6-deoxy-β-cyclodextrin was 30 %, while the yield of the three di-tosylate regioisomers was 7 %.

4.8 Synthesis of 6-guanidinium-β-CD

The synthesis of 6-guanidinium-β-cyclodextrin was performed as described in Figure 4.35.

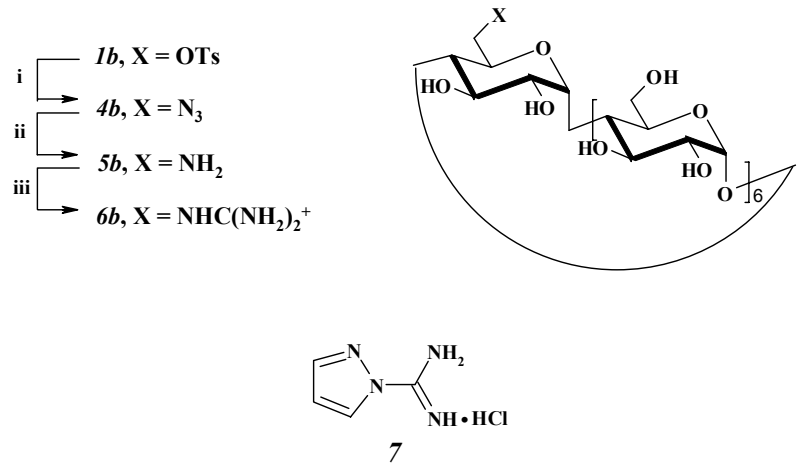

i: KI, NaN_3, DMF dry (90%); **ii**: 1) TPP, DMF, 2) H_2O (90%); **iii**: *7*, $(i\text{-}Pr)_2NEt$, DMF (40%).

Figure 4.35: Synthetic procedures for the synthesis of *6b*.

As it can be seen, compound ***1b*** was converted to the azido derivative ***4b*** *via* nucleophilic substitution of the tosyl group by sodium azide in DMF. Then, the azido derivative ***4b*** was reduced in the presence of triphenylphosphine to the amino derivative ***5b*** *via* the Staudinger reaction. Finally, the reaction between 6-amino-6-deoxy-β-cyclodextrin and the guanilating reagent *7* in DMF gave the desired product ***6b*** with a yield that was not higher than 40 % for the same reason explained for the compound ***6a***.

4.9 Synthesis of multi-charged CD derivatives

With the purpose to favour OTA complexation in its dianionic form, we thought to insert two positive charges on the upper rim of the β-cyclodextrin. In particular, we placed two amino groups at different distances one from another on the upper rim (AB, AC and AD).

Moreover, we also wanted to see the effect of the presence of many positive charges on the upper rim of the cyclodextrin on ochratoxin A recognition; for this reason we have synthesized the per(6-guanidinium) derivative of β-cyclodextrin.

4.9.1 Diamino β-CD derivatives functionalized at the 6-position.

The synthesis of the three diamino regioisomers of β-cyclodextrins functionalized on the upper rim is based on the derivatization of the 6A,6X-ditosyl-β-cyclodextrins that have been prepared by tosylation of β-cyclodextrin performed in pyridine.

The synthesis of the diamino derivatives starting from the correspondents ditosylate species is shown in Figure 4.36.

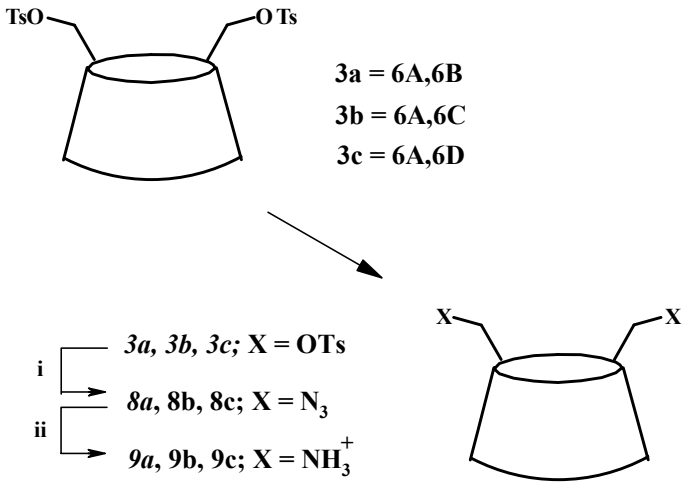

i: KI, NaN_3, DMF dry (85%); **ii**: 1) TPP, DMF, 2) H_2O (88%).

Figure 4.36: Synthetic procedures followed for the synthesis of AB, AC and AD diamino derivatives.

4.9.2 Per(6-guanidinium)-β-CD.

Because of several difficulties associated with the regioselective functionalization of cyclodextrins, which involve non-uniform, incomplete substitution, purification of the products from starting materials and finally comprehensive characterization, reliable procedures affording cleanly substituted, well characterized per–substituted derivatives continue to be in need. Furthermore, the preparation of per-substituted cyclodextrins bearing charged groups has received particular attentions[35] since the presence of a geometrically defined charged region on the upper or the lower rim may presents a significant alternative receptor to the cavity itself.

The synthesis of the per(6-guanidinium)-β-cyclodextrin is shown in Figure 4.37.

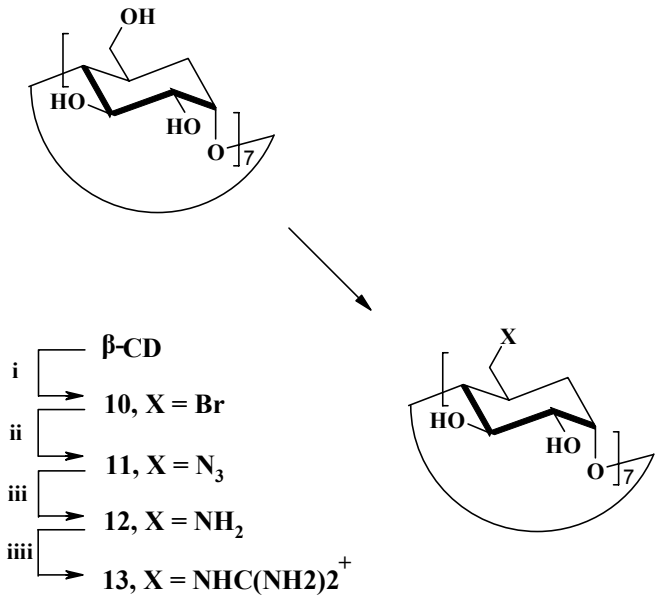

i: Br_2, TPP, DMF (70%); **ii**: KI, NaN_3, DMF (90%); **iii**: 1) TPP, DMF, 2) $NH_{3\ aq}$ (90 %); **iiii**: ***7***, $(i\text{-}Pr)_2NEt$, DMF (40%).

Figure 4.37: Synthesis of per(6-guanidinium)-β-CD.

Using literature procedures, the natural β-cyclodextrin was first converted to the corresponding per(6-bromo)-dirivative ***10***.[36] Since the direct guanidilation of ***10*** does not allow to obtain the target molecule, as reported by Yannakopoulou,[37] a longer but efficient route was followed, where the per(6-bromo)-β-cyclodextrin was converted to per (6-azido)-β-cyclodextrin ***11***, then to per(6-amino)-β-cyclodextrin ***12***[38], and finally to per(6-guanidinium)-β-cyclodextrin ***13*** after treatment of ***12*** with 1-H-pyrazolecarboxyamidine hydrochloride ***7*** as the guanidilating agent.[37] The final product was purified with chloroform washing with the aim to remove small molecules and solvents.

A very useful indication for the sequential functional group transformations were the chemical shifts of the carbon atoms C-6 of the primary side, which changed from ~62 ppm in the natural β-cyclodextrin to 34 ppm in ***10***, 51 ppm in ***11***, 43 ppm in ***12*** and 45.5 ppm in ***13***.

4.10 Experimental

4.10.1 General.

The following materials were obtained from commercial suppliers and were used without further purification: β-cyclodextrin hydrate (Aldrich), tosyl chloride (Fluka), P_2O_5 (Aldrich), NaH (Sigma). DMF (Backer) was dried over molecular sieves (3 Å). Thin layer chromatographic analyses were conducted using precoated TLC silica gel plates (60 F-254, Merck). The detection of cyclodextrin derivatives on SiO_2 TLC plates was achieved using the anisaldehyde test. HPLC chromatography was performed on a Waters HPLC Chromatograph, equipped with a model 4000 pump and a model 2487 UV detector, set at 254 nm, with a C18 spherisorb column (25 x 250 mm). ^{1}H NMR and ^{13}C NMR were recorded on Bruker AC300 and Varian INOVA 600. ESI-MS experiments were performed on Micromass ZMD mass spectrometer (Micromass, Manchester, UK), fitted with an electrospray source and a single quadrupole mass analyser. Data were acquired by use of Masslynx 3.4 software (Micromass, Manchester, UK).

4.10.2 Syntheses.

2-Tosyl-2-deoxy-β-CD (*1a*) and 2A,2X-ditosyl-2A,2X-dideoxy-β-CD (*2a, 2b, 2c*):

To a solution of 3g (2.64 mmol) of β-cyclodextrin (dried overnight at 100 °C in the presence of P_2O_5) in 55 ml of DMF (dried over molecular sieves), 0.127 mg (60% in oil; 3.17 mmol) of NaH were added and the mixture was stirred overnight at room temperature until the solution became clear. To this solution, tosyl chloride (0.605g, 3.17 mmol) in 5 ml of DMF was added drop wise. After 2 hours, the solution was added to 1 L of acetone and the precipitate was filtered. TLC on silica gel using n-butanol, ethanol, water (5:4:3 by volume) showed more than one spot: one at Rf = 0.35 for cyclodextrin, another one at Rf = 0.54 for the mono-derivative and a last one at Rf = 0.6 for the diderivatives. Preparative HPLC (Water Delta Prep 4000, water spherisorb Column, 20 x 250 mm, 10 μm, linear gradient elution from water : methanol 72% : 28% to methanol in 25 min, flow 15 ml/min) allowed the purification of the mono tosylate and the di-derivatives, as white solids. Yield of the mono-substituted: 0.85g (25 %); yield of the AB isomer: 0.19g (5 %); yield of AC and AD isomers: 0.11g (3 %).

2-tosyl-2-deoxy-β-CD

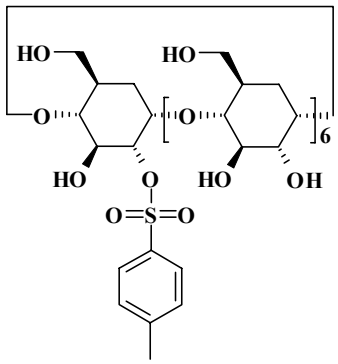

(***1a***)

^{1}H NMR (300 MHz, DMSO-d_6) δ: 2.41 (s, 3H, CH_3), 3.25-3.40 (m, 14 H, H-6), 3.45-3.65 (m, 25 H, H-2, 3, 4, 5), 3.70-3.80 (m, 1H, H-4'), 3.85-3.95 (m, 1H, H-5'), 4.02-4.06 (m, 1H, H-3'), 4.22 (d, 1H, J = 3.9 Hz, H-2'), 4.43-4.49 (m, 7H, OH-6), 4.82 (s, 7H, H-1), 5.67-5.90 (m, 13H, OH-2, 3), 7.44 (d, 2H, J = 9.0 Hz, aromatic H), 7.85 (d, 2H, J = 9.0 Hz, aromatic H).

^{13}C NMR (75 MHz, DMSO-d_6) δ:21.0 (CH_3), 59.70 (C-6, C6'), 69.12 (C-3'), 71.86 (C-5, C-5'), 72.20 (C-2), 72.85 (C-3), 79.50 (C-2'), 80.70 (C-4'), 81.33 (C-4), 97.90 (C-1'), 101.70 (C-1), 127.90, 129.70, 132.70 and 144.80 (aromatic C).

ESI MS (m/z): 1311 $[M + Na]^{+}$, 667 $[M + 2Na]^{++}$.

*Symbol 'indicate hydrogen and carbon signals of the substituted glucosidic unit.

2A,2B-ditosyl-2A,2B-dideoxy-β-CD

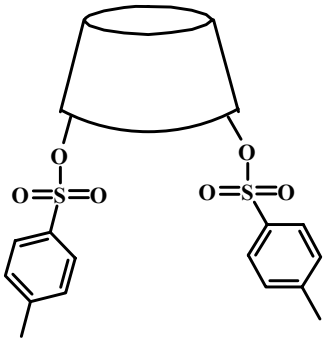

(***2a***)

^{1}H NMR (600 MHz, DMSO-d_6) δ: 2.41 (s, 6H, CH_3), 3.47-3.23 (m, 12H, H-2, 4, 4', 4''), 3.67-3.52 (m, 26H, H-3, 5, 5', 5'', 6, 6', 6''), 3.90-3,83 (m, 2H, H-3', 3''), 4.01 (dd, 1H, J = 10.02, 3.46 Hz, H-2''), 4.09-4.03 (bs, 1H, H-2'), 4.49-4.36 (m, 7H, OH-6), 4.74 (d, 1H, J = 3.56 Hz, H-1''), 4.81-4.75 (m, 5H, H-1), 4.88 (d, 1H, J = 3.33 Hz, H-1'), 5.78-5.57 (m, 12H, OH-2, 3, 3', 3''), 7.34 (d, 2H, J = 8.22 Hz, aromatic H), 7.41 (d, 2H, J = 8.22 Hz, aromatic H), 7.72 (d, 2H, J = 8.22 Hz, aromatic H), 7.85 (d, 2H, J = 8.22 Hz, aromatic H).

^{13}C-NMR (75 MHz, DMSO-d_6) δ: 21.0 (CH_3), 21.2 (CH_3), 59.8 (C-6, 6', 6''), 68.7 (C-3'), 69.0 (C-3''), 71.6 (C-5,5',5''), 72.3 (C-2), 72.8 (C-3), 79.1 (C-2', 2''), 81.0 (C-4',4''), 81.5 (C-4), 96.9 (C-1''), 97.5 (C-1'), 101.8 (C-1), 127.90, 129.60, 133.0 and 144.6 (aromatic C).

ESI-MS (m/z): 1466 $[M+Na]^{++}$, 744 $[M+2Na]^{++}$.

*Symbols ' and '' indicate hydrogen and carbon signals of the unit A and B, respectively.

2A,2C-ditosyl-2A,2C-dideoxy-β-CD

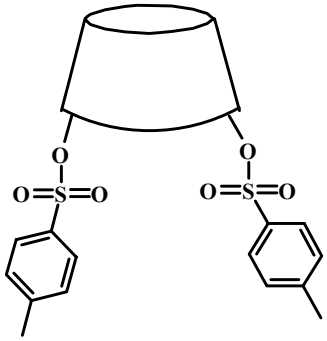

(***2b***)

^{1}H NMR (600 MHz, DMSO-d_6) δ: 2.41 (d, 6H, J = 4.32 Hz, CH_3), 3.41-3.22 (m, 10H, H-2, 4, 4', 4''), 3.79-3.45 (m, 26H, H-3, 5, 5', 5'', 6, 6', 6''), 3.96-3.86 (m, 2H, H-3', 3''), 4.07-4.01 (m, 2H, H-2', 2'), 4.24-4.22 (m, 2H, H-4), 4.50-4.39 (m, 7H, OH-6, 6', 6''), 4.88-4.78 (m, 7H, H-1, 1', 1''), 5.69-5.63 (m, 7H, OH-3, 3', 3''), 5.73 (d, 1H, J = 6.6 Hz, OH-2), 5.77 (d, 1H, J = 6.6 Hz, OH-2), 5.83 (d, 1H, J = 6.6 Hz, OH-2), 5.90 (d, 1H, J = 6.6 Hz, OH-2), 5.99 (d, 1H, J = 6.6 Hz, OH-2), 7.45 (dd, 4H, J = 7.95, 5.36 Hz, aromatic H), 7.85 (dd, 4H, J = 7.95, 5.36 Hz, aromatic H).

^{13}C-NMR (75 MHz, DMSO-d_6) δ: 21.0 (2 x CH_3), 59.70 (C-6, 6', 6''), 69.08 (C-3', 3''), 71.46 (C-5, 5', 5''), 72.19 (C-2), 72.87 (C-3), 79.5 (C-2', 2'') 80.6 (C-4', 4''), 81.40 (C-4), 97.90 (C-1', 1''), 101.70 (C-1), 127.90, 129.68, 132.74 and 132.76 (aromatic C).

ESI-MS (m/z): 1466 $[M+Na]^{++}$, 744 $[M+2Na]^{++}$.

*Symbols ' and '' indicate hydrogen and carbon signals of the unit A and C, respectively.

2A,2D-ditosyl-2A,2D-dideoxy-β-CD

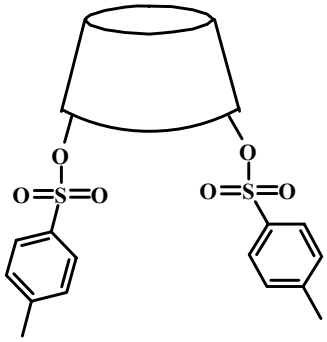

(***2c***)

^{1}H NMR (600 MHz, DMSO-d_6) δ: 2.41 (s, 6 H, CH_3), 3.42-3.20 (m, 12 H, H-2, 4, 4', 4''), 3.70-3.50 (m, 26 H, H-3, 5, 5', 5'', 6, 6', 6''), 3.92-3.80 (t, 2 H, J = 10 Hz, H-3', 3''), 4.03 (dd, 2 H, J = 10, 3.6 Hz, H-2', 2''), 4.19 (d, 2 H, J = 3.6 Hz, H-4), 4.48-4.15 (m, 7 H, OH-6, 6', 6''), 4.86-4.79 (m, 7 H, H-1, 1', 1''), 5.71-5.64 (m, 7 H, OH-3, 3', 3''), 5.78 (d, 1 H, J =
7 Hz, OH-2), 5.85 (t, 2 H, J = 6 Hz, OH-2), 5.885 (d, 1 H, J = 6 Hz, OH-2), 5.93 (d, 1 H, J = 6 Hz, OH-2), 7.436 (d, 4 H, J = 7.8 Hz, aromatic H), 7.84 (dd, 4H, J = 8, 2 Hz, aromatic H).

^{13}C-NMR (75 MHz, DMSO-d_6) δ: 21 (2 x CH_3), 59.64 (C-6, 6', 6''), 69.1 (C-3', 3''), 71.9 (C-5, 5'', 5''), 72.1 (C-2), 73.0 (C-3), 79.2 (C-2', 2''), 80.1 (C-4', 4''), 81.5 (C-4), 97.8 (C-1', 1''), 101.73 (C-1), 127.91, 129.69, 132.70 and 144,76 (aromatic C).

ESI-MS (m/z): 1466 $[M+Na]^{++}$, 744 $[M+2Na]^{++}$.

*Symbols ‘ and ’’ indicate hydrogen and carbon signals of the unit A and D, respectively.

6-Tosyl-6-deoxy-β-CD (*1b*) and 6A,6X-ditosyl-6A,6X-dideoxy-β-CD (*3a, 3b 3c*):

A solution of p-toluenesulfonyl chloride (1.5g, 7.9 mmol) in 15 ml of anhydrous pyridine was added to a solution of 5g (4.4 mmol) of β-cyclodextrin (dried overnight at 100°C in the presence of P_2O_5) in 50 ml of anhydrous pyridine at 5°C. This solution was stirred at room temperature; after 9h it was added to 1 L of acetone and the precipitate was filtered to recover a colourless solid containing the cyclodextrin products. TLC on silica gel using n-butanol, ethanol, water (5:4:3 by volume) as eluent showed more than one spot. Preparative HPLC (Water Delta Prep 4000, water spherisorb Coloumn, 20 x 250 mm, 10 μm, linear gradient elution from water : methanol 72% : 28% to methanol in 25min, flow 15 ml/min) allowed the purification of the mono-tosyl derivative and the three di-substituted isomers as white solids. Yield of the mono-substituted: 3g (30 %); yield of the AB, AC and AD isomers: 0.8g (7 %).

6-tosyl-6-deoxy-β-CD

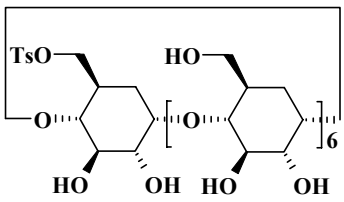

(***1b***)

^{1}H NMR (300 MHz, DMSO-d_6) δ: 3.17 (s, 3 H, CH_3), 3.84-3.00 (m, 42 H, H-2, 3, 4, 5, 6), 4.70-4.00 (m, 6 H, OH-6), 4.84 (bs, 7 H, H-1), 5.71 (bs, 14 H, OH-2, 3), 7.43 (d, 2 H, J = 8.2 Hz, aromatic H), 7.76 (d, 2 H, J = 8.2 Hz, aromatic H).

^{13}C-NMR (75 MHz, DMSO-d_6) δ:

ESI-MS (m/z): 1290 $[M+H]^+$.

6A,6B-ditosyl-6A,6B-dideoxy-β-CD

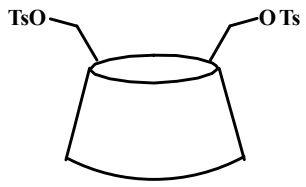

(***3a***)

^{1}H NMR (600 MHz, CD_3OD-d_4) δ: 2.49 (s, 3 H, CH_3), 2.50 (s, 3 H, CH_3), 3.92-3.25 (m, 38 H, H-2, 3, 4 ,5, 6), 4.27 (td, 2 H, J = 11.2, 5.1 Hz, H-6), 4.38 (d, 1 H, J = 10.8 Hz, H-6), 4.495 (d, 1 H, J = 10.8 Hz, H-6), 4.72 (d, 1H, J = 3 Hz, H-1), 4.886 (d, 1H, J = 3 Hz, H-1), 4.94-4.90 (m, 1 H, H-1), 4.948 (d, 1H, J = 3 Hz, H-1), 4.97 (d, 1H, J = 3 Hz, H-1), 4.99 (bs, 1 H, H-1), 7.445 (t, 4 H, J = 7.2 Hz, aromatic H), 7.79 (dd, 4 H, J = 16.8, 8.4 Hz, aromatic H).

^{13}C-NMR (75 MHz, CD_3OD-d_4) δ: 21.82 (2xCH_3), 61.34

(C-6), 61.64 (C-6), 61.73 (C-6), 61.89 (C-6), 70.68 (C-5), 70.76 (C-5), 71.14 (C-5), 73.43 (C-3), 74.09 (C-2), 82.30 (C-4), 82.71 (C-4), 83.30 (C-4), 103.17 (C-1), 103.29 (C-1) 103.99 (C-1), 129.14, 131.07, 134.69 and 146.70 (aromatic C).

ESI-MS (m/z): 1466 $[M+Na]^{++}$, 744 $[M+2Na]^{++}$.

Data for the complete characterization of 6A,6C- and 6A,6D-ditosyl-β-CD (***3b*** and ***3c***) are reported on the thesis of laurea in Chemistry of G. Buccella – "*Sintesi e proprietà operative di una β-ciclodestrina funzionalizzata con un ponte tetraammidico chirale"* (**1994-95**).

2A-azido-2A-deoxy-2(S)-β-cyclodextrin (*4a*):

A mixture of ***1a*** (0.1g, $7.75*10^{-2}$ mmol) and sodium azide (0.075g, 1.15 mmol) in water (0.5 ml) was stirred at 80° C for two days. The resulting solution was then concentrated to half its volume and added to 200 ml of acetone. A white solid precipitated. This process was repeated again to provide the azido derivative as a white solid. Yield: 0.085g (90 %).

<u>*2A-azido-2A-deoxy-2(S)-βCD*</u>

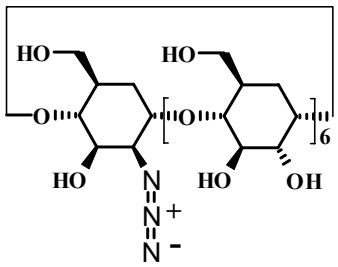

(***4a***)

^{1}H NMR (300 MHz, DMSO-d_6) δ: 3.27-3.24 (m, 14 H, H-2, 4), 3.95-3.53 (m, 28 H, H-3, 5, 6), 4.50 (m, 7 H, OH-6), 4.80 (m, 7 H, H-1), 5.80-5.60 (m, 13 H, OH-2, 3).

^{13}C-NMR (75 MHz, DMSO-d_6) δ: 30.5 (C-2'), 59.7 (C-6, 6'), 61.1 (C-6'), 69.7 (C-3'), 71.6 (C-5, 5'), 71.9 (C-2), 73.1 (C-3), 80.0 (C-2'), 80.9 (C-4, 4'), 101.6 (C-1), 103.1 (C-1').

ESI-MS (m/z): 1182 $[M+Na]^{+}$, 1160 $[M+H]^{+}$,
599 $[M+Na+NH_4]^{++}$

*Symbols ' indicate carbon signals of the unit A.

2-amino-2-deoxy-2(S)-β-CD (*5a*):

Triphenylphosphine (0.018g, $7.0*10^{-2}$ mmol) was stirred with ***4a*** (0.062g, $5.3*10^{-2}$) in dry DMF (0.7 ml) for 2h at room temperature. Then, deionized water (0.1 ml) was added and the solution was kept to 70° C for 2 days. After that the solvent was removed, acetone was added to wash the solid from the triphenylphosphine and the triphenylphosphinoxyde. The solid was collected by filtration and dried under high vacuum. Yield: 0.047g (90 %).

2-amino-2-deoxy-2(S)-β-CD

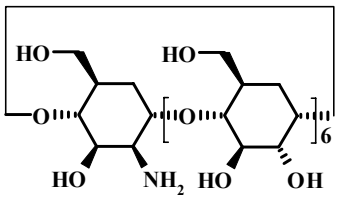

(***5a***)

^{1}H NMR (300 MHz, DMSO-d_6) δ: 3.36-3.30 (m, 14 H, H-6), 3.80-3.53 (m, 28 H, H-3, 5, 6), 4.64-4.44 (m, 7 H, OH-6), 4.90-4.70 (m, 7 H, H-1), 5.85-5.58 (m, 13 H, OH-2, 3), 7.64-7.53 (m, 2 H, NH2).

^{13}C-NMR (75 MHz, DMSO-d_6) δ: 52.7 (C-2'), 59.6 (C-6, 6'), 71.5 (C-5, 5'), 72.1 (C-2), 73 (C-3), 79.8 (C-4'), 81.6 (C-4), 101.9 (C-1), 103.8 (C-1').

ESI-MS (m/z): 1156 $[M+Na]^+$, 1134 $[M+H]^+$, 579 $[M+H+Na]^+$.

*Symbols ' indicate carbon signals of the unit A.

2-guanidinium-2-deoxy-2(S)-β-CD (*6a*):

Crude ***5a*** (0.04g, $3,5*10^{-2}$ mmol) was suspended in 400 µl of dry DMF and 1-H-pyrazolecarboxamidine hydrochloride (0.034g, 0.23 mmol) and DIEA (43 µl) were added. The reaction was stirred 2 days under N_2 and, after this time, the solution was dropped in a flask containing 20 ml of ether; the resulting suspension was stirred for 2h. The precipitate collected by filtration was dissolved in water and the solution was applied to a column of CM-Sephadex C-25 resin (in NH_4^+ form). The column was initially eluted with water (100 ml) and then with a linear gradient of aqueous ammonium hydrogen carbonate (10-200 mM). The collected fractions were assayed by TLC. Fractions that gave only one spot with R_f = 0.04 (eluent 7:7:5:4 EtOAc/2-propanol/NH_4OH/H_2O) were combined, concentrated and repeatedly lyophilized from deionized water to provide the bicarbonate salt of ***6a*** as a fluffy white solid. Yield: 0.014g (40 %).

2-guanidinium-2-deoxy-2(S)-β-CD

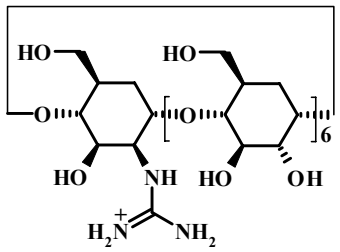

(***6a***)

^{1}H NMR (300 MHz, D_2O) δ: 3.60-3.45 (m, 16 H), 3.90-3.70 (m, 26 H), 3.97 (t, 1 H, H-3'), 4.12-4.08 (m, 1 H, H-2'), 5.05-4.87 (m, 7 H, H-1).

^{13}C-NMR (75 MHz, D_2O) δ: 57.0 (C-2'), 73.5 (C-3'), 75.2 (C-3), 76.3 (C-2), 76.5 (C-5), 82.9 (C-4'), 84.0 (C-4), 105.2 (C-1), 107.0 (C-1'), 160.6 (C of the guanidinio group).

ESI-MS (m/z): 1177 $[M + H]^{+}$, 608 $[M + H + Na]^{++}$, 600 $[M + H + K]^{++}$.

*Symbols ' indicate hydrogen carbon signals of the unit A.

6-azido-6-deoxy-β-CD (*4b*):

To a solution of mono-6-tosyl-β-CD (0.48g; 0.37 mmol) in dry DMF (2 ml) warmed at 60°, KI (0.080 g; 0.5 mmol) and NaN_3 (0.24g; 3.7 mmol) were added. The reaction mixture was stirred at 60° C for 24h. The reaction mixture was then cooled to room temperature and treated with an anion exchange resin (amberlite IRA-400) and a cation exchange resin (Amberlite IR-120) to remove the salt. The solution was then concentrated to half volume and added drop wise to 100 ml of acetone. The white solid obtained was separated by filtration and washed with acetone. Yield: 0.38g (90 %).

6-azido-6-deoxy-β-CD

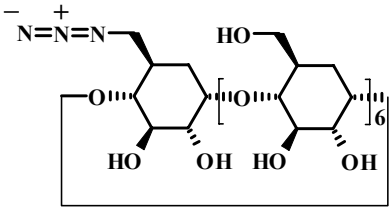

(***4b***)

^{1}H NMR (300 MHz, DMSO-d_6) δ: 3.45-3.25 (m, 14 H, H-2, 2', 4, 4'), 4.06-3.91 (m, 28 H, H-3, 3', 5, 5', 6, 6'), 4.60-4.45 (m, 6H, OH-6), 4.90-4.80 (m, 7 H, H-1, 1'), 5.80-5.60 (m, 14 H, OH-2, 3).

ESI-MS (m/z): 1182 $[M + Na]^{+}$, 599.8 $[M + Na + NH_4]^{++}$.

*Symbols ' indicate hydrogen and carbon signals of the unit A.

6-amino-6-deoxy-β-CD (*5b*):

The title compound was obtained from ***4b*** using the same procedure described for ***5a*** (yield: 90 %).

6-amino-6-deoxy-β-CD

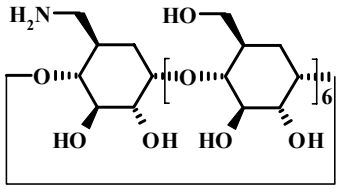

(***5b***)

^{1}H NMR (300 MHz, DMSO-d_6) δ: 3.50-3.26 (m, 30H, H2, 2', 3, 3', 4, 4', 5, 5', NH_2), 3.65-3.56 (m, 14 H, H-6, 6', 6''), 4.46, 4.43 (m, 6 H, OH-6), 4.89-4.82 (m, 7 H, H-1, 1'), 5.77-5.61 (m, 14 H, OH-2, 3).

^{13}C-NMR (75 MHz, DMSO-d_6) δ: 41.7 (C-6'), 59.9 (C-6), 72.0 (C-2), 72.4 (C-3), 73.0 (C-5), 81.6 (C-4'), 82.8 (C-4), 101.9 (C-1).

ESI-MS (m/z): 1134.50 $[M+H]^+$.

*Symbols ' indicate hydrogen and carbon signals of the unit A.

6-guanidinium-6-deoxy-β-CD (6*b*):

The title compound was obtained from ***4b*** using the same procedure described for ***6a*** (yield 40 %).

6-guanidinium-6-deoxy-β-CD

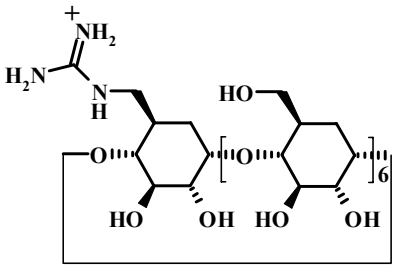

(***6b***)

^{1}H NMR (300 MHz, D_2O) δ: 3.70-3.50 (m, 16 H), 4.04-3.78 (m, 26 H), 5.13-5.03 (m, 7 H, H-1).

^{13}C-NMR (75 MHz, D_2O) δ: 42.98 (C-6'), 61.34 (C-6), 72.63 (C-3'), 73.73 (C-3), 73.86 (C-2, 2'), 81.90 (C-4'), 83.20 (C-4), 102.77 (C-1, 1'), 158.61 (C of the guanidinium group).

ESI-MS (m/z):1176.50 $[M+H]^+$, 599.80 $[M+H+Na]^{++}$.

*Symbols ' indicate carbon signals of the unit A.

6A,6B-diazido-6A,6B-dideoxy-β-CD (*8a*):

A,B-ditosyl-β-CD ***3a*** (0.062g, $4.36*10^{-2}$ mmol), KI (0.009g, $4.36*10^{-2}$ mmol) and NaN_3 (0.057g, 0.87 mmol) were dissolved in 5 ml of dry DMF, and the mixture was heated at 65 °C for one day with stirring under nitrogen. Then, the solvent was removed and acetone (100 ml) was added to the residue. The precipitate thus obtained was recovered by filtration and vacuum-dried to give the diazido derivative. Yield: 0.043g (85 %).

6A,6B-diazido-6A,6B-dideoxy-β-CD

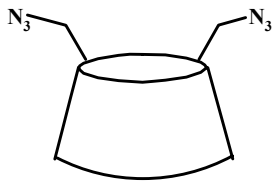

(***8a***)

^{1}H NMR (600 MHz, D_2O) δ: 5.13-5.07 (m, 7 H, H-1), 4.06-3.82 (m, 24 H, H-3, 5, 6), 3.72-3.56 (m, 18 H, H-2, 4, 6', 6'')

ESI-MS (m/z): 1223.2 $[M + K]^+$, 1207.2 $[M + Na]^+$.

*Symbols ' and '' indicate hydrogen signals of the unit A and B, respectively.

6A,6C-diazido-6A,6C-dideoxy-β-CD (*8b*):

Synthetic procedures and data for the characterization of compound ***8b*** are reported in the thesis of laurea in chemistry of S. Buonocore – "*β-ciclodestrine mono- e difunzionalizzate con gruppi cationici come selettori chirali in elettroforesi capillare"* (**1996-97**).

6A,6D-diazido-6A,6D-dideoxy-β-CD (*8c*):

Synthetic procedures and data for the characterization of compound ***8c*** are reported in the thesis of laurea in Chemistry of G. Buccella – "*Sintesi e proprietà operative di una β-ciclodestrina funzionalizzata con un ponte.tetraammidico chirale"* (**1994-95**).

6A,6B-diamino-6A,6B-dideoxy-β-CD (*9a*):

The diazido derivative ***8a*** (0.040g, $3.37*10^{-2}$ mmol) in 3 ml of dry DMF was treated with triphenylphosphine (0.052g, 0.2 mmol) for two hours. Then, deionized water was added (0.1 ml) to the solution and the mixture was kept to room temperature for one day. After removal of the solvent and acidification to pH 4 with hydrochloric acid, the unreacted triphenylphosphine and the triphenylphosphineoxyde produced were completely extracted with chloroform. Lyophilization of the aqueous solution gave the hydrochloride of the A,B-diamino-β-CD. Yield: 0.038g (88 %).

6A,6B-diamino-6A,6B-dideoxy-β-CD

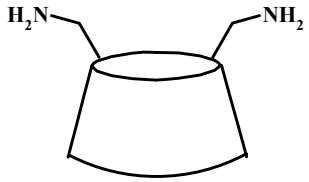

(***9a***)

^{1}H NMR (600 MHz, D_2O) δ: 3.22-3.10 (m, 2 H, H-6), 3.32 (dd, 1 H, J = 13.8, 4.8 Hz, H-6), 3.60-3.40 (m, 15 H, H-2, 4, 6), 4.02-3.68 (m, 24 H, H-3, 5, 6), 5.05-4.96 (m, 7 H, H-1).

^{13}C-NMR (75 MHz, D_2O) δ: 43.8 (C-6', 6''), 62.9 (C-6), 75.7-74.4 (C-5, 2, 3), 83.8 (C-4), 85.4 (C-4', 4''), 104.5 (C-1).
ESI-MS (m/z): 1136 $[M + H]^+$.

6A,6C-diamino-6A,6C-dideoxy-β-CD (*9b*):

Synthetic procedures and data for the characterization of compound ***9b*** are reported in the thesis of laurea in Chemistry of S. Buonocore – "*β-ciclodestrine mono- e difunzionalizzate con gruppi cationici come selettori chirali in elettroforesi capillare"* (**1996-97**).

6A,6D-diamino-6A,6D-dideoxy-β-CD (*9c*):

Synthetic procedures and data for the characterization of compound ***9c*** are reported in the thesis of laurea in Chemistry of S. Buonocore – "*β-ciclodestrine mono- e difunzionalizzate con gruppi cationici come selettori chirali in elettroforesi capillare"* (**1996-97**).

Per-6-bromo-6-deoxy-β-CD (*10*):

The bromination of β-cyclodextrin was carried out using the Vilsmeier-Haack reagent $[(CH_3)_2NCHBr]Br$, which was prepared by dropwise addition of Br_2 (3.2 ml, 62 mmol), to a solution of triphenylphosphine (16g, 62 mmol) in 70 ml of dry DMF with vigorous stirring, at 0 °C, under N_2. The resulting precipitate was further stirred at room temperature for 40 min. Then, 16 ml of dry DMF and β-CD (4g, 3.52 mmol) (previously dried over P_2O_5) were added to the Vilsmeier-Haack reagent, and the reaction mixture was heated at 75-80 °C, under N_2 (it is extremely important not to exceed 80 °C, in which case the solution turns dark-brown and the yield is severely diminished). After 12 h, the DMF was removed under vacuum and the remaining oil was poured into 50 ml of a 3 M sodium methoxyde solution in methanol, previously cooled to 0 °C. After 1 h of stirring at room temperature, the mixture was precipitated in 2 L of acetone and the white precipitate thus obtained was recovered by filtration. The per-6-bromo derivative was then dried under vacuum. Yield: 3.9g (70 %).

per-6-bromo-6-deoxy-β-CD

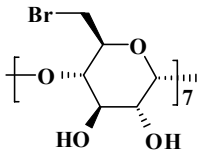

(***10***)

^{1}H NMR (300 MHz, DMSO) δ: 3.45- 3.30 (m, 14 H), 3.64 (m, 14 H), 3.83 (t, 7 H, J = 8.4 Hz), 4.01 (d, 7 H, J = 9.8 Hz), 4.98 (d, 7 H, J = 3.2 Hz), 5.90 (d, 7 H, J = 2 Hz,), 6.04 (d, 7 H, J = 7 Hz).

^{13}C-NMR (75 MHz, DMSO) δ: 34.28 (C-6), 70.84 (C-5), 71.90 (C-2), 72.12 (C-3), 84.47 (C4), 101.95 (C-1).

Per-6-azido-6-deoxy-β-CD (*11*):

Compound ***10*** (1.30g, 0.83 mmol), KI (0.07g, 0.34 mmol) and NaN_3 (0.51g, 7.8 mmol) were dissolved in 15 ml of dry DMF, and the mixture was heated at 65 °C for 40 h with stirring under nitrogen. The suspension was then concentrated under reduced pressure to a few milliliters before a large excess of water was added. A fine white precipitate was formed and recovered by centrifugation. The precipitate was washed with water and dried under vacuum to yield a stable white powder. Yield: 0.97g (90 %).

Per-6-azido-6-deoxy-β-CD

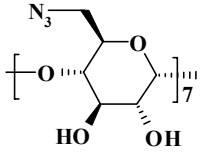

(***11***)

^{1}H NMR (300 MHz, DMSO) δ: 3.42-3.30 (m, 14 H), 3.65-3.53 (m, 14 H), 3.82-3.68 (m, 14 H), 4.91 (d, 7 H, J = 3 Hz), 5.77 (d, 7 H, J = 2 Hz), 5.92 (d, 7 H, 7 Hz).

^{13}C-NMR (75 MHz, DMSO) δ: 51.4, 70.4, 72.1, 72.7, 83.3, 102.1.

Per-6-amino-6-deoxy-β-CD (*12*):

Compound ***11*** (0.74g, 0.57 mmol) was dissolved in 15 ml of dry DMF, and triphenylphosphine (2.26g, 8.6 mmol) was added. After 1 h, concentrated aqueous ammonia (3 ml, approximately 35 %) was added dropwise to the solution. Shortly after the addition of the NH_3 solution was complete, the reaction mixture turned into a white suspension. It was stirred at room temperature for 20 h before the resulting suspension was concentrated under reduced pressure to a few millilitres. The product was then added dropwise to a large excess of acetone obtaining thus a white precipitate. The precipitate was washed with acetone and dried under vacuum to yield a stable white powder. Yield 0.57g (90 %).

Per-6-amino-6-deoxy-β-CD

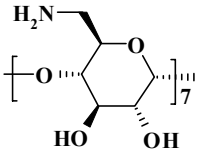

(***12***)

^{1}H NMR (300 MHz, D_2O) δ: 3.30-3.20 (m, 7 H), 3.44 (dd, 7 H, J = 13, 7 Hz), 3.57 (t, 7 H, J = 9 Hz), 3.68 (dd, 7 H, J = 9.5, 3.5 Hz), 4.03-3.94 (m, 7 H), 4.25-4.15 (m, 7 H), 5.15 (d, 7 H, J = 3.25 Hz).

^{13}C-NMR (75 MHz, D_2O) δ: 42.9, 70.5, 74.3, 74.8, 84.8, 104.1.

ESI-MS (m/z):1128 $[M + H]^+$

Per-6-guanidinio-6-deoxy-β-CD (*13*):

Crude ***12*** (0.39g, 0.35 mmol) was suspended in 7.5 ml of dry DMF and 1-H-pyrazolecarboxamidine hydrochloride (0.7g, 4.8 mmol) and DIEA (1.6 ml) were added. The whole was stirred at 70 °C for 8h under a nitrogen atmosphere and then a second addition of the same quantities of 1-H-pyrazolecarboxamidine hydrochloride and DIEA as before, followed. The mixture was heated at 70 °C and stirred continuously for a further 1 day. Then diethyl ether (60 ml) was added drop wise and the suspension formed was stirred for 1h. The solvent was decanted and the collected sticky solid was dissolved in a very small amount of water (0.3 ml). Addition of ethanol resulted in the precipitation of a white substance, which was recovered by centrifugation and dried under vacuum. This precipitate was redissolved in water, the pH was adjusted to 8.5 with sodium hydrogen carbonate and the solution was washed with chloroform (3 x 5 ml). Finally, the product was lyophilized. Yield (40 %).

Per-6-guanidinio-6-deoxy-β-CD

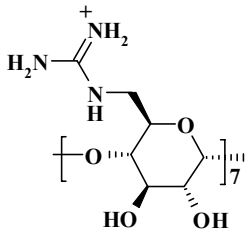

(***13***)

^{1}H NMR (300 MHz, DMSO) δ: 5.10-5.0 (m, 7 H-1), 4.10-3.90 (m, 14 H, H-3, 5), 3.70-3.58 (m, 14 H, H-2, 6), 3.50-3.35 (m, H-4, 6).

^{13}C-NMR (75 MHz, DMSO) δ: 161.17 (C of the guanidinium group), 105.17 (C-1), 86.80 (C-4), 77.0 (C-5), 75.9 (C-2), 75.15 (C-3), 45.55 (C-6).

ESI-MS (m/z): 204.2 ($[M + 7H^+]/7$, 100%),
1423 ($[M +H]^+$, 2%).

4.10.3 Mass spectrometry analysis.

All the β-cyclodextrin solutions for the mass spectrometry analyses reported were prepared at a 50 μM concentration in the presence of sodium chloride (100 μM). Mass spectra were obtained by perfusing the solutions into the mass spectrometer at a 10 μl/min rate. MS conditions: ESI interface, positive ions, single quadrupole analyzer. Capillary voltage 3500 V, cone voltage 190 V, source temperature 80 °C, desolvation temperature 150 °C, cone gas (N_2) 60 l/h, desolvation gas (N_2) 450 l/h. Spectra were acquired in total ion mode (300-1700 Da), scan time 4.0 s, inter-scan delay 0.1 s.

4.10.4 NMR spectrometry analysis.

The TOCSY spectra were recorded at 25 °C with different mixing times: 30, 90 and 160 ms for the 2A,2B-ditosyl-β-cyclodextrin and 30 and 160 ms for the 2A,2C- and 2A,2D-ditosyl-β-cyclodextrin. Relax delay 1.0 s., acquisition time 0.2 s., 32 repetitions, 2 x 256 increments.

The ROESY spectra were recorded at 25 °C. Mixing time: 200 ms. Relax delay 1 s, acquisition time 0.25 s, 32 repetitions, 2 x 128 increments.

All spectra were elaborated by using MestReC 4.9.9.9. Data processing: SineBell apodization 90.0 degree, first point 0.50.

[1] J. Szejtli, *Cyclodextrins and Their Inclusion Complexes*; Akadémiae Kiadò: Budapest, **1982**.

[2] Y. Okabe, H. Yamamura, K. I. Obe, K. Otha, M. Kawai, K. Fujita, *J. Chem. Soc. Chem. Commun.* **1995**, 581.

[3] J. Szejtli, *Cyclodextrin Technology*, Kluwer Academic Publisher , Dordrecht, The Netherlands, **1988**.

[4] A. Ueno, R. Breslow, *Tetrahedron Lett.* **1982**, 23, 3451.

[5] a) P. B. Weisz, M. M. Joullie, C. M. Hunter, K. M. Kumor, Z. Zhang, E. Levine, E. Macarak, D. Weiner, E. S. Barnathan, *Biochem. Pharm.* **1997**, 54, 149; b) J. Fojk, P. B. Weisz, M. M. Joullie, W. W. Li, W. R. Ewing, *Science*, **1989**, 243, 1490.

[6] D. W. Armstrong, U.S. Pat. 4539399, 1985 (Chem. Abstr. **1985**, 103, 226754).

[7] P. Fügedi, P. Nanasi, *Carbohydr Res.* **1988**, 175, 173.

[8] K. Fujita, T. Ishizu, K. Oshiro, K. Obe, *Bull. Chem. Soc. Jpn*. **1989**, 62, 2960.

[9] a) A. Hybl, R. E. Rundle, D. E. William, *J. Am. Chem. Soc.* **1965**, 87, 2779; b) W. Saenger, M. Noltemeyer, P. C. Manor, B. Himgerty, B. Klar, *Bioorg. Chem.* **1976**, 5, 187.

[10] A. R. Khan, P. Forgo, K. J. Stine, V. T. D'Souza, *Chem. Rev.* **1998**, 98, 1977-1996.

[11] K. Takeo, K. Uemura, H. Mitoh, *J. Carbohidr. Chem.* **1988**, 7, 293.

[12] F. Cramer, G. Mackensen, K. Kensse, *Chem. Ber.* **1969**, 102, 494.

[13] D. Rong, V. T. D'Souza, *Tetrahedron Lett.* **1990**, 31, 4275.

[14] K. Fujita, S. Nagamura, T. Imoto, T. Tahara, T. Koga, *J. Am. Chem. Soc.* **1985**, 107, 3233.

[15] A. W. Coleman, P. Zhang, H. Parrot-Lopez, C. C. Ling, M. Miocque, L. Mascrier, *Tetrahedron Lett.* **1991**, 32, 3997.

[16] K. Takeo, H. Mitoh, K. Uemura, *Carbohydr. Res*. **1989**, 187, 203.

[17] S. Tian, Ph. D. Dissertation, University of Missouri-St. Louis, **1997**, p. 26.

[18] K. Fujita, A. Mantsunaga, T. Imoto, *J. Am. Chem. Soc,* **1984**, 106, 5740.

[19] P. R. Ashton, P. Ellwood, I. Staton, J. F. Stoddart, *J. Org. Chem.* **1991**, 56, 7274.

[20] a) I. Tabushi, T. Nabeshima, K. Fujita, A. Mantsunaga, T. Imoto, *J. Org. Chem.* **1985**, 50, 2638; b) K. Fujita, T. Imoto, T. Tahara, H. Yamamura, T. Koga, T. Fujioka, K. Mihashi, *J. Org. Chem.* **1990**, 55, 877.

[21] K. Fujita, H. Yamamura, A. Mantsunaga, T. Imoto, K. Mihashi, T. Fujioka, *J. Am. Chem. Soc.* **1986**, 108, 4509.

[22] K. Fujita, A. Mantsunaga, T. Imoto, *Tetrahedron Lett.* **1984**, 25, 5533.

[23] K. Fujita, T. Tahara, T. Imoto, T. Koga, *J. Am. Chem. Soc.* **1986**, 108, 2030.

[24] a) *Comprehensive Supramolecular chemistry*; J. L. Atwood, J. M. Lehn, Eds. Vol 3, Cyclodextrins; J. Szejtli, T. Osa, Eds. Pergamon; Oxford, U. K. **1996**; b) G. Gattuso, S. A. Napogodiev, J. F. Stoddart, *Chem. Rev.* **1998**, 98, 1959; c) A. P. Croft, R. A. Bartsch, *Tetrahedron*, **1983**, 39, 1417.

[25] a) I. Tabushi, K. Shimokawa, K. Fujita, *Tetrahedron Lett.* **1977**, 18, 1527; b) I. Tabushi, Y. Kuroda, K. Yokata, L. C. Yuan, *J. Am. Chem. Soc.* **1981**, 103, 711.

[26] I. Tabushi, K. Yamamura, T. Nabeshima, *J. Am. Chem. Soc*. **1984**, 106, 5267.

[27] W. Considine, *J. Organometal. Chem.* **1966**, 5, 263.

[28] R. M. Munavu, H. H. Szmant, *J. Org. Chem.* **1976**, 41, 1832.

[29] F. M. Menger, M. A. Dulany, *Tetrahedron Lett.* **1985**, 26, 267.

[30] J. A. Rendleman, *Carbohydrates in Solution*; R. F. Gould Ed.; Advanced in Chemistry Series 117, American Chemical Society; Washington DC. **1973**, p 54.

[31] S. P. Rowland, *Carbohydr. Res*. **1971**, 16, 243.

[32] S. Sforza, G. Galaverna, R. Corradini, A. Dossena, R. Marchelli, *J. Am. Soc. Mass Spectrom.* **2003**, 14, 124.

[33] a) S. Edwards, C. J. Smith, P. J. Smith, *J. Org. Chem.* **1998**, 63, 1737-1739; b) M. S. Bernatowicz, Y. Wu, G. R. Mastueda, *J. Org. Chem*. **1992**, 57, 2497-2502.

[34] K. Takahashi, K. Hattori, F. Toda; *Tetrahedron Lett*. **1984**, 3331.

[35] a) F. Grillo, B. Hamelin, L. Jullien, J. Canceill, J. M. Lehn, L. De Robertis and H. Driguez, *Bull. Soc. Chem. Fr.* **1995**, 132, 857-866; b) T. Kraus, M. Budesinsky and J. Zavada, *Eur. J. Org. Chem.* **2000**, 3133-3137; c) A. Bom, M. Bradley, K. Cameron, J. K. Clark, J. van Egmond, H. Feliden, E. J. MacLean, A. W. Muir, R. Palin, D. C. Rees and M. Q. Zhang, *Angew. Chem. Int. Ed.* **2002**, 41, 265-270; d) T. Kraus, M. Budesinsky, I. Cisarova and J. Zavada, *Angw. Chem. Int. Ed.* **2002**, 41, 1715-1717; e) T. Kraus, M. Budesinsky and J. Zavada, *J. Org. Chem.* **2001**, 66, 4595-4600.

[36] D. Vizitiu, C. S. Walkinshaw, B. I. Gorin, G. R. Tatcher, *J. Org. Chem.* **1997**, 62, 8760-8766.

[37] N. Mourtzis, K. Eliadou, C. Aggelidou, V. Sophianopoulou, I. M. Mavridis, K. Yannalopoulou, *Org. Biomol. Chem.* **2007**, 5, 125-131.

[38] P. R. Ashton, R. Königer, J. F. Stoddart, *J. Org. Chem.* **1996**, 61, (3), 903-908.

Chapter 5

Positively Charged CDs for the Recognition of Ochtatoxin A

5.1 Introduction

Chemically, ochratoxin A (OTA) has a pentaketide skeleton and contains a chlorinated isocoumarin moiety linked through a carboxylic group to a L-phenylalanine *via* an amide bond. This family of mycotoxins includes also ochratoxin B and C, which are the dechlorinated analogue and the methyl ester respectively. The isocoumarinic carboxylic acid (ochratoxin α) and its dechlorinated analogue (ochratoxin β) are also detectable in cultures of OTA-producing strains of *Aspergillus* and *Penicillium* and 4-hydroxy OTA has also been found in cultures of *Aspergillus ochraceus*. The structure of OTA and the related compounds are shown in Figure 5.1.

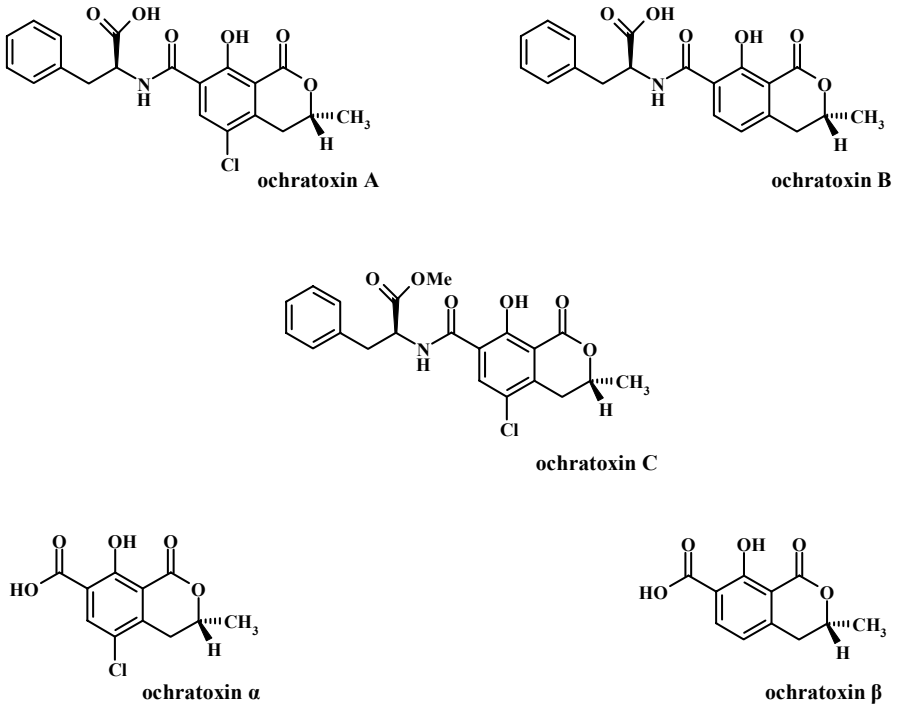

Figure 5.1: Structures of the main naturally occurring ochratoxins.

As mentioned in the chapter 3, the International Agency for Research on Cancer (IARC) evaluated ochratoxin A in 1993, annhd classified it as possibly carcinogenic to humans (group 2B), based on sufficient evidence for carcinogenicity in animal studies and inadequate evidence in humans (IARC, 1993).

The most recent international exposure assessments were performed respectively by the Scientific Committee on Food (SCF) and the JECFA (Joint FAO/WHO Expert Committee on Food Additives, 2001). The SFC estimated that the mean dietary intake ranged from 0.7 to 4.6 ng/Kg b.w. per day. The JECFA estimated a dietary exposure of approximately 90 ng/Kg b.w. per week corresponding to about 13 ng/Kg b.w. per day.

A recent (9 June 2006) Panel on Contaminants in the Food Chain of the European Food Safety Authority (EFSA), taking into account all data currently available, derived a tolerable weekly intake (TWI) of 120 ng/Kg b.w. for OTA. Currently, the weekly exposure of the general population to OTA varies between 15 and 60 ng/Kg b.w. and is therefore well below this value.

The methods currently used to determine OTA require clean up and concentration of the sample, when low detection limits are required. Classical methods are liquid-liquid and solid-phase extraction (SPE), although recently, immunoaffinity columns (IACs) have been extensively used for the sample clean up procedure. The main advantage offered by the IAC columns are that, being OTA specifically bound to antibodies, it is possible to isolate the toxin avoiding the matrix interferents. However, some drawbacks concern the lack of reproducibility eventually occurring in different column batches, on account of the heterogeneous packing, the high costs and the relatively short storage time: each column can be used only ones.

Recently, also selective molecularly imprinted polymers for solid phase extraction of OTA have been reported, which are promising candidates for selective SPE applications.[1] Enzyme-like immunosorbent assays (ELISA) can be used for OTA determination: this technique is particularly attractive for rapid screening, but it may cause systematic overestimates if compared with chromatographic methods.

The necessity of monitoring a large number of samples requires methods which allow a rapid screening and confirmation of the identity of the molecule.

High performance liquid chromatography (HPLC), preceded by extraction of OTA using a commercially available immunoaffinity column (IAC), has been the most popular among the reference centers but it is too slow for large numbers of samples.[2] Capillary electrophoresis with laser-induced fluorescence[3] and electrospray-tandem mass spectrometry[4-5] have been employed for various matrices, but they require highly expensive and technically sophisticated equipments.

Another assay for the determination of OTA, particularly in wine and beer, is based on Gas Chromatography Mass Selective detection,[6] monitoring specific ions. Previously the mycotoxin has to be extracted and derivatized with bis(trimethylsilyl)trifluoroacetamide, with a LOD of 0.1 ng/ml. This method is not suitable for routine analyses but it is useful as a confirmatory tool for OTA > 0.1 ng/ml.

OTA detection methods are generally based on RP-HPLC with fluorimetric detection, using C18 columns and an acid eluent at pH 5 or at slightly alkaline pH, using the ion-pair technique.[7-8]

Some studies were performed using an ammonia solution as a post-column fluorescence enhancer, reaching a detection limit of 0.003 ng/ml based on a standard solution.[9]

Also, a LC-MS-MS method proposed by Laitner et al,[10] based on the extraction with a RP-C18 SPE column has been reported; however, this method requires the use of expensive equipment not commonly available in most laboratories. Moreover, this methodology require preliminary clean up and/or concentration of the sample.

5.2 Aim of the work

The aim of the work was to build up a receptor able to complex OTA and thus to enhance the fluorescence of the toxin. To obtain this goal we have studied by molecular modelling (see the chapter 3) the potential inclusion of OTA inside the cavity of the β-cyclodextrin (Figure 5.2), and we synthesized several β-cyclodextrin modified with one, two or a number of positively charged groups either on the upper or the lower rim.

In this chapter we report the results obtained by investigating the interaction of OTA with the modified β-cyclodextrins previously synthesized.

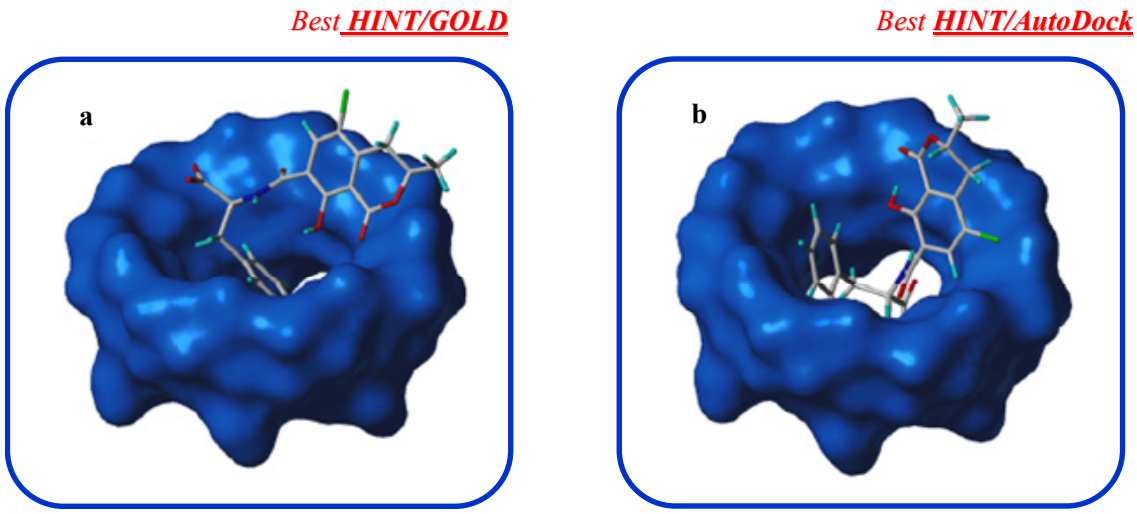

Figure 5.2: a) Best HINT/GOLD for OTA in β-CD. b) Best HINT/AutoDock for OTA in β-CD.

5.3 Results and discussion

As it underlined in chapter 3, observing the chemical structure of OTA it is possible to note the presence of two acid groups: the carboxylic function on the phenylalaninic residue (pK_{a1} = 4.4) and the phenolic group on the isocoumarinic ring (pK_{a2} = 7.1), (Figure 5.3).

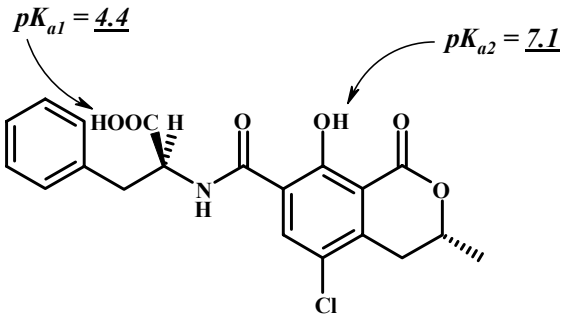

Figure 5.3: K_a values for the two acidic groups present in the OTA structure.

The natural fluorescence of the mycotoxin is given by the presence of the isocoumarinic moiety, enhanced by the presence of a rigid system due to the formation of an intramolecular hydrogen bond between the phenolic moiety and the amidic carbonyl (α-form) or the esteric carbonyl group (β-form), as it is schematised in Figure 5.4.

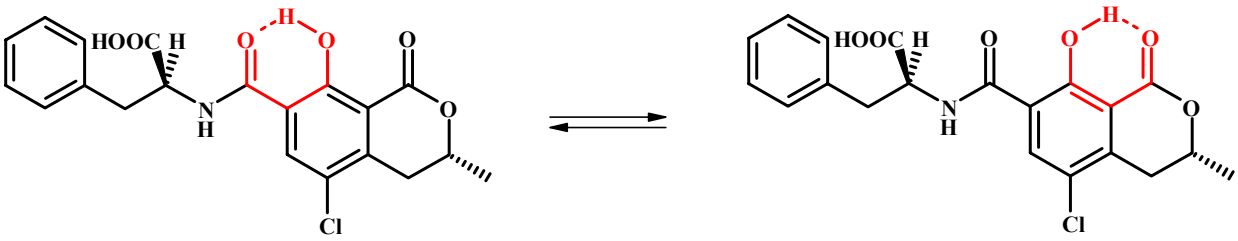

Figure 5.4: Equilibrium between α- and β-forms for OTA at an acidic pH value.

Instead, in an alkaline environment, the presence of a phenate moiety allows a higher conjugation of the system, suggesting a more rigid structure where the amidic hydrogen is involved in a hydrogen bond with both the phenate and the carboxylate groups (Figure 5.5).

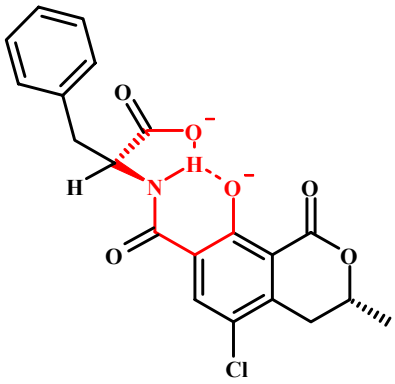

Figure 5.5: Chemical structure of OTA in an alkaline environment.

Spectroscopic studies conducted by Dall'Asta et al.[11] revealed for OTA a strong dependence of its spectroscopic properties (UV absorption and fluorescence emission) from the pH of the aqueous solution in which it is dissolved.

The UV spectra of aqueous solutions of ochratoxin A at different pH values is reported in Figure 5.6.

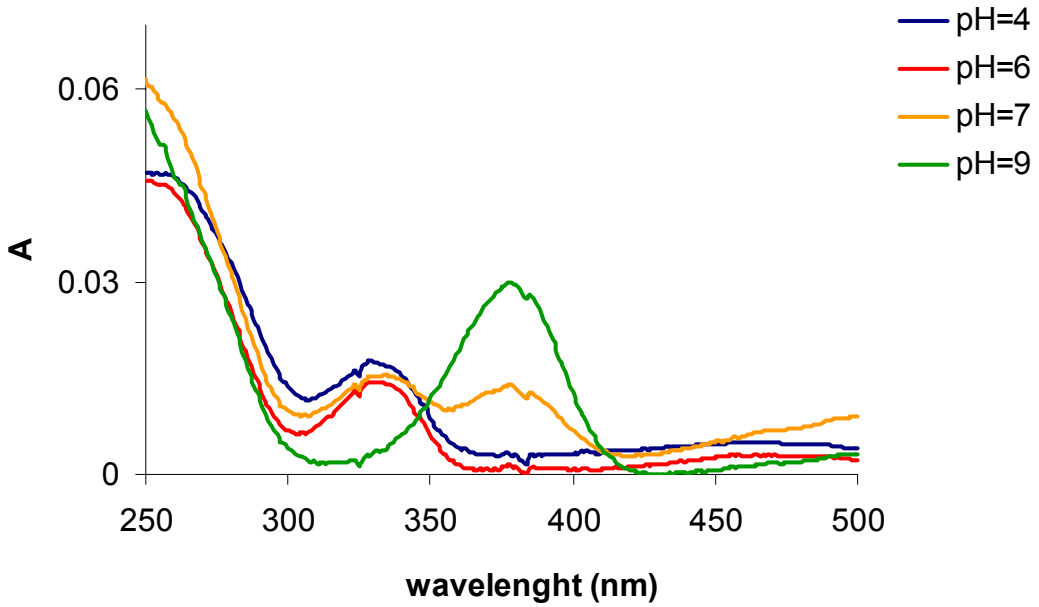

Figure 5.6: UV spectra of OTA at different pH values. Concentration of OTA: 1 μg/ml.

As it can be seen in Figure 5.6, at pH = 6 or lower, the predominant specie is the monoanionic ochratoxin A, with an absorption maximum at 330 nm. When the pH is 7, both species, the

monoanionic and the dianionic species, are present since the absorption spectrum shows two different maxima, the former at 335 nm and the latter at 370 nm. At alkaline pH (pH = 9), only the dianionic specie is present, with an absorption maximum at 380 nm and a higher absorbance due to the increasing conjugation of the system.

Similarly, the fluorescence spectra of ochratoxin A performed at different pH values revealed greater emission properties for the dianionic form (Figure 5.7).

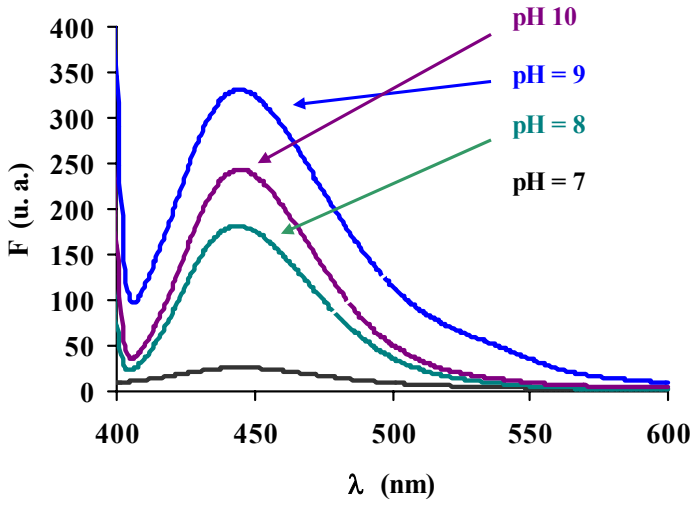

Figure 5.7: Fluorescence enhancements at different pH values.

As outlined in Figure 5.7, the fluorescence increases sharply from pH 7 to pH 9, consistently with the increasing concentration of the deprotonated form, while at higher pH values, a slight fluorescence decrease is observed, probably due to the hydrolysis of the lactone ring. Moreover, going from neutral to alkaline solutions a 9-fold fluorescence enhancement was obtained.

5.3.1 Spectroscopic measurements with neutral and negatively charged β-CDs.

First, we performed a screening of complexing properties of different commercially available cyclodextrins for OTA by fluorescence experiments (Table 5.1).

Table 5.1: Emission of OTA (10^{-7} M) in water in the presence of different commercially available CDs. pH of the solutions: 9.

Complex	F/F_0
water, pH = 9	1.0 ± 0.1
OTA-α-CD	1.0 ± 0.1
OTA-β-CD	1.2 ± 0.2
OTA-γ-CD	1.0 ± 0.1
DIMEB	0.99 ± 0.1
Hyp-β-CD	1.00 ± 0.2
Su-β-CD	0.13 ± 0.2
SBE-β-CD	0.99 ± 0.1

ΔF = F/F0 where F is the OTA fluorescence intensity recorded in the presence of CD and F_0 is the OTA fluorescence intensity recorded in water. Molar ratio OTA:CD = $1:10^5$

As shown in Table 5.1, none of the commercially available cyclodextrins, neither neutral such as native α-, β- and γ-cyclodextrins, 2,6-di-O-methyl-β-cyclodextrin (DIMEB) and 2-hydroxypropyl-β-cyclodextrin (Hyp-β-CD), nor negatively charged such as succinyl-β-cyclodextrin (Su-β-CD) or tetra(6-O(sulfo-n-butyl))-β-cyclodextrin (SBE-β-CD) showed affinity for OTA. In particular, except for the case of the succinyl-β-cyclodextrin, where the number of the negative charges for molecule is high (from 4 to 6), the presence of substituents did not allow significant modifications of the interaction between the toxin and the hydrophobic cavity.

5.3.2 Spectroscopic measurements with positively charged β-CDs.

With the aim of evaluating the effect of electrostatic interactions on the OTA:cyclodextrins complex, we performed fluorescence measurements of aqueous solution of OTA, at pH 9, in the presence of β-cyclodextrin derivatives opportunely synthesized (see chapter 4) bearing one or more positively functional groups on the upper or on the lower rim.

5.3.2.1 Cyclodextrins bearing a single positive charge.

Although the mode of inclusion obtained by docking techniques suggested that the interaction of β-cyclodextrin with the mycotoxin occurred preferentially at the wider opening side of the host, we placed positive functional groups such as ammonium or guanidinium on both rims, in order to verify if the position of the charge could induce some differences in the host:guest interactions.

First of all, 2-amino-2-deoxy-β-cyclodextrin and 6-amino-6-deoxy-β-cyclodextrin were studied. In the former case, only a little fluorescence enhancement was obtained, as shown by the emission spectrum reported in Figure 5.8.

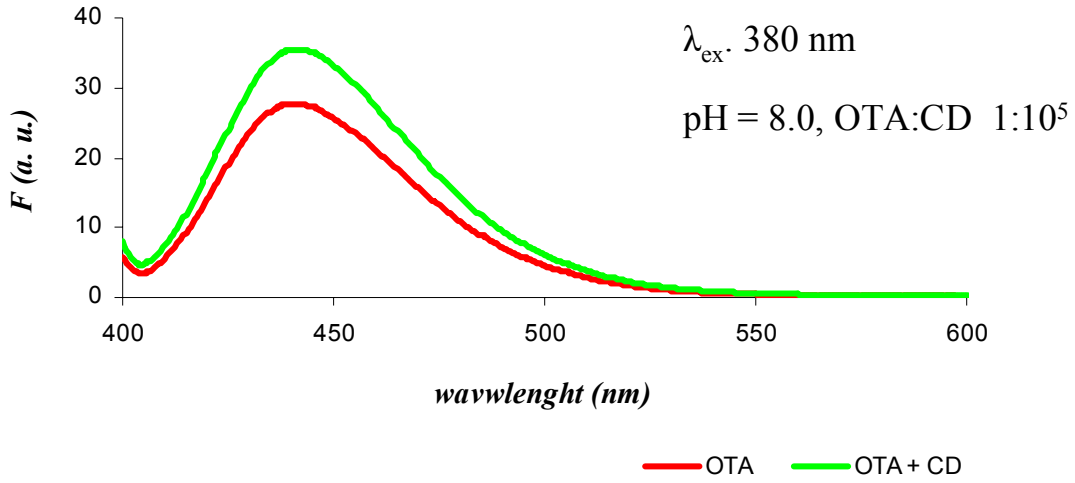

Figure 5.8: OTA fluorescence in the presence and in the absence of 2-amino-2-deoxy-β-CD. [OTA] = 20 ng/ml; buffer solution: NH_3/NH_4Cl (20 mM).

In the case of the amino derivative at the 6-position no enhancement was observed since an F/F_0 ratio of 1.0 (where F is the fluorescence of an aqueous solution of OTA at pH = 9 in the presence of the 6-amino-6-deoxy-β-cyclodextrin and F_0 is the OTA fluorescence at pH = 9) was obtained.

Since the aim of these measures was to verify the capacity of cyclodextrin derivatives to promote significative enhancements of the emission of alkaline solutions of OTA (pH = 9), in both cases presented above it wasn't possible to record the emission at pH grater than 8.0, since the pK_a of the ammonium group is ≈ 8.0. Therefore, the conditions used were not the best since at similar pH values, only 50 % of the guests added to the solutions were in the protonated form.

In order to overcome this problem, guanidinium derivatives of β-cyclodextrins were used, since the pK_a of the guanidinium group is ≈ 13. The fluorescence spectra of OTA at pH = 9, in presence of 2-guanidinium-2-deoxy-2-(S)-β-cyclodextrin or 6-guanidinium-6-deoxy-β-cyclodextrin are shown in Figure 5.9 and Figure 5.10.

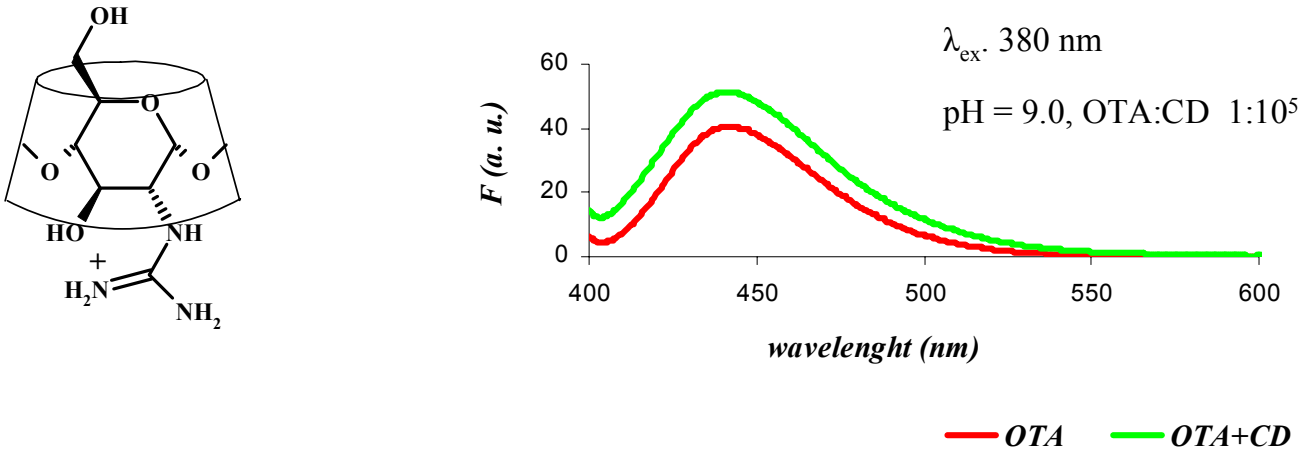

Figure 5.9: OTA fluorescence in the presence and in the absence of 2-guanidinium-2-(S)-β-CD. [OTA]= 20 ng/ml; buffer solution: NH_3/NH_4Cl (20 mM).

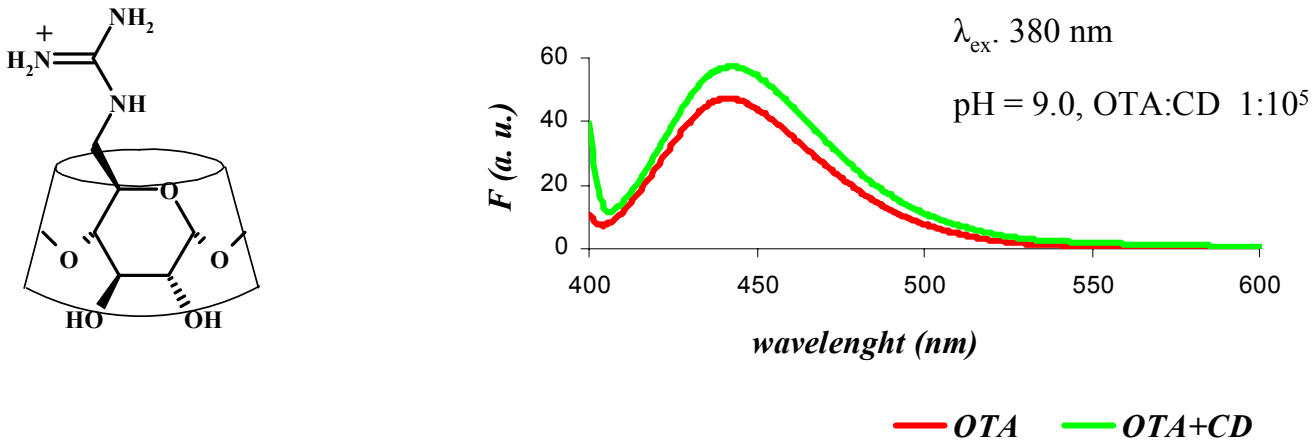

Figure 5.10: OTA fluorescence in the presence and in the absence of 6-guanidinium-β-CD. [OTA]= 20 ng/ml; buffer solution: NH_3/NH_4Cl (20 mM).

In both cases no significative fluorescence enhancement was induced, suggesting that, electrostatic interactions due to the presence of a single positive charge placed on the upper or on the lower rim do not induce modifications of the mode of complexation of OTA.

5.3.2.2 Cyclodextrin derivatives bearing two positive charges on the upper rim.

All three 6A,6X-diamino-6A,6X-dideoxy-β-cyclodextrin isomers (Figure 5.11), synthesized as described in chapter 4, were tested as fluorescence enhancers for OTA emission.

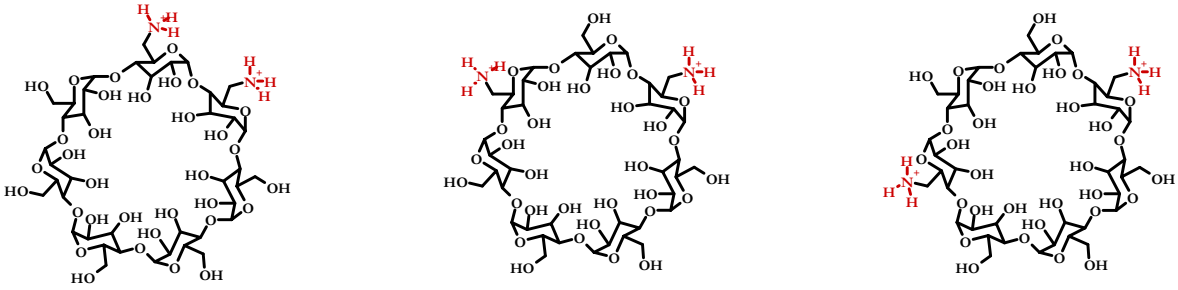

6A,6B-diamino-β-CD 6A,6C-diamino-β-CD 6A,6D-diamino-β-CD

Figure 5.11: 6A,6X-diamino-β-CD derivatives.

The fluorescence spectra obtained adding the AB regioisomer to a solution of OTA, at pH 8.0 is reported in Figure 5.12.

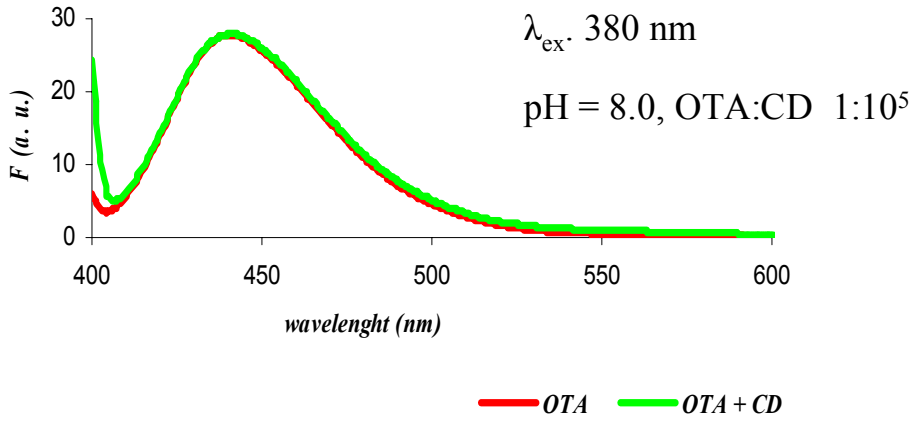

Figure 5.12: OTA fluorescence in the presence and in the absence of 6A,6B-diamino-6A,6B-dideoxy- β-CD. [OTA] = 20 ng/ml; buffer solution: NH_3/NH_4Cl (20 mM).

Similarly, also in the case of the A,C and A,D diamino isomers, no fluorescence enhancements for OTA were obtained.

5.3.2.3 Application of per(6-guanidinium)-β-CD.

In order to check the performance of a perguanidilated β-cyclodextrin, rich of positive charges on the upper rim, the per-(6-guanidinium)-6-deoxy-β-cyclodextrn, synthesized as described in the chapter 4, was used as fluorescence enhancer. Below, the fluorescent spectrum recorded for a solution of OTA at pH = 9, in the absence and in the presence of the per-guanidilated derivative, is reported (Figure 5.13).

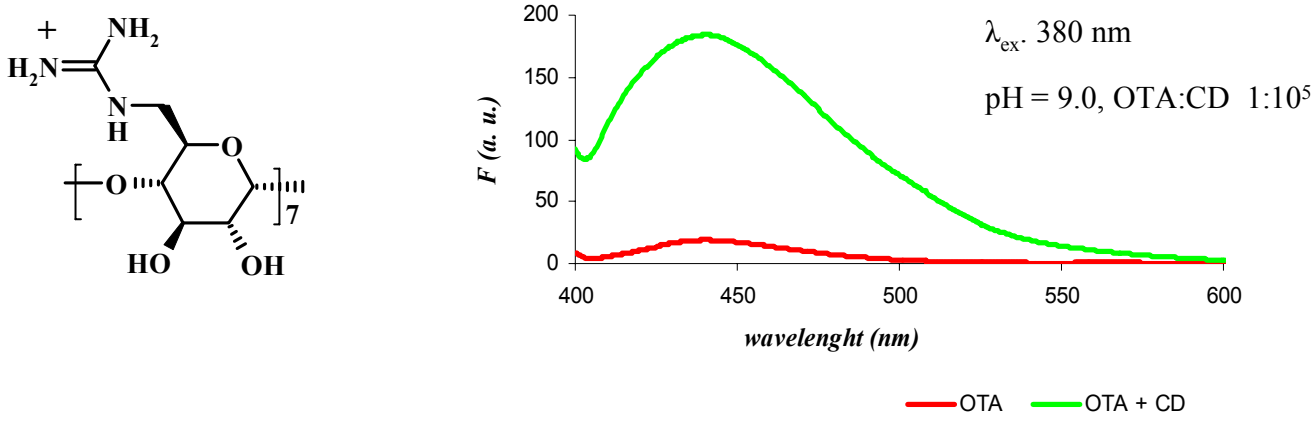

Figure 5.13: OTA fluorescence in the presence and in the absence of per(6-guanidinium)-6-deoxy-β-CD. [OTA] = 20 ng/ml; buffer solution: NH_3/NH_4Cl (20 mM).

Although the experiment is preliminary, it is promising, but it deserves further attention.

5.4 Conclusions

The effectiveness of additional coulombic forces components on the overall OTA:cyclodextrin interaction was investigated. On the basis of the results obtained, cyclodextrins bearing one or two positive charges on their structure did not show any significant change in the mode of inclusion of OTA in the hydrophobic cavity of a β-cyclodextrin derivative. In particular, mono-positively charged cyclodextrin derivatives, such as 2- and 6- ammonium or 2- and 6-guanidinium-β-cyclodextrins, did not induce fluorescence enhancement of OTA, suggesting that neither the presence of a single charge, nor its position, are crucial factors for promoting OTA inclusion. Finally, preliminary experiments with a perguanidilated derivative bearing seven charges at the 6-positions showed an effective fluorescence enhancement of OTA. However, further researches are needed.

5.5 Materials and methods

5.5.1 Reagents.

Ochtatoxin A (OTA) standards were from Sigma Biochemicals (St. Louis, MO, USA). Doubly distilled water was produced in our laboratory utilising an Alpha-Q system Millipore (Marlborough, MA, USA). α-, β- and γ-cyclodextrin were purchased from ACROS (Carlo Erba, Italy); heptakis(2, 6-di-O-methyl)-β-CD (DIMEB), tetra(6-O-(sulfon-butyl))-β-CD (SBE-β-CD; substitution degree n = 4); (2-hydroxypropyl)-β-CD (Hyp-β-CD) were purchased from ALDRICH (Steinheim, Germany). Succinyl-β-CD (Su-β-CD; randonmly substituted, substitution degree n = 4-6) was purchased from FLUKA.

Ammonium chloride buffer (pH 9, 20 mM) was freshly prepared by dissolving the proper amount of salts in 1 L of doubly distilled water and adjusting pH to the desired value with a NH_3 solution (35% v/v).

5.5.2 Preparation of OTA solutions and decontamination.

A standard stock solution of ochratoxin A was prepared by dissolving the powder (1 mg) in a proper volume of acetonitrile. Working solutions of ochratoxin A (10^{-7} M and $4.95*10^{-8}$ M,) were prepared from standard stock solutions by evaporating the organic phase under nitrogen and dissolving the residue in water. These solutions are stable at −4 ◦C for a month. Decontamination of waste solutions and glassware was performed with sodium hypochlorite (10% aqueous solution) for 12 hours.

5.5.3 Fluorescence measurements.

Fluorescence spectra were recorded on a PERKIN ELMER LS50 instrument in a 0.2 × 0.2 cm quartz microcuvette (Hellam; type: 105.251-QS, light path: 3 mm, centre: 15 mm). Due to the solvent effects on the absorption and luminescence spectra, the proper excitation wavelengths was selected by scanning the excitation spectra of the ochratoxin A solutions (20 ppb). The emission scan was performed in the wavelength range 400–600 nm. Both emission and excitation slits were set at 15 nm. Each spectrum was recorded in triplicate.

5.5.4 Measurements of fluorescence enhancements by CDs.

The solutions of OTA and cyclodextrins were prepared in doubly distilled water and the spectra of each analyte alone (blank) and in the presence of cyclodextrin (molar ratio toxin:CD = $1:10^5$) were recorded; the F/F_0 ratio was calculated, where F and F_0 are the fluorescence intensities in the presence (sample) or in the absence (blank) of the CDs, respectively.

[1] J. Jodlbauer, N. M. Marier, W. Lindner, *J. Chromatogr. A*, **2002**, 945, 45-63.

[2] A. Visconti, M. Pascale, G. Centone, *J. Chromatogr. A,* **1999**, 864, 89-101; b) M. Castellari, S. Fabbri, A. Fagiani, A. Amati, S. Galassi, *J. Chromatogr. A*, **2000**, 888, 129-136.

[3] S. Cimeli, C. Maragos, *J. Agric. Food Chem.* **1998**, 46, 3162-3165.

[4] M. Becker, P. Delgelmann, M. Herderich, P. Schreier, H. Humpf, *J. Chrom. A*, **1998**, 818, 260-264.

[5] B. P. Lau, P. M. Scott, D. A. Lewis, S. R. Kahnere, *J. Mass Spectrom.* **2000**, 35, 22-32.

[6] J. G. Soleas, J. Yan, D. M. Goldberg, *J. Agric. Food Chem.* **2001**, 49, 2733-2740.

[7] A. Visconti, M. Pascale, G. Centone, *J. Chromatogr. A*, **1999**, 864, 89-101.

[8] M. Castellari, S. Fabbri, A. Fagiani, A. Amati, S. Galassi, *J. Chromatogr. A*, **2000**, 888, 129-136.

[9] B. Zimmerli, R. Dick, *J. Chromatogr. B*, **1995**, 666, 85-99.

[10] A. Leitner et al., Anal. Chimica Acta, 2002, 453, 33-41.

[11] C. Dall'Asta, G. Galaverna, A. Dossena, R. Marchelli, J. Chromatogr. A, 2004, 1024, 275-279.

Chapter 6

Host:Guest Interactions of β-CD with Zearalenone: Spectroscopic Evidences

6.1 Introduction

Zearalenone (ZEN) is a toxic secondary metabolite produced by several species of *Fusarium* fungi, mainly *F. graminearum* and *F. culmorum*, which grow on several food commodities, especially cereals such as maize, barley, oats, wheat, and sorghum.

The structure of ZEN consists of a resorcinol moiety fused to a 14-membered macrocyclic lactone ring, which includes a *trans* double bond, a ketone, and a methyl side group.

Of the numerous ZEN derivatives, only *trans*-α-zearalenol (α-ZOL) occurs naturally in cereal grains, whereas after consumption of ZEN, the two stereoisomeric metabolites α- and β-ZOL are produced in mammals by reduction of the keto-group in C-6' (Figure 6.1). Zearalenone and related metabolites display a strong estrogenic activity and can result in severe reproductive and infertility problems when they are fed to domestic animals in sufficient amounts.

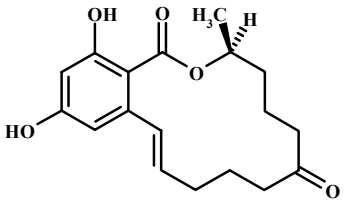

Zearalenone (ZEN)

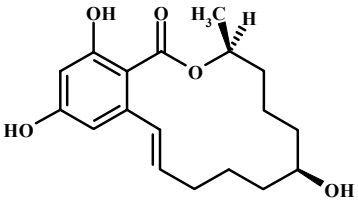

α-Zearalenol (α-ZOL)

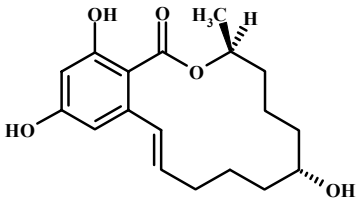

β-Zearalenol (β-ZOL)

Figure 6.1: Structure of ZEN and its metabolites.

Zearalenone is primarly estrogenic in its actions and its LD_{50} values are very high, ranging from 2 to 10 g/Kg body weight.

The highest incidence rates of ZEN are reported from North America and central and northern Europe. Depending on climatic, harvest and storage conditions, the most contaminated commodities are maize and maize-based products. From some areas of Europe, incidence rate up to 90% has been reported for maize. Zearalenone has also been detected at high concentrations in Africa beers. However, since ZEN is metabolized to β-ZOL by strains of *S. cereviasiae*, this metabolite should be detected in beer.

Since ZEN usually occurs at μg/Kg (ppb) levels, there is a special interest in analytical procedures for reliable detection and quantification of ZEN between 10 and 100 μg/Kg.

Analysis of ZEN is commonly performed by applying a clean up step after extraction and using HPLC with fluorescence detection, on account of the native fluorescence of this mycotoxin and its derivatives. While conventional analytical methods generally use liquid-liquid partition or solid phase extraction steps during sample clean up, recently immunoaffinity columns (IAC) for sample purification have been developed. Despite their high recoveries and good reproducibility, the IAC method does not allow for the simultaneous detection of zearalenone and its derivatives.

Electrophoretic and chromatographic separations of zearalenone and other mycotoxins were studied using cyclodextrins as additives in order to improve the efficiency of separation,[1] although in many cases UV detection was used and the potential effect of the inclusion complex formation on ZEN fluorescence was not described. Very recently, the fluorescence enhancement of zearalenone in the presence of cyclodextrins was used by Maragos et al.[2] for improving its analytical detection by capillary electrophoresis with laser-induced fluorescence detection (CE-LIF).

As an alternative to fluorescence detection, liquid chromatography–mass spectrometry (LC-MS) methods have been developed with various interfaces. In all cases the quantitative determinations always had problems concerning the choice of an appropriate standard.

Rosenberg et al. described an atmospheric pressure chemical ionization (APCI) LC-MS method for the determination of zearalenone in grains. In the single ion mode (SIM), zearalenone could be measured in maize down to 0.12 μg/Kg.[3]

Zoellner et al. used LC-negative ion APCI-MS/MS for the determination of zearalenone in grains and beer, using the C1'- C2' saturated zearalanone as internal standard.[4] Similarly, this group determined ZEN, α- and β-ZOL, zeranol and taleranol in urine; however the use of zearalenone as internal standard seems unwise because of the interrelationship between the analytes.[5]

The same LC-APCI-MS/MS technique was applied by Lagana et al. for the determination of six resorcyclic acid lactones in environmental samples using the structurally unrelated 4-octylbenzenesulfonic acids standard.[6]

LC-MS analysis with negative ion electrospray interface (ESI) was used by Horie and Nakazawa for the determination of zeranol in muscle and liver using external calibration.[7]

Very recently, since the application of liquid chromatography coupled with mass spectrometric detection has opened the possibility to use the isotope-dilution approach, an innovative approach for

the application of isotope dilution methods to the quantification of ZEN was developed by Sforza et al.[8] The principle underlying this approach was that derivatives labelled with stable isotopes could be obtained in the derivatization reaction itself, by using simple derivatizing reagents which can be found in two pure isotopic forms, a "light" one or a "heavy" one.

6.2 Aim of the work

The only systematic study concerning the fluorescence enhancement of zearalenone in the presence of cyclodextrins is that of Maragos,[2] who examined a wide variety of cyclodextrins for enhancing the fluorescence intensity of ZEN using CE-LIF and for developing a CE-LIF method to detect ZEN in maize. The enhancement effect is ascribed to inclusion complex formation, but no data have been produced so far to characterize the complex. Thus, the aim of this work was to investigate which factors affect the ZEN fluorescence enhancement in the presence of cyclodextrins and to characterize the host-guest ZEN-CD inclusion complex. In particular, we wished to study the effect of unsubstituted and polysubstituted β-cyclodextrins on the fluorescence properties of zearalenone and its main metabolite α-zearalenol (ZOL) in aqueous solution, as well as the nature of the ZEN-CD and ZOL-CD interactions by spectroscopic experiments, such as NMR, circular dichroism, fluorescence and UV measurements. Stability constants of the ZEN-CD and ZOLs-CD complexes were also evaluated by performing fluorescence titrations with β-cyclodextrin (β-CD), 2,6-di-O-methyl-β-cyclodextrin (DIMEB) and 2-hydroxypropyl-β-cyclodextrin (Hyp-β-CD).

6.3 Results and discussion

6.3.1 Screening of the ZEN fluorescence enhancement with different CDs.

In order to evaluate which cyclodextrin induced the highest fluorescence enhancement for zearalenone and its derivatives, a spectroscopic screening of native β-CD and of the substituted hydroxypropyl-β-CD and dimethyl-β-CD was carried out in aqueous solution. These three CDs were chosen on account of their commercial availability: in particular, β-CD as the reference compound, DIMEB as one of the most efficient enhancer of fluorescence intensity on the base of Maragos' results and Hyp-β-CD for its high solubility in water. The aim was that of investigating the role played by the CD cavity and by the nature of the substituents on the zearalenone fluorescence enhancement.

The recorded fluorescence enhancements due to the addition of CDs to a molar ratio ZEN (ZOLs):CD = 1:10^3 are reported in Figure 6.2. All the tested CDs induced a high enhancement in the fluorescence spectra of the analytes and a blue shift in the emission maximum wavelength (from 457 nm to 452 nm), both phenomena suggesting a strong interaction between the mycotoxins and the CDs. In particular, blue shifts of 3–6 nm in the emission maximum were similar to those recorded for the analytes in media less polar than water, as methanol or ethanol, and were consistent with the lower polarity of the environment experienced by the fluorophore due to the inclusion into the cyclodextrin cavity.

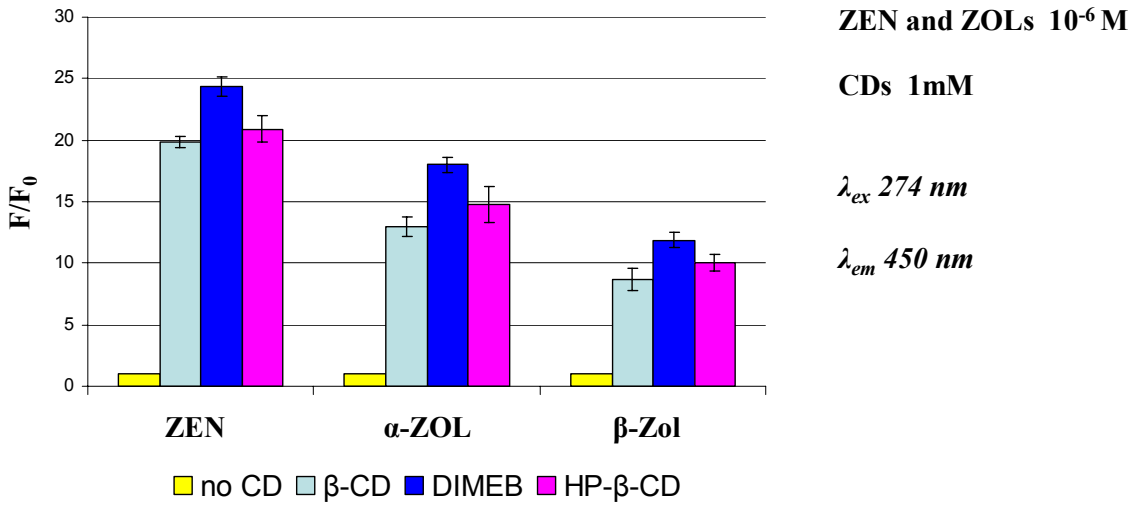

Figure 6.2: Fluorescence enhancements of ZEN and ZOLs with different CDs in water solution at pH = 7.6.

The best enhancement was recorded for zearalenone, whereas α- and β-zearalenol showed lower enhancement. The most effective enhancement is observed, for all the three analytes, for

dimethyl-β-cyclodextrin (DIMEB), followed by hydroxypropyl-β-cyclodextrin (Hyp-β-CD) and the native β-cyclodextrin. The fluorescence switch on suggests the inclusion of the phenolic moiety, but also the C6 moiety seems to has an important role in the inclusion mechanism: the highest enhancement is recorded for zearalenone, which present a sp^2 carbonyl group in C6. The isomeric forms α-zearalenol and β-zearalenol showed lower fluorescence enhancement in the presence of CDs, suggesting that the hydroxyl group on C6 may hinder the inclusion of the toxin.

6.3.2 Effect of pH on the fluorescence of ZEN and ZOLs in the presence and in the absence of β-CD.

Since zearalenone and zearalenols have a phenolic moiety, they are acidic compounds; therefore, the spectroscopic properties may be different for the neutral and the anionic forms, and strictly depend on the pH of the medium. In the paper by Maragos,[2] a borate buffer at pH 8.5 was used. The pK_a values of the two phenolic groups are not known, but comparing the structure with similar compounds it can be envisaged that the OH group in the *para* position should have a pK_a value around 8.5, whereas the *ortho* OH should have a pK_a slightly higher than 10, also on account of the possible hydrogen bond with the ester carbonyl oxygen. The systematic evaluation of the spectroscopic properties of zearalenone at different pH values have never been reported so far. For this reason, we studied the changes in the absorption and emission spectra of ZEN at different pH values and how the pH affects the β-CD complexation. In particular, the ZEN and ZOLs (10^{-5} M) emission was recorded in aqueous buffer at different pH values (5.5 and 9.0) in the presence and in the absence of β-CD (10^{-2} M). Data collected for ZEN are reported in Figure 6.3.

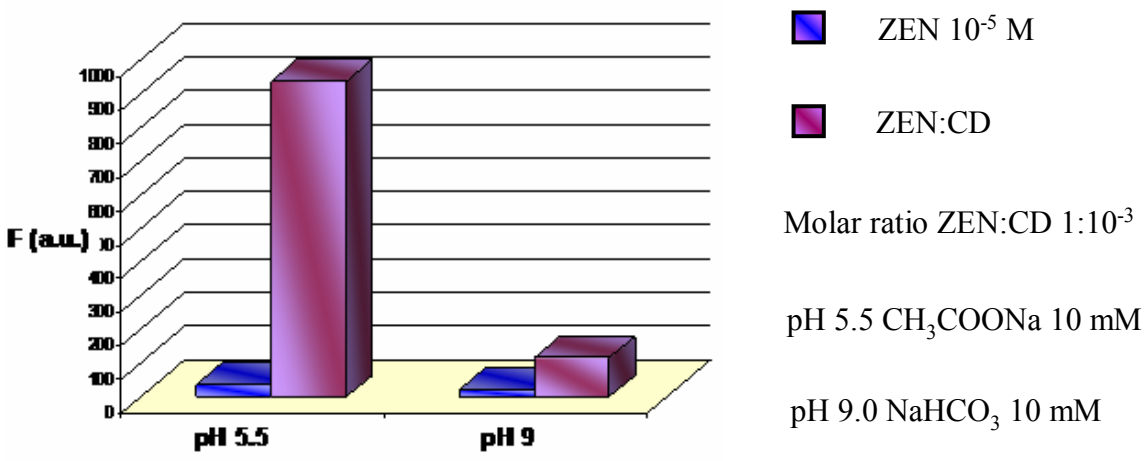

Figure 6.3: ZEN emission intensities in buffer solution recorded at different pH values in the presence or in the absence of β-CD.

As shown in Figure 6.3, the fluorescence of ZEN was only slightly higher in acidic conditions, whereas the pH affected very significantly the emission of the ZEN:β-cyclodextrin complex. Indeed, an enhancement of about 9 times was observed at pH = 9, in agreement with results obtained by Maragos, whereas the enhancement induced by the addition of cyclodextrin at pH ≤ 5.5 was 100 times than in the absence of β-cyclodextrin. This effect is probably due to the lower affinity of the ionized toxin for the cyclodextrin apolar cavity.

6.3.3 Influence of the temperature and the buffer molarity on the fluorescence of ZEN and ZOLs in the presence of β-CD.

The fluorescence emission is usually affected by the temperature: in particular, at low temperatures the energy dissipation in the medium is reduced, on account of the reduced vibration of the molecule, and the emission usually increases. On the other hand, at higher temperature the formation of the ZEN:cyclodextrin complex is faster. The fluorescence spectra of the ZEN:β-cyclodextrin complexes were evaluated at different temperatures (20 °C, 30 °C, 40 °C and 50 °C), by using a thermostat connected to the spectrofluorimeter. Before recording the spectra, the solutions were equilibrated to the temperature required for 15 minutes. The results, reported in Figure 6.4, clearly indicated that the best fluorescence was obtained at 20 °C for the ZEN:β-cyclodextrin complex.

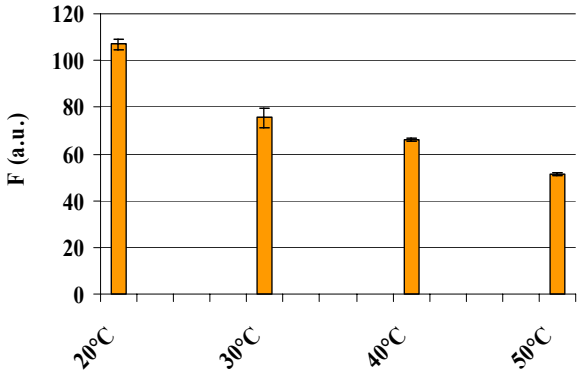

Figure 6.4: Fluorescent spectra of ZEN:β-CD complex at different temperature. Molar ratio ZEN:CD 1:10^3; pH of the solutions 5.5; buffer solution CH_3COOH/CH_3COONa (10 mM).

The effect of the ionic strength on the emission spectra of ZEN and ZOLs in the presence and in the absence of β-cyclodextrin was also evaluated. The experiments were performed at 20 °C, using the acetate buffer (pH 5.5) at different molarities (0.5 mM, 1 mM, 2mM, 5 mM and 10 mM).

The results reported in Figure 6.5 indicated that the highest fluorescence intensity was obtained using a buffer solution with a 10 mM concentration, whereas lower values were recorded for lower buffer molarities, which are related to a lower ionic strength.

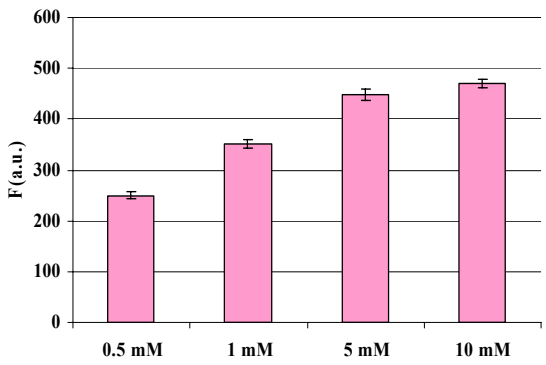

Acetate buffer, pH 5.5

Temperature: 20° C

Figure 6.5: Fluorescent emission recorded for several ZEN:β-CD complex solutions at different buffer molarities.

6.3.4 Determination of the mycotoxins:CD stability constants.

The formation constants of the ZEN-CD and ZOLs-CD complexes were evaluated for the native β-CD. In order to calculate the binding constants and the stoichiometry of the host-guest complex, fluorescence titrations of ZEN and ZOLs with increasing amounts of β-CD were performed. The results obtained for the mycotoxins are reported in Figure 6.7.

The stoichiometry was tentatively evaluated by Job Plot. This approach is based on the fluorescence emission obtained by varying the host-guest molar fractions, using host and guest solutions at the same concentration. Unfortunately, the fluorescence change of the ZEN:β-CD complex in these conditions was too small to obtain an accurate measurement. Thus, the binding constants of ZEN and ZOLs with β-CD were calculated according to the Benesi–Hildebrand equations,[9] assuming the formation of a 1:1 and of a 1:2 toxin-cyclodextrin inclusion complex (equations 1 and 2 in Figure 6.6) and evaluating in which condition the best fitting was obtained.

$$\frac{1}{(F_i - F_0)} = \frac{1}{(F_\infty - F_0)K[CD]_i} + \frac{1}{(F_\infty - F_0)} \qquad (1)$$

$$\frac{1}{(F_i - F_0)} = \frac{1}{(F_\infty - F_0)K[CD]^2_i} + \frac{1}{(F_\infty - F_0)} \qquad (2)$$

Figure 6.6: Benesi-Hildebrand equations assuming the formation of a 1:1 or a 1:2 toxin-CD complexes.

F_i and F_0 are the fluorescence intensities of the toxin in the presence and in the absence (blank) of cyclodextrin, respectively; F_∞ is the fluorescence intensity of the complex and $[CD]_i$ is the cyclodextrin concentration after each addition.

The regression curves obtained for ZEN and ZOLs assuming a 1:1 stoichiometry are reported in Figure 6.8, in Figure 6.9 and in Figure 6.10.

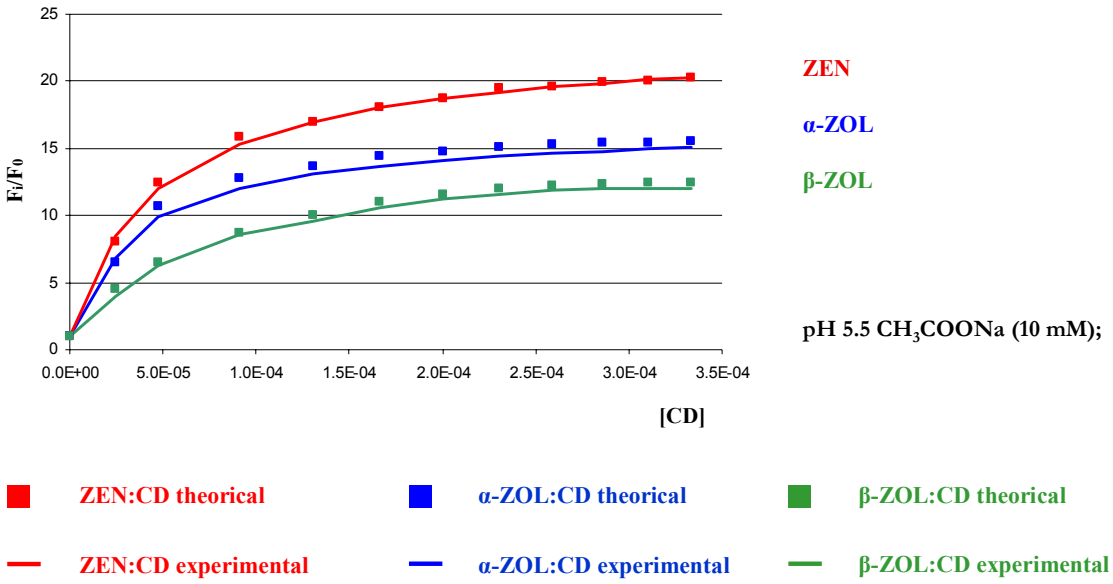

Figure 6.7: Fluorescent titration of ZEN and ZOLs with increasing amounts of β-CD.

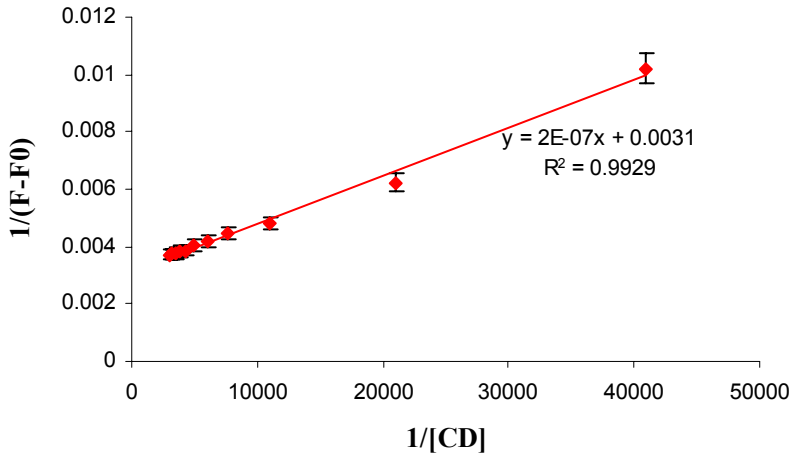

Figure 6.8: Benesi-Hildebrand regression curve for ZEN with β-CD.

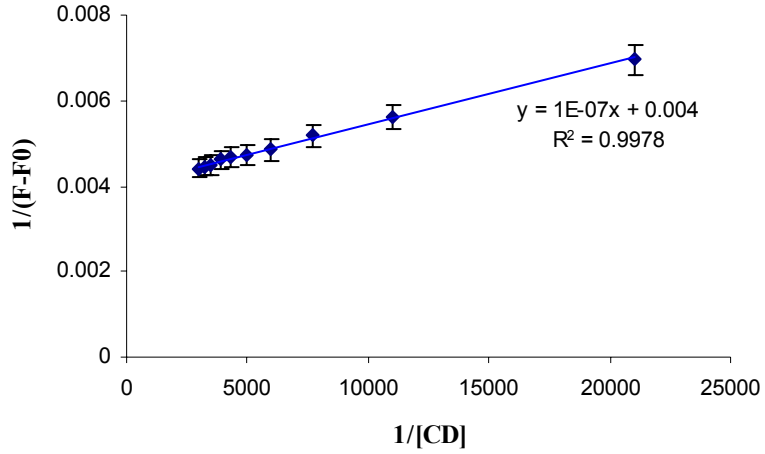

Figure 6.9: Benesi-Hildebrand regression curve for α-ZOL with β-CD.

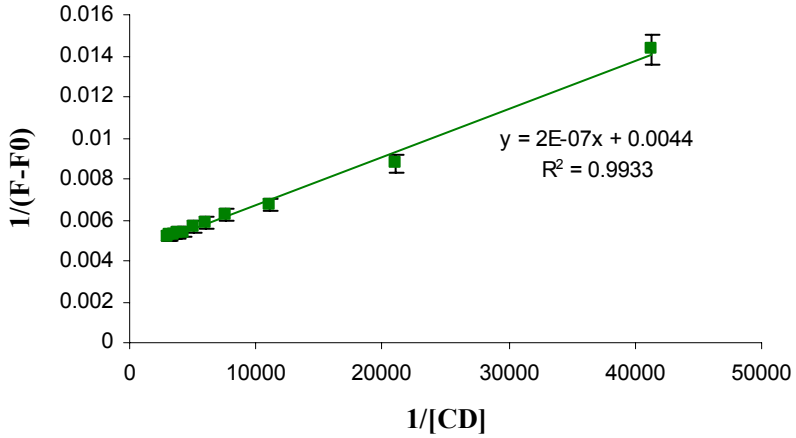

Figure 6.10: Benesi-Hildebrand regression curve for β-ZOL with β-CD.

All the regression coefficients calculated for complexes of ZEN and ZOLs with β-CD showed very good correlation values (>0.99) for the 1:1 stoichiometry and lower correlation values for the 1:2 toxin-cyclodextrin complex. According to the results, the best fitting supported a ZEN:β-CD 1:1 stoichiometry. The calculated binding constants are reported in Table 6.1.

Table 6.1: Data obtained for the calculations of the binding constants of ZEN, α-ZOL and β-ZOL with β-CD considering both the host:guest stoichiometries 1:1 and 1:2.

	Stoichiometry	Slope	Intercept	R^2	log K
ZEN:CD	1:1	2.0e-07	3.1e-03	0.9929	**4.27 ± 0.21**
	2:1	3.1e-03	4.0e-03	0.9882	
α-ZOL:CD	1:1	1.0e-07	4.2e-03	0.9978	**4.45 ± 0.27**
	2:1	6.0e-12	4.6e-03	0.9710	
β-ZOL:CD	1:1	2.0e-07	4.4e-03	0.9933	**4.34 ± 0.32**
	2:1	5.0e-10	8.83-03	0.9601	

When comparing the formation constants and the fluorescence enhancements recorded in the presence of β-CD for each analyte (Table 6.1), we can observe that the data are consistent.

Although the fluorescence of ZOLs resulted lower in the presence of CDs than ZEN (see Figure 6.2), on account of their higher flexibility due to the presence of an hydroxyl instead of a keto group at the C6', similar stability constants for ZEN or ZOLs:β-cyclodextrin complexes were obtained indicating that the aromatic moiety is probably the main moiety involved in the complexation inside the cyclodextrin cavity.

6.3.5 NMR experiments.

The nature of the ZEN:β-CD complex was investigated by NMR spectroscopy. 1D and 2D NMR spectra of zearalenone, in D_2O, in the presence or in the absence of β-cyclodextrin were performed. Zearalenone shows a very complex ^{1}H-NMR spectrum since signal relative to the aliphatic hydrogens have chemical shifts very close to each other; however, by comparing 1D and 2D NMR spectra it was possible to assign their exact chemical shifts (Figure 6.11).

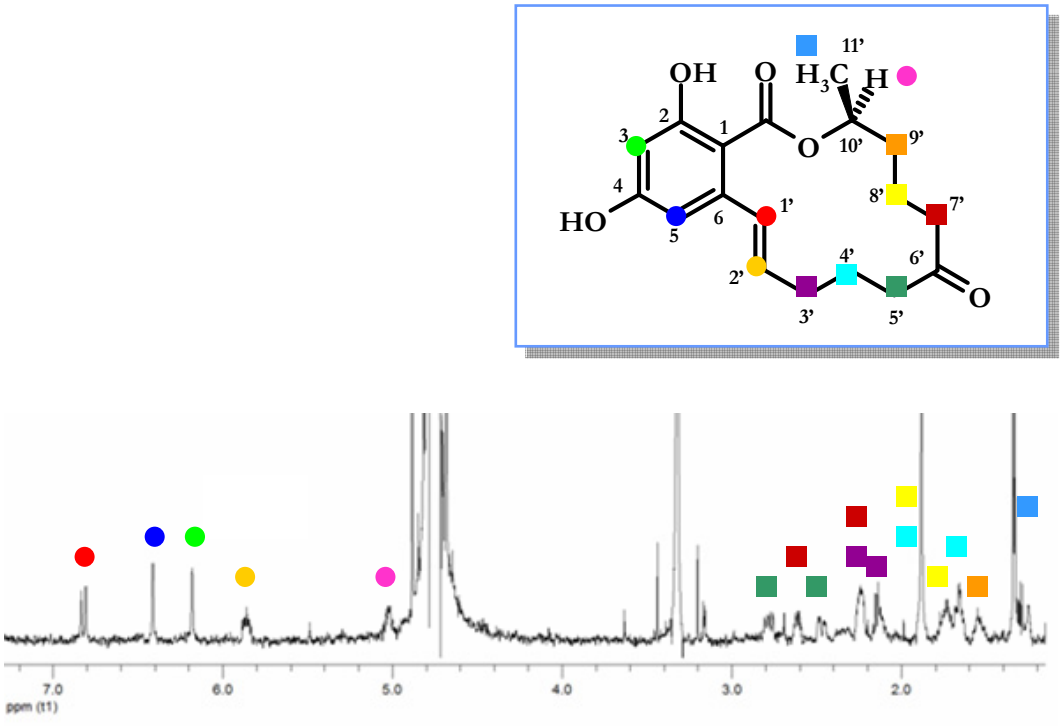

Figure 6.11: ^{1}H-NMR spectrum of ZEN in D_2O.

The increased solubility of zearalenone in the presence of β-cyclodextrin was a first proof of some kind of interaction between the host and the guest. Furthermore, the comparison of the ^{1}H-NMR spectra of the toxin alone and of the toxin with β-cyclodextrin offered proof of an inclusion inside the hydrophobic cavity. Indeed, the host induced modifications of the chemical shifts of the toxin hydrogens. In particular, significative downfield shifts observed for H-5, H-1', H-10', and an upfield shift for H-2', suggested a partial inclusion of zearalenone interesting the aromatic moiety of the overall structure, as previously hypothesized by fluorescence experiments.

The comparison between the ^{1}H-NMR spectra of ZEN and ZEN:β-CD relatively to the protons cited above are reported below (Figure 6.12 and Table 6.2).

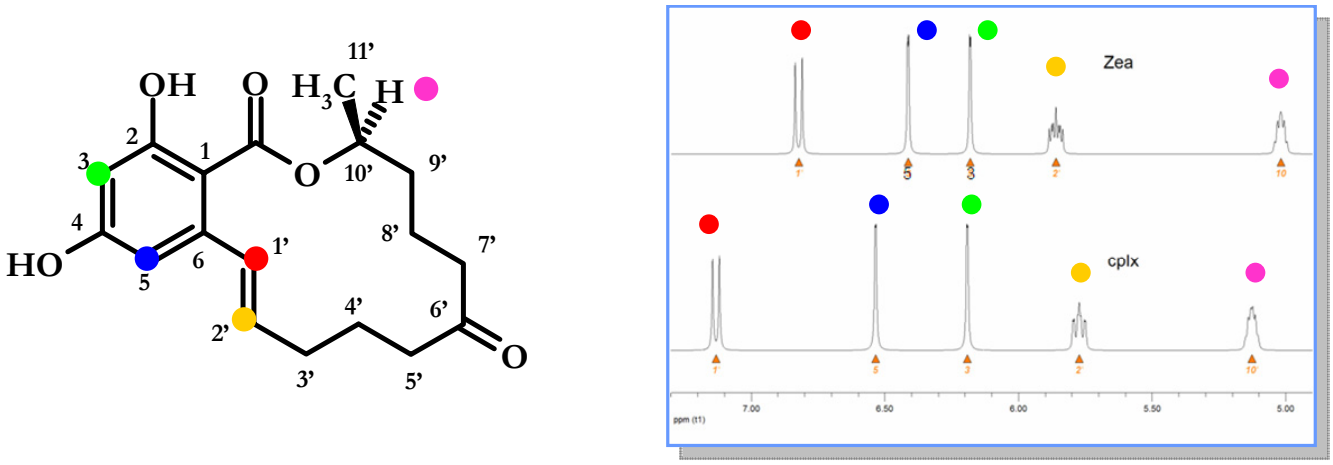

Figure 6.12: Downfield shifts for H-5, H-1' and H10', and upfield shift for H-2' of ZEN observed in the presence of β-CD in D_2O.

Table 6.2: ^{1}H-NMR chemical shifts (ppm) for selected protons of ZEN and ZEN:β-CD in D_2O.

Hydrogen:	ZEN (ppm)	ZEN:β-CD (ppm)
H-3	6.181	6.192
H-5	**6.413**	**6.535**
H-1'	**6.822**	**7.132**
H-2'	**5.860**	**5.773**
H-10'	**5.019**	**5.127**

Similarly, a large shielding of the cyclodextrin protons was observed. In particular, significative upfield of the chemical shifts of hydrogens H-3 and H-5, which are directed towards the inside of the cavity, due to the closeness with the ZEN aromatic ring was observed, as shown in Table 6.3.

Table 6.3: ^{1}H-NMR chemical shifts (ppm) for protons of β-CD in the absence and in the presence of ZEN in D_2O.

Hydrogen:	β-CD (ppm)	ZEN:β-CD (ppm)
H-1	5.049	5.033
H-2	3.627	3.622
H-3	**3.943**	**3.923**
H-4	3.563	3.551
H-5	**3.853**	**3.799**
H-6	**3.855**	**3.835**

The inclusion was also confirmed by a ROESY experiment. Correlation peaks between the cyclodextrin hydrogens and the aromatic and the double bond protons of zearalenone were observed (Figure 6.13, a and b).

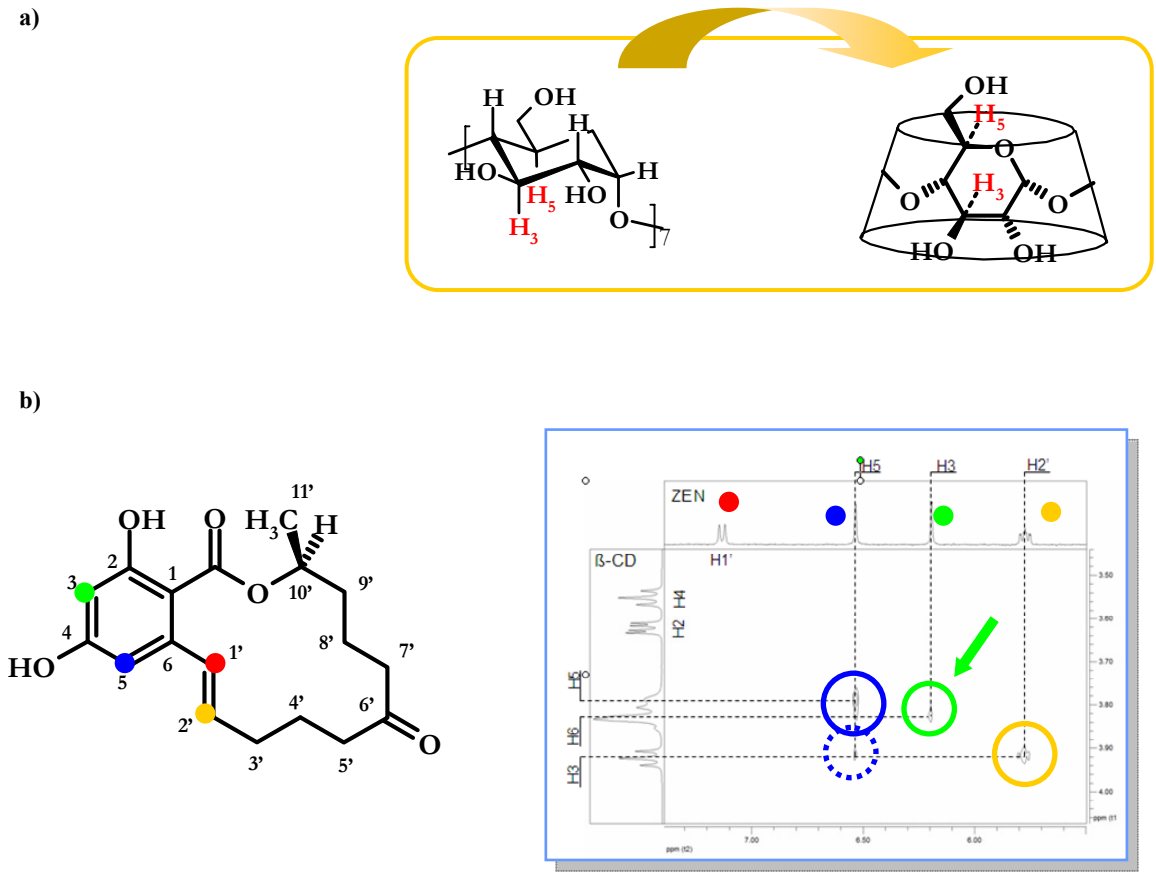

Figure 6.13: a) Hydrogen H-3 and H-5 of the β-CD, which are directed towards the cavity; b) a portion of the ^{1}H-^{1}H ROESY spectrum for a solution of ZEN:β-CD complex in D_2O.

As shown in Figure 6.13 b, correlation peaks between H-2' and H-5 of zearalenone and H-3 of cyclodextrin were found. In particular, for the aromatic H-5, two cross peaks, one stronger and one weaker, with H-5 and H-3 of β-cyclodextrins, respectively, were clearly visible.

However, in order to obtain an exhaustive comprehension of the zearalenone:β-cyclodextrin inclusion mode, the correlation peak between the aromatic hydrogen H-3 of the toxin with the protons H-6 of the host was crucial. Indeed, this correlation together with the absence of any others correlation between the toxin protons with neither H-3 nor H-5, the inside hydrogens of the cavity, demonstrated that the inclusion of the phenyl ring was feasible but only a portion of the aromatic ring was interested in the inclusion complex. The interaction with the aromatic hydrogen H-3 of ZEN, moreover, allows to explain the upfield shift observed for the H-6 protons of β-cyclodextrin reported in Table 6.3, and the stronger downfield shift obtained for the H-5 proton respect to the H-3 proton of zearalenone, reported in Table 6.2.

However, the absence of other significant correlations with the inside hydrogens of the cavity, as well as the alternate upfield and downfield shift observed in the ^{1}H-NMR spectra for several aliphatic protons, such as H-4', H-5' and H-7', revealed the presence of interactions between the same aliphatic portion of zearalenone with the lower rim of the β-cyclodextrin. Moreover, modification of the coupling constants observed for ZEN and CD respect to the case of the complex solution indicated conformational changes in the host as well as in the guest as a consequence of the formation of an inclusion complex.

Finally, in agreement with all the results obtained by the NMR investigation, the inclusion complex formed between zearalenone and the hydrophobic cavity of β-cyclodextrin has been hypothesized. In particular, considering the upfield shifts observed for the cyclodextrin hydrogens H-5 and H-6 and taking into account the correlation between the host and the guest revealed by ROESY spectrum, the inclusion complex can be described by the model proposed in Figure 6.14.

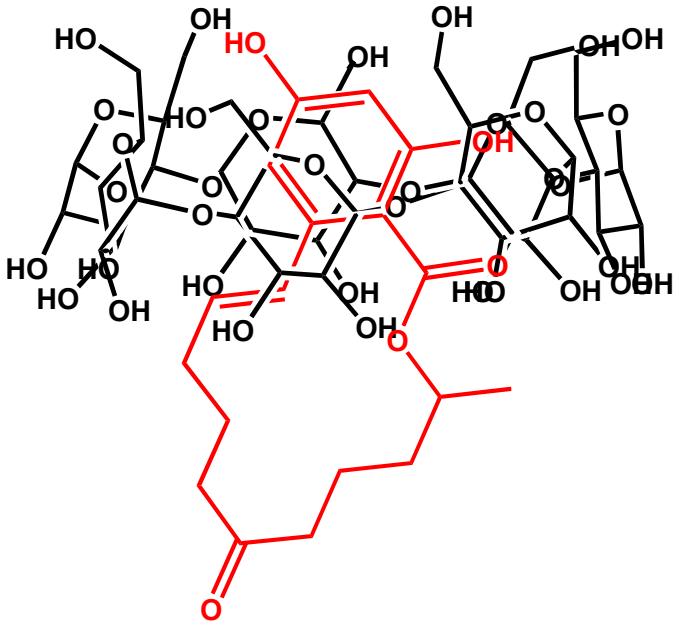

Figure 6.14: Proposed model for the ZEN:β-CD inclusion complex.

6.3.6 Circular dichroism experiments.

In order to achieve further evidence for the proposed inclusion model for the zearalenone:β-CD complex, circular dichroism experiments were performed. The spectra were acquired separately for aqueous solutions of ZEN and β-CD, and for aqueous solutions of ZEN + β-CD (molar ratio: 1:10^{3}). The results are reported in Figure 6.15.

The circular dichroism signal of β-CD was not significantly different from the baseline. When comparing the spectrum obtained for the complex with that registered for ZEN in aqueous solution, it is possible to see that both bands in the circular dichroism spectrum obtained for the ZEN:β-CD

complex are stronger than those observed for ZEN. These data suggest that the inclusion of ZEN into the β-CD cavity involves the phenolic system, which is responsible for the absorption at 280–230 nm.

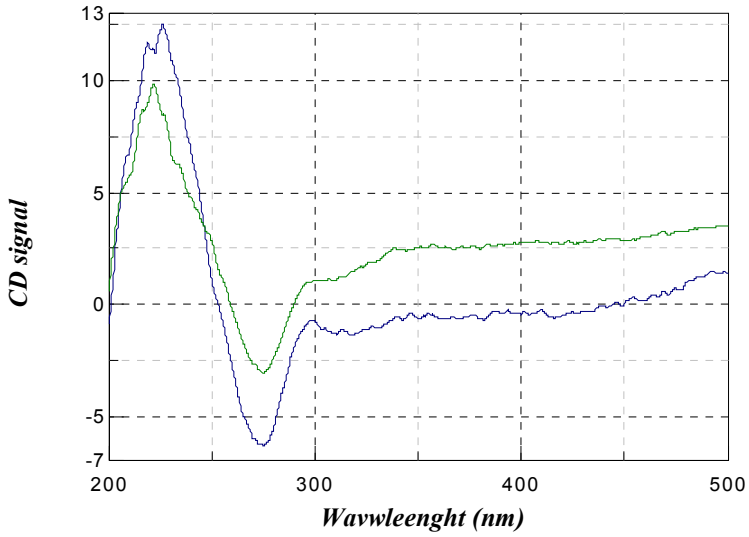

Figure 6.15: CD spectra of aqueous solution of ZEN and ZEN:β-CD complex. The green line indicates the CD signal of ZEN in water, while the blue line indicates the CD signal of the complex.

6.3.7 Electrospray-mass spectrometry experiments.

The study of host–guest interactions in the gas phase allows the detection of specific interactions not necessarily present in solution, giving a complementary picture of the intrinsic phenomena responsible for molecular recognition.[10] There are interpretation ambiguities on ESI-MS spectra of supramolecular assemblies, e.g. deciding whether the species present in the mass spectra correspond to those present in solution, or rather, they result from processes occurring under high-vacuum conditions. Moreover, it is not clear, whether the molecular ions observed are real inclusion complexes or only ion-dipole external adducts, so called "false positives", as reported by Cunnif et al.[11] In our particular case, however, a comparison is easily made by results obtained from independent solution-phase techniques (fluorescence and NMR).

The identification of major peaks recorded for a solution of β-cyclodextrin in water (1 mM) is reported in Table 6.4 while the ESI-MS spectrum recorded for an aqueous solution of zearalenone (1 mM) and the main peaks identification are reported in Figure 6.16 and Table 6.5.

Table 6.4: Major peaks (m/z) identified from an ESI-MS spectrum of an aqueous sol. of β-CD (1 mM).

Mass (m/z)	Identification
579	$[CD+H+Na]^{2+}$
587	$[CD+H+K]^{2+}$
1135	$[CD+H]^{+}$
1157	$[CD+Na]^{+}$

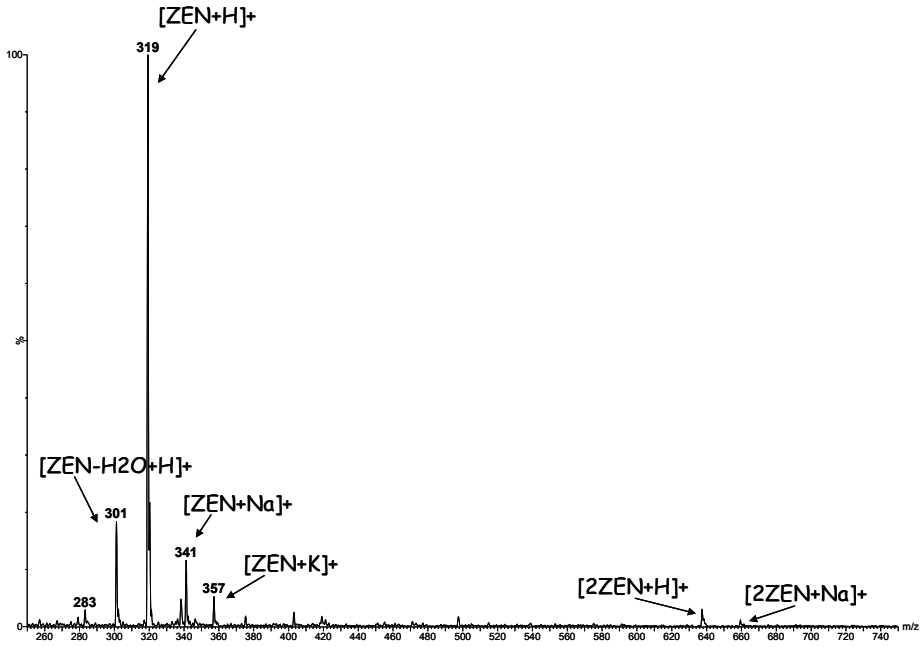

Figure 6.16: ESI-MS spectrum of an aqueous solution of ZEN (1 mM).

Table 6.5: Major peaks (m/z) identified from an ESI-MS spectrum of an aqueous sol. of ZEN (1 mM).

Mass (m/z)	Identification
283	$[ZEN+2H_2O+H]^{+}$
301	$[ZEN+H_2O+H]^{+}$
319	$[ZEN+H]^{+}$
341	$[ZEN+Na]^{+}$
357	$[ZEN+K]^{+}$
637	$[2ZEN+H]^{+}$
659	$[2ZEN+Na]^{+}$

Instead, in the case of the study of the ZEN:β-CD complex, the mass spectrum obtained was characterized by the presence of several multicharged adducts relatively to the cyclodextrin alone and the complex (Figure 6.17). In particular, the cationization involved mainly sodium and potassium: this behaviour is typical for cyclodextrins, as recently reported by Sforza et al.[12]

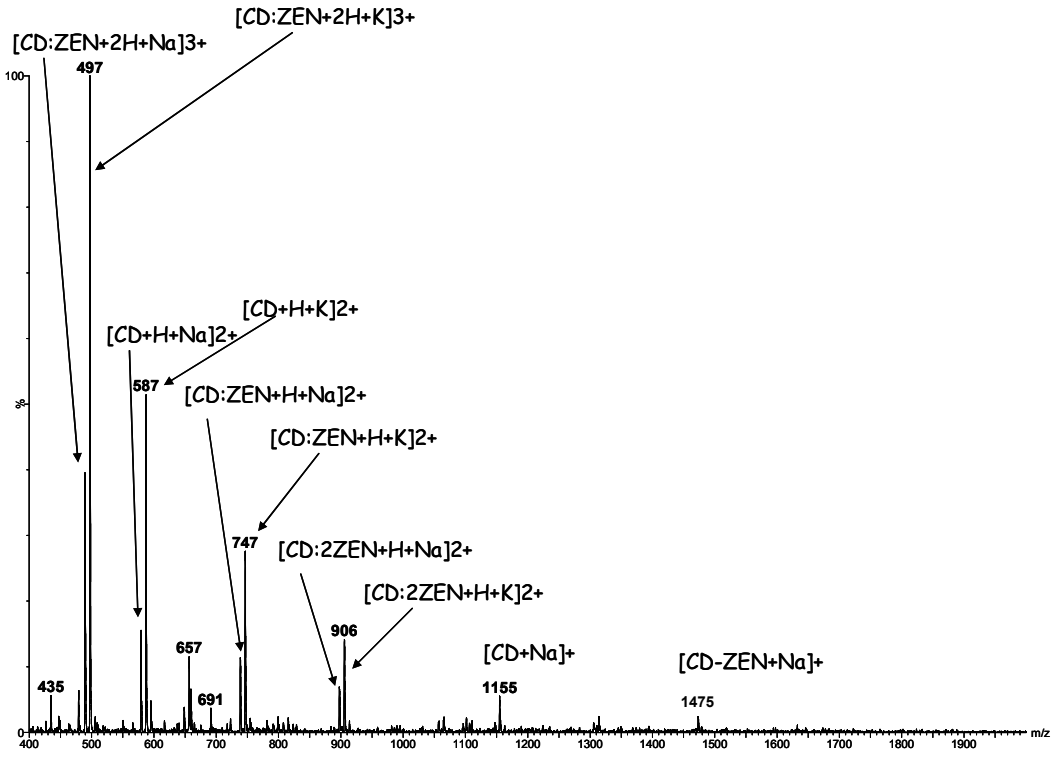

Figure 6.17: ESI-MS spectrum of the ZEN:β-CD complex.

The most intense peaks of the depicted range at *m*/*z* 492.3 and 497.6 were assumed to be the triple charged ion adducts $[CD:ZEN+2H+Na]^{3+}$ and $[CD:ZEN+2H+K]^{3+}$, while the peaks at *m*/*z* 738 and 746 was ascribed to the double charged adducts of the 1:1 complex. Moreover, the sodium adduct $[CD\text{-}ZEN+Na]^{+}$ also occurred, although at lower intensity. The signals due to uncomplexed cyclodextrin were also present in the spectrum: in particular, $[CD+H+Na]^{2+}$ and $[CD+H+K]^{2+}$ have a good intensity with the same cationization pattern. Finally, the signals at *m*/*z* 897 and 905 support the formation of the doubly charged 1:2 CD:ZEN complex, which occurs only in the gas phase. According to this statement, zearalenone seems to be able to easily form dimeric adducts in the gas phase, as reported in Table 6.6.

Table 6.6: Major peaks (m/z) identified from an ESI-MS spectrum of an aqueous sol. of ZEN:β-CD complex (1 mM).

Mass (m/z)	Identification
492	**$[ZEN+CD+2H+Na]^{3+}$**
497	**$[ZEN+CD+2H+K]^{3+}$**
579	$[CD+H+Na]^{2+}$
587	$[CD+H+K]^{2+}$
738	**$[ZEN+CD+H+Na]^{2+}$**
746	**$[ZEN+CD+H+K]^{2+}$**
897	$[2ZEN+CD+H+Na]^{2+}$
905	$[2ZEN+CD+H+K]^{2+}$
1135	$[CD+H]^{+}$
1157	$[CD+Na]^{+}$
1475	**$[ZEN+CD+H+Na]^{+}$**

6.4 Conclusions

In conclusion, all the data obtained suggest that zearalenone, α- and β-zearalenols and cyclodextrins give rise to host-guest complexes, involving inclusion of the phenolic moiety inside the CD cavity, causing fluorescence enhancement. In particular, in the case of zearalenone, the stoichiometry of the complex with β-cyclodextrin resulted to be 1:1.

Functional groups linked to the upper rim of CDs do not greatly influence the intensity of the fluorescence emission. The higher fluorescence enhancements observed in the presence of HP-β-CD might be due to its higher solubility in water and its higher flexibility when compared to the native β-CD.

An exhaustive comprehension of the ZEN-CD inclusion mechanism may lead to the design of chemosensor devices based on fluorescence. The well-known specificity of fluorescent probes would allow for more sensitive and accurate detection of mycotoxins, even at very low concentrations, minimizing the risk of false negative/positive results usually associated with ELISA tests. Cyclodextrins will be tested in HPLC analyses as fluorescence enhacers for zearalenone and zearalenols detection, in order to achieve lower detection limits. Moreover, chemosensors based on a luminescence response may be integrated into microarray systems, which could be applied for early detection of post-harvest contamination, providing for an easy-to-use control tool for mycotoxin analysis.

6.5 Materials and methods

6.5.1 Reagents.

Zearalenone (ZEN), α- and β-zearalenol (α- and β-ZOL) standards were from Sigma Biochemicals (St. Louis, MO, USA). All solvents were LC grade from Carlo Erba (Milan, Italy) and doubly distilled water was produced in our laboratory utilising an Alpha-Q System Millipore (Marlborough, MA, USA). β-CD was purchased from ACROS (Carlo Erba, Italy). 2-Hydroxypropyl-β-CD (HP-β-CD) and deuterium oxide (99.96 atom %D) were purchased from ALDRICH (Steinheim, Germany). NaOH and NaCl were from Carlo Erba (Milan, Italy). PBS solution was prepared dissolving 8 g NaCl, 1.2 g Na_2HPO_4, 0.2 g K_2HPO_4 and 0.2 g KCl in 1L bidistilled water and adjusting pH to 7.6 with 2N HCl. Sodium acetate buffer (pH 5; 5 mM) and sodium bicarbonate buffer (pH 8.5; 5 mM) solutions were freshly prepared by dissolving the proper amount of salts in 1 L doubly distilled water and adjusting the pH to the desired value with CH_3COOH or NaOH (1M), respectively.

6.5.2 ZEN and ZOLs solutions: preparation and decontamination.

Standard stock solutions of zearalenone and of its metabolites α- and β-zearalenol were prepared by dissolving the powder (10 mg) in a proper volume of acetonitrile. Working solutions of zearalenone and zearalenols (10^{-6} - 10^{-5} M) were prepared from standard stock solutions by evaporating the organic phase under nitrogen and dissolving the residue in water. These solutions are stable at −4 ◦C for a month. Decontamination of waste solutions and glassware was performed with sodium hypochlorite (10% aqueous solution) for 12 hours.

6.5.3 Fluorescence measurements.

Fluorescence spectra were recorded on a PERKIN ELMER LS50 instrument in a 0.2 × 0.2 cm quartz microcuvette (Hellma; type: 105.251-QS, light path: 3 mm, centre: 15 mm). Due to the solvent effects on the absorption and luminescence spectra, the proper excitation wavelengths were selected by scanning the excitation spectra of the different zearalenone and zearalenols solutions (10^{-6} M). The emission scan was performed in the wavelength range 380–600 nm. Both emission and excitation slits were set at 15 nm. Each spectrum was recorded in triplicate.

6.5.4 Measurements of fluorescence enhancements by CDs.

The solutions of ZEN or ZOLs (10^{-6} M) and cyclodextrins (1 mM) were prepared in doubly distilled water and the spectra of each analyte alone (blank) and in the presence of cyclodextrin (molar ratio Guest:CD = 1:10^3) were recorded; the F/F_0 ratio was calculated, where F and F_0 are the fluorescence intensities in the presence (sample) or in the absence (blank) of the CDs, respectively.

Moreover, the fluorescence spectra of ZEN in the presence of CDs (molar ratio ZEN:CD 1:10^3) have been recorded at two different pH values (pH 5.5 and pH 8.5), using acetate buffer (5 mM, pH 5.5) and bicarbonate buffer (5 mM, pH 8.5), in order to obtain the emission spectra of the neutral and the anionic form of the guest in the presence and in the absence of cyclodextrins.

6.5.5 Effect of pH on the fluorescence of ZEN and ZOLs in the presence and in the absence of β-CD.

The fluorescence spectra of ZEN (10^{-5} M) and ZEN:β-CD (molar ratio: 1:10^3) solutions were also recorded at different pH values. In particular, the experiments were performed at pH 5.5 and 9.0, using acetate buffer (10 mM) and bicarbonate buffer (10 mM), respectively.

6.5.6 Experimental procedures for the determination of the stoichiometry and association constants.

Aqueous solutions of β-CD (1 mM) were prepared and diluted to the desired concentrations. The concentration of ZEN or ZOLs was fixed at 1×10^{-6} M and the concentration of β-CD was changed from 1×10^{-4} to 1×10^{-3} M.

Suitable aliquots of the CD solutions were added to the zearalenone or zearalenol solution and the fluorescence spectra were recorded, measuring the variation of the F/F_0 ratio as a function of the aliquots of CDs added. The fluorescence intensities were corrected for dilution effects.

The fluorescence intensity of the inclusion complex was measured by excitation at wavelength corresponding to the maximum absorption wavelength of ZEN and ZOLs (276 nm). The complex formation constants were calculated by assuming a 1:1 or a 1:2 ZEN:CD stoichiometry ratio, according to the Benesi–Hildebrand equation.[9]

6.5.7 NMR experiments.

^{1}H-NMR spectra were recorded on a NMR Varian Inova 600 MHz at 25°C. The measurement were carried out with saturated solution of ZEN and ZEN:β-CD (molar ratio 1:1). A stock solution of zearalenone was prepared by dissolving 10 mg of the mycotoxin into 1.5 ml of acetonitrile. The ZEN working solutions (10^{-3} M in doubly distilled water) were prepared daily as follows: a proper amount of stock solution was dried under nitrogen flow and then under vacuum for few hours, the residue was dissolved in 750 µl of deuterium oxide, degassed, spun and transferred into the NMR tube. The working solution of ZEN:β-CD 1:1 was prepared in the same way, by dissolving the dried ZEN residue in β-CD solution (10^{-3} M in deuterium oxide). The chemical shift and the ^{1}H-^{1}H correlation were obtained from the proton spectra (^{1}H-NMR) and from the homonuclear correlation spectra (gCOSY); ROESY spectra was recorded to evaluate the interaction between ZEN and β-CD.

NMR spectra were processed with MestReC 4.9.9.9; the constants coupling were determined by line fitting and simulation of the real spectra.

Table 6.7: ^{1}H-NMR chemical shifts (ppm) for ZEN, in the absence and in the presence of β-CD, in D_2O.

Proton:	β-CD	ZEN:β-CD
H-3	6.181	6.192
H-5	6.413	6.535
H-1’	6.822	7.132
H-2’	5.860	5.773
H-3’ (a)	2.131	2.202
H-3’ (b)	2.256	2.453
H-4’ (a)	1.600	1.595
H-4’ (b)	1.875	2.073
H-5’ (a)	2.471	2.894
H-5’ (b)	2.781	2.408
H-7’ (a)	2.613	2.796
H-7’ (b)	2.224	2.144
H-8’ (a)	1.731	1.678
H-8’ (b)	1.900	1.872
H-9’ (a)	1.580	1.556
H-9’ (b)	1.538	1.691
H-10’	5.019	5.127
H-11’	1.336	1.435

6.5.8 Circular dichroism experiments.

Circular dichroism spectra were recorded on a JASCO J-715 spectropolarimeter equipped with a Peltier thermostat: acquisition range 200-500 nm, accumulations 3, band width 1.0 nm, response 1s, scan speed 100 nm/min, temperature 20°C. Quartz cells (0.1 x 1 cm) were used. The CD spectra of ZEN (10^{-5} M) and ZEN:β-CD (molar ratio: $1:10^3$) were recorded. All spectra were treated with the noise reduction software included in the program J-700 for Windows Standard Analysis, version 1.33.00.

6.5.9 ESI-MS experiments.

Mass spectrometry experiments were performed on a Waters Acquity SQ (single quadrupole) mass spectrometer using electrospray ionization. The source temperature was set at 180°C and the probe voltage was 3.2 kV in positive ion mode. Nitrogen was applied as both the nebulizer and desolvation gas. Data were acquired across a mass range of 200–2000 *m*/*z*.

Each working solution (1 mM β-CD, 1 mM zearalenone and 1 mM β-CD:ZEN 1:1 complex) was infused in the equipment at an infusion rate of 10 µl/min and the mass spectra were recorded in the continuous mode for 2 minutes.

[1] E. Chiavaro, C. Dall'Asta, G. Galaverna, A. Biancardi, E. Gambarelli, A. Dossena, R. Marchelli, J. Chromatogr. A, 2001, 937 (1-2), 31-40.

[2] C. M. Maragos, M. Appell, J. Chromatogr. A, 2007, 1142 (1-2), 252-257;

[3] E. Rosenberg, R. Krska, R. Wissiak, V. Kemetov, R. Josephs, E. Razzazzi, M. Grassbauer, *J. Chromatogr. A*, **1998**, 819, 277.

[4] P. Zoellner, J. Jodlbauer, W. Lindner, *J. Chromatogr. A*, **1999**, 858, 167.

[5] P. Zoellner, D. Berner, J. Jodlbauer, W. Lindner, *Chromatographia*, **2000**, 51, 681.

[6] A. Lagana, G. Fago, A. Marino, D. Santarelli, *Rapid Commun. Mass Spectrom.* **2001**, 15, 304.

[7] M. Horie, H. Nakazawa, *J. Chromatogr. A*, **2000**, 51, 681.

[8] S. Sforza, C. Dall'Asta, A. Moseriti, G. Galaverna, A. Dossena, R. Marchelli, *Angew. Chem. Int. Ed.* **2005**, 44, 5126-5130.

[9] H. A. Benesi, L. H. Hildebrand, *J. Am. Chem. Soc.* **1949**, 71, 2703.

[10] I. Osaka, M. Koudda, N. Selvapalau, S. Samol, K. Shashadhar, R. Kimono, M. V. Rekarsky, Y. Inova, R. Arakawa, *J. Mass Spectrom.* **2006**, 41 (2), 202-207.

[11] J. B. Cunnif, P. Kouros, *J. Am. Chem. Soc. Mass Spectrom.* **1995**, 6 (5), 437-447.

[12] S. Sforza, G. Galaverna, R. Corradini, A. Dossena, R. Marchelli, *J. Am. Soc. Mass Spectrom.* **2003**, 14, 124.

Acknowledgements:

I would like to thank all people who helped me in writing this thesis, in particular Professor Rosangela Marchelli and Professor Arnaldo Dossena.

I'm grateful to Prof. Roberto Corradini and Prof. Stefano Sforza for their supervision concerning the synthetic and characterization parts of my work.

Finally, I would like to extend my special thanks to Dr. Chiara Dall'Asta and to Dr. Andrea Faccini (without their help, the realization of this thesis would not have been possible) and all people I met during the last three years.

Roberto